Involvement of *miR164* and its Targets in Tomato Flower Development

Anat Hendelman

Department of Life Science

The Mina &Everard Goodman Faculty

Ph.D. Thesis

Submitted to the Senate of Bar-Ilan University

Ramat-Gan, Israel October 2013

This work was carried out under the supervision of

Dr. Tzahi Arazi (Plant sciences institute), Agricultural Research Organization, Volcani center.

Prof. Rafael Perl-Treves (The Mina &Everard Goodman Faculty of Life Science), Bar Ilan University.

Table of Contents

Abbreviations

Abbreviations

PTGS	post-transcriptional gene silencing
RNAi	RNA interference
dsRNA	double-stranded RNA
siRNA	small interfering RNA
tasi-RNA	*trans*-acting siRNA
miRNA	microRNA
Pol II	RNA polymerase II
DCL1	DICER-LIKE1
AGO1	ARGONAUTE1
RISC	RNA-Induced Silencing Complex
SAM	Shoot Apical Meristem
VSR	viral suppressors silencing
BWYV	*Beet western yellows virus*
ARF	AUXIN RESPONSE FACTOR
CUC	CUP SHAPED COTYLEDONS
NAM	NO APICAL MERISTEM
GOB	GOBLET
vsiRNAs	virus-derived small RNAs
Tomato	*Solanum lycopersicum*
nt	Nucleotide
SEM	Scanning Electron Microscopy

Abstract

MicroRNAs are an abundant class of 21–22 nt, non-coding RNAs that play a critical role in a wide range of developmental pathways in plants through ARGONAUTE1 (AGO1) post-transcriptional regulation of target mRNAs. Genetic analysis of *ago1* mutants with informative defects has provided valuable insights into AGO1's biological functions and its corresponding miRNAs. Tomato encodes two AGO1 homologs (SlAGO1s), but mutants have not been described to date. The first goal of this thesis was to analyze SlAGO1s' involvement in tomato flower development. The *Polerovirus* P0 silencing suppressor is an F box protein that suppress viral silencing by binding to RNA induced silencing complex (RISC) thus preventing the incorporation of the miRNA/siRNA duplexes into AGO1, leading to its degradation. This study confirmed that both SlAGO1s' undergo decay in the presence of P0, and accordingly transgenic responder line (*OP:P0HA*) were produced which, upon transactivation, expresses P0 C-terminally fused to a hemagglutinin (HA) tag (P0HA) and destabilizes SlAGO1s at the site of expression. By crossing *OP:P0HA* with a battery of driver lines, constitutive as well as organ- and stage-specific, SlAGO1 downregulation was induced in the F1 progeny. Activated plants exhibited various developmental phenotypes that partially overlapped with those of *Arabidopsis ago1* mutants. Plants that constitutively expressed P0HA had reduced SlAGO1 levels and increased accumulation of miRNA targets, indicating compromised SlAGO1-mediated silencing. Consistent with this, they exhibited pleiotropic morphological defects and their growth was arrested post-germination. Transactivation of P0HA in young leaf (*FIL>>P0HA*) and floral organ primordia (*AP1>>P0HA/ AP3>>P0HA*) dramatically modified corresponding organ morphology, including the radialization of leaflets, petals and anthers, suggesting that SlAGO1s' activities are required for normal lateral organ development and polarity. Additionally, *AP1>>P0HA* and *AP3>>P0HA* produced flowers with extra floral-organs and abnormal floral-organs separation, suggesting that SlAGO1s' activities are also essential for normal flower boundary morphogenesis. Being composed of several whorls of distinct floral organs, the flower is one of the most complex organs in the plant. As such, the formation and maintenance of boundaries that separate the meristem from the floral organ

primordium and adjacent organs are critical for its normal development. Among the tested miRNA-target genes, *Solyc03g115850* (*SlNAM2*) was most influenced by P0HA expression. The yet uncharacterized *SlNAM2* gene is a member of the NAM, ATAF1/2, and CUC2 (NAC) domain transcription factor family, which was predicted as a miR164 target gene. In *Arabidopsis*, the *NAM*-miR164-regulated genes, *CUP SHAPED COTYLYDON1* (*CUC1*) and *CUC2*, play key roles in floral-boundary specification. In contrast, much less is known about floral-boundary establishment in the model crop tomato. The miR164-regulated *NAM* gene *GOBLET* is expressed in the floral meristem–organ boundaries and its loss-of-function mutant produces flowers with fused sepals and fewer locules, indicating its requirement for tomato floral-boundary formation. Here sly-miR164 was found to target the transcripts of an additional three (*SlNAM2, SlNAM3 and SlNAC1*) uncharacterized *NAM* genes in developing flowers. Since *SlNAM2* was upregulated in the P0HA expressing plants, a possible role of *SlNAM2* in floral-boundary specification was further investigated during this work. After floral-boundary initiation, *SlNAM2* is expressed as stripes that mark the boundaries between sepals and between different floral whorls. Furthermore, ectopic accumulation of SlNAM2-encoding transcripts caused various growth-suppression and extra-organ phenotypes typically observed in plants overexpressing known boundary genes. Flower-specific silencing of sly-miR164-targeted *NAM* genes (*AP1>>MIR164*) caused defects in the separation of sepals and floral whorls indicating abnormal boundary specification. However, supplementing these *NAM*-deficient flowers with miR164-resistant *SlNAM2* suppressed their fusion phenotypes and completely restored floral boundaries. Taken together, these results strongly suggest that *SlNAM2* participates in the establishment of tomato flower whorl and sepal boundaries.

A. Introduction

A.1. Small RNA in plants

Small RNAs (sRNAs, 20- to 24-nucleotides) are key regulators of gene expression in plants (Chen, 2009). In recent years next generation sequencing techniques enabled the mass identification and quantification of sRNAs, revealing complex populations of these molecules. Plant sRNAs can be divided into small interfering RNAs (siRNAs) and microARNAs (miRNAs) based on differences in biogenesis. SiRNAs are generated from long double-stranded RNAs (dsRNAs), which usually give rise to multiple siRNAs species from both strands and can act in *cis* or *trans* (Axtell, 2013). This group contains the heterochromatic siRNAs (hc-siRNAs) that guide DNA methylation and histone methylation machineries to homologous loci for transcriptional gene silencing (Lu *et al.*, 2005; Kasschau *et al.*, 2007; Zhang *et al.*, 2007; Mosher *et al.*, 2008), secondary siRNAs including phased or tasi-RNAs that regulate developmental (Chitwood *et al.*, 2007; Allen *et al.*, 2007; Yifhar *et al.*, 2012) and disease resistance genes (Zhai *et al.*, 2011; Li *et al.*, 2012; Shivaprasad *et al.*, 2012), and natural sense-antisense transcript siRNAs pairs (NAT-siRNAs) that were found to play a role in reproductive function (Ron *et al.*, 2010) and biotic and abiotic stresses (Borsani *et al.*, 2005; Katiyar-Agarwal *et al.*, 2007). In contrast, miRNAs, which play critical roles in modulating metabolism, development and physiology, are derived from single-stranded RNA transcripts, pri-miRNAs, that can fold into a hairpin RNA secondary structure (Xie *et al.*, 2005). The biogenesis of plant sRNAs requires several evolutionary conserved components, of which few are encoded by multigene families with conserved clades that were found to be specialized for the production or use of a certain class of sRNAs (Margis *et al.*, 2006; Vaucheret, 2008). The first component is the DICER-LIKE (DCL) endonuclease that slices the double stranded regions of the RNA precursors and releases a 20–24 nt long double-stranded duplex, with 2-nt 3’ overhang (Margis *et al.*, 2006). *Arabidopsis thaliana* encodes four DCLs each specialized in the generation of certain small RNAs with overlapping functions (Park *et al.*, 2002; Xie *et al.*, 2004; Gasciolli *et al.*, 2005; Henderson *et al.*, 2006). DCL1 catalyzes the formation of predominantly 20-22-nt miRNAs, certain siRNAs that derived from inverted repeats and NAT-siRNAs (Park *et al.*, 2002; Allen *et al.*, 2005; Borsani *et al.*, 2005; Henderson *et al.*, 2006; Li *et al.*, 2012; Shivaprasad

et al., 2012). DCL2 catalyzes the formation of 22-nt siRNAs and 22-24-nt NAT-siRNAs (Xie *et al.*, 2004; Borsani *et al.*, 2005; Deleris *et al.*, 2006). DCL3 is required for the production of 24-nt hc-siRNAs and long miRNAs (Qi *et al.*, 2005; Wu *et al.*, 2010; Xie *et al.*, 2004). DCL4 sequentially processes 21-nt secondary siRNAs derived from RDR6-depedent dsRNA including phased and ta-siRNAs and is also required for the production of young miRNAs such as miR822 and miR839, presumably because of their perfect stem–loop structure resembling a dsRNA (Gasciolli *et al.*, 2005; Howell *et al.*, 2007; Rajagopalan *et al.*, 2006; Xie *et al.*, 2004). The second important component is the ARGONAUTE (AGO), a part of the RNA-Induced Silencing Complex (RISC) (Baumberger and Baulcombe, 2005). This complex incorporates the mature single strand sRNA and uses it as a guide to target complementary RNAs resulting in its slicing, translational inhibition or epigenetic silencing (Baumberger and Baulcombe, 2005; Vaucheret, 2008; Li *et al.*, 2013). *Arabidopsis* encode ten AGO proteins that fall into three distinct clades: AGO1, AGO5 and AGO10 clade, the AGO2, AGO3 and AGO7 clade, and the AGO4, AGO6 and AGO8 and AGO9 clade (Vaucheret, 2008). Sequencing of sRNAs bound by each AGO protein, defined their roles in various small RNA pathways. AGO1, preferentially binds sRNAs with a 5’ uridine characteristic of most 20-22-nt miRNAs (Baumberger and Baulcombe, 2005; Mi *et al.*, 2008), whereas AGO5, binds sRNAs of different sizes that have a 5’ cytosine (Takeda *et al.*, 2008). Lately, it was found out that AGO10 primarily associates with miR165/166 in the SAM thus preventing their incorporation into AGO1 complexes (Zhu *et al.*, 2011). AGO2 (and probably the very similar AGO3) has a preference for 21-nt sRNAs with a 5’ adenine. Additionally, AGO2 is supposed to have an antiviral role as it associates with several virus-derived siRNAs (Takeda *et al.*, 2008). AGO7 associates largely with a single miRNA, miR390, required for TAS3 (trans-acting siRNA locus 3) dependent ta-siRNA production (Montgomery *et al.*, 2008). Finally, it is thought that 24-nt siRNAs with a 5’ adenine guide AGO4, AGO6 and AGO9 to noncoding RNAs that mediate DNA methylation and chromatin modifications (Qi *et al.*, 2006; Zheng *et al.*, 2007; Havecker *et al.*, 2010). AGO8 shows low-level expression in all stages and tissues and thus is considered to be a pseudo gene (Takeda *et al.*, 2008; Mallory and Vaucheret, 2010).

A.2. The biogenesis and regulatory roles of plant miRNAs

The miRNA encoding genes (*MIRs*) are transcribed by RNA polymerase II (Pol II) (Xie *et al.*, 2005; Kim *et al.*, 2011) into a pri-miRNA, which is capped and polyadenylated. The pri-miRNA is processed into the pre-miRNA, which is further processed into the miRNA/miRNA∗ duplex. The duplex is methylated by HEN1 and finally, most of the mature miRNAs are incorporated into AGO1 (Baumberger and Baulcombe, 2005), and act in *trans* to modulate the spatial and temporal expression of partially complementary mRNAs (Fig. 1). Most plant miRNAs exhibit up to four or less mismatches with their targets and these mismatches are usually located in the 3' region of the miRNA (Mallory *et al.*, 2004*b*; Schwab *et al.*, 2005). Further experiments with mutated targets show that mismatches between positions 3 and 11 of the miRNAs result in poor cleavage, whereas mismatches at the 3' end had a slighter effect (Mallory *et al.*, 2004*b*). By those roles, several bioinformatics algorithms were developed and many prediction miRNA-target tools are now available (Dai and Zhao, 2011; Wu *et al.*, 2012; Sun *et al.*, 2013). Strikingly, in *Arabidopsis* both DCL1 and AGO1 undergo homeostatic regulations through the action of miR162 and miR168, respectively (Xie *et al.*, 2003; Vaucheret *et al.*, 2004). Moreover, the maintenance of AGO1 homeostasis is not only by miR168 but also by secondary siRNA arising from miR168-guided *AGO1* mRNA cleavage products (Mallory and Vaucheret, 2009). Up to date, three types of miRNA regulatory modes have been described at the PTGS level (Garcia, 2008). The first regulatory mode is spatial restriction, where the miRNA has a complementary accumulation pattern with its target genes and spatially confine their transcriptionally expression domain. For example, in *Arabidopsis* miR166 restricts the expression of *PHABULOSA* (*PHB*) to the adaxial domain of the developing leaf to enable proper polarity formation (McConnell *et al.*, 2001; Kidner and Martienssen, 2004). The second regulatory mode is dampening expression, where the miRNA and its target genes are sharing overlapping expression domain and the miRNA act to buffer the target gene accumulation level. For example, in *Arabidopsis* both miR164 and its *CUP SHAPED COTYLEDON1* (*CUC1*) and *CUC2* target genes, are expressed in the bud at the interwhorl regions where miR164 refine their accumulation levels to insure proper boundaries formation (Baker *et al.*, 2005; Sieber *et al.*, 2007). The third regulatory mode is temporal regulation, where the miRNA act as a developmental clock and the developmental transition occurs when

the target reaches a critical threshold. like transition to reproductive phase in *Arabidopsis* is controlled by the accumulation of miR172 and its *APETALA2-like (AP2-like)* target genes (Aukerman and Sakai, 2003; Chen, 2004).

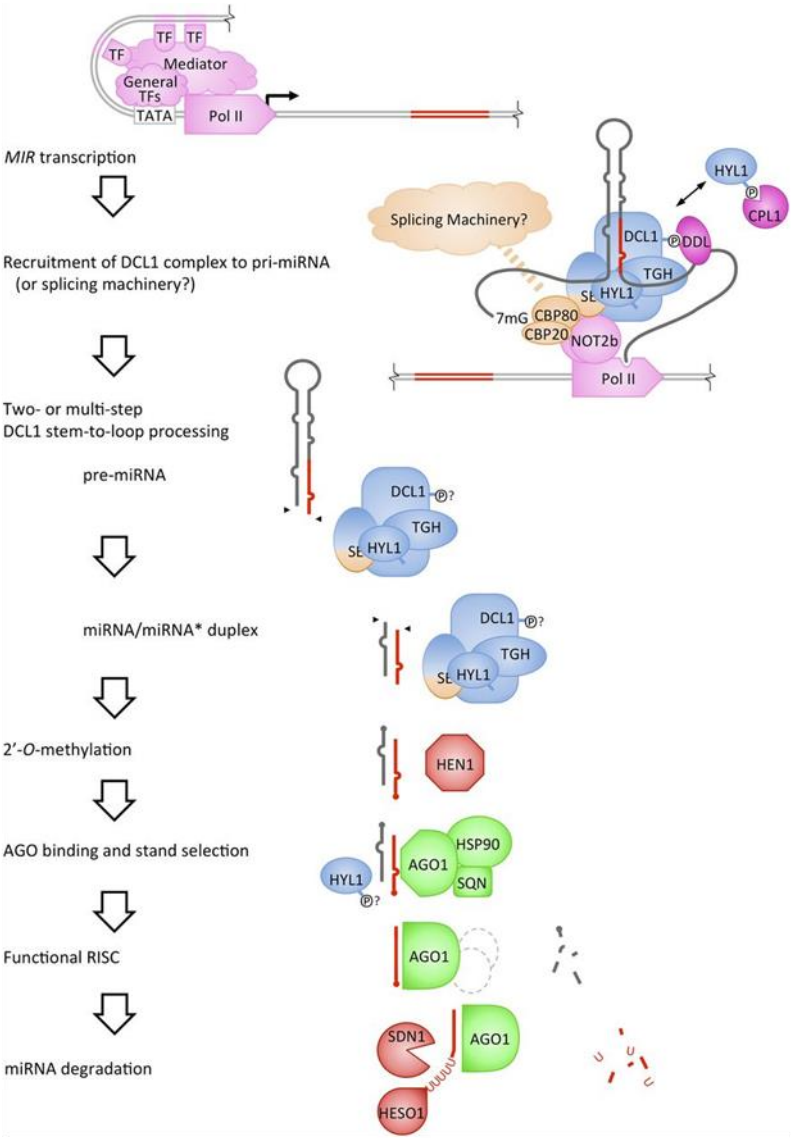

Fig. 1. Summary of the major steps in miRNA biogenesis and turnover. Proteins are colour coded according to known functions in *MIR* transcription (pink), splicing (orange), DCL processing (light blue), phospho-regulation (purple), RISC assembly (green), and miRNA stabilization and turnover (red). Adopted from Rogers K , and Chen X Plant Cell 2013;25:2383-2399(Rogers and Chen, 2013)

A.3. ARGONAUTE1 and its role in plant development

AGO proteins contain a variable N-terminal domain and conserved C-terminal PAZ, MID, and PIWI domains. The PAZ domain recognizes the 3' ends of sRNAs and bind

to it with low affinity in a sequence-independent manner while the MID domain binds to the 5' phosphate of the sRNAs (Tolia and Joshua-Tor, 2007). The PIWI domain has an RNaseH-like structure and slices target RNAs (Tolia and Joshua-Tor, 2007). AGO1 is a key component of miRNA RISCs as well as transgene (Baumberger and Baulcombe, 2005) and antiviral (Zhang *et al.*, 2006) RISCs. Because most plant miRNAs have a 5' uridine, AGO1 is considered the most important AGO in the miRNA pathway. Indeed, in *ago1* mutants, miRNA accumulation is reduced and their target mRNAs accumulate (Vaucheret *et al.*, 2004). Consistent with the major function played by AGO1 in the miRNA pathway, *Arabidopsis ago1* null mutants exhibit severe developmental phenotypes, including various defects in organ polarity and occasional growth arrest (Bohmert *et al.*, 1998; Lynn *et al.*, 1999; Kidner and Martienssen, 2004, 2005). The *ago1-3* and *ago1-8* null mutants exhibit narrow thickened rosette leaves, which completely lose their polar identity, and radialized cauline leaves and petals (Bohmert *et al.*, 1998; Lynn *et al.*, 1999). Growth arrest occurs in *ago1-7* and *ago1-8* seedlings upon replacement of the primary shoot apical meristem (SAM) with a single determinate pin-like organ, and in a*go1-10* null mutant seedlings due to lack of post-embryonic organs (Lynn *et al.*, 1999; Kidner and Martienssen, 2005). In contrast to *ago1* mutants, other *ago* null mutants exhibit no obvious (*ago2-6* and *ago9*) or very limited (*ago7/zippy* and *ago10/pinhead/zwille*) developmental defects (Vaucheret, 2008) in *Arabidopsis*. Ler but not Col ecotype *ago10* null mutants exhibit, with incomplete penetrance, a severely defective SAM (Lynn *et al.*, 1999; Takeda *et al.*, 2008), whereas *ago7* null mutants display premature transition from juvenile to adult vegetative phase, as indicated mainly by precocious appearance of adult leaf traits (Hunter *et al.*, 2003).

A.4. Viral suppressors of RNA silencing

RNA silencing constitutes the primary plant immune system against viruses. Upon virus infection the plant host induce the production of virus-derived small RNAs (vsiRNAs) that are incorporated into the RISC and guide it to cleave the viral RNAs (Csorba *et al.*, 2009). In return, plant viruses evolved diverse viral suppressors of RNA silencing (VSRs) which can suppress either the production or the antiviral activity of vsiRNAs (Csorba *et al.*, 2009). Interestedly, it has been found that the antiviral and the miRNA pathways are reminiscent and even share certain functional

components (Baulcombe, 2004). For example both pathways use small RNAs that incorporate into AGO1 as their effector. As a result, VSRs not only inhibits the antiviral mechanism but, also perturb the miRNA pathway (Voinnet, 2005). For example, the P19 protein a *Tomato busy stunt virus* (TBSV) VSR, functions to sequester 20-21 long siRNA-duplexes thus preventing their incorporation into RISCs (Lakatos *et al.*, 2006). Moreover, P19 was found to inhibit the translational capacity of *AGO1* mRNA by modulating the endogenous miR168 level to alleviate the anti-viral function of AGO1 protein (Várallyay *et al.*, 2010). In addition it was shown that the developmental aberrations exhibited by P19 in *Arabidopsis* P19 transgenic plants were caused due to impaired levels of miR167, that led to misregulation of the miR167 target *AUXIN RESPONSE FACTOR 8* (*ARF8*) (Jay *et al.*, 2011). The 2b protein of *Cucumber mosaic virus* (CMV), binds to both AGO1 and sRNAs duplexes, causing to inhibition of the host RdRP-dependent synthesis of viral secondary siRNAs by inhibiting the RISC activity via physical interaction with the PAZ domain of AGO1 (Zhang *et al.*, 2006; Burgyán and Havelda, 2011). The P0 protein of the *Beet western yellows virus* (BWYV) encodes an F-box protein that promote the degradation of AGO1 preventing de novo formation of siRNA/miRNA RISC effector complexes (Pazhouhandeh *et al.*, 2006; Baumberger *et al.*, 2007; Bortolamiol *et al.*, 2007; Csorba *et al.*, 2010). Consistent with this, transgenic P0 expression causes pleiotropic developmental phenotypes, including growth arrest as well as enhanced accumulation of several miRNA-target transcripts, mimicking the effects observed in *ago1* mutants (Bortolamiol *et al.*, 2007). Furthermore, in *Arabidopsis* AGO5, AGO6, AGO2 and AGO9 have also been shown to decay in the presence of P0 (Baumberger *et al.*, 2007). Nevertheless, since *Arabidopsis* mutants of these AGOs do not show developmental phenotypes (Vaucheret, 2008), the effect of such decay on plant development is likely to be very limited. Thus, in the absence of an *ago1* mutant, the expression of P0 in an organ offers a potent strategy to downregulate AGO1 in that organ, thereby exposing its involvement in organogenesis.

A.5. miRNAs in tomato plants

Solanum lycopersicum (tomato) is one of the most important crops in the fresh vegetable market and the food-processing industry. In 2007, tomato joined the miRNAs race (Pilcher *et al.*, 2007) and by now the Tomato Functional Genomics

database contains more than 5.3 million unique tomato small RNAs from leaf, buds, flowers and several stages of developing tomato fruits libraries, generated by traditional cloning of cDNA libraries and high-throughput sequencing of sRNAs (Itaya *et al.*, 2008; Moxon *et al.*, 2008; Mohorianu *et al.*, 2011; Karlova *et al.*, 2013). More than 100 known miRNAs were identified in those libraries and 46 known miRNAs were deposit to miRBase (release 20; http://www.mirbase.org/). The target of many of these miRNAs were predicted to be transcription factors involved in plant growth and developmental patterning (Itaya *et al.*, 2008; Moxon *et al.*, 2008; Mohorianu *et al.*, 2011). Moreover, the recent annotation of the complete tomato genome sequence (Tomato Genome Consortium, 2012) enabled an identification of target genes on a genome-wide scale and parallel analysis of RNA ends (PARE) enabled verification to some of those predicted target genes (Karlova *et al.*, 2013). *Lanceolate* (*La*), a member of the TCP transcription factor family, was the first tomato miRNA target gene to be characterized (Ori *et al.*, 2007). Point mutations within the sly-miR319-binding site of several *La* alleles caused to dominant mutation which produced very small leaves with entire margins as a result of accelerated differentiation of leaf margins, while downregulation of all sly-miR319 target genes by ectopic expression of *MIR319* by *FIL* promoter produced larger leaflets and continuous growth of leaf margins. The resulted phenotypes together with the expression patterns of both sly-miR319 and *La*, suggested that the spatial and temporal regulation of *La* by sly-miR319 is essential for proper differentiation of leaf margins while the leaf elaboration occur (Ori *et al.*, 2007). Sly-miR159 is probably also crucial for normal flower development as transgenic expression of miR159-resistant *SGN-U567133*-target gene led to pleiotropic developmental defects in leaves, flowers, and fruits (Buxdorf *et al.*, 2010). Sly-miR164 is another conserved miRNA that regulates the expression of *GOBLET* (*GOB*), a member of the NAM, ATAF1/2, CUC2 (NAC) domain transcription factor family, which involved in boundary formation. A loss-of-function mutant of this gene produced goblet-shaped fused cotyledons, and similar to its *CUC2* homolog, the spatial and temporal expression of *GOB* is post-transcriptionally regulated by sly-miR164. This regulation limits *GOB* expression to the boundaries between the shoot apical meristem and leaf primordia and between leaflet primaordia (Berger *et al.*, 2009; Blein *et al.*, 2008). Accordingly, a loss-of-function *gob-3* mutant produced simpler leaves with smooth leaflet margins lacking secondary leaflets, and gain-of-function *Gob-4d* produced extra lobed

cotyledons and deeply lobed leaves, together indicating that *GOB* is required for the formation of the boundaries between leaflets in compound tomato leaves (Berger *et al.*, 2009). In the flower, *GOB* is expressed at the boundaries between floral meristem and floral-organ primordia (Blein *et al.*, 2008). In addition, *gob-3* and *Gob-4d* mutants produced flowers with fused sepals and fewer locules or with extra carpals, respectively, together suggesting that *GOB* functions in the formation of floral-organ boundaries as well (Berger *et al.*, 2009).

A.6. The role of miRNAs in flower development

Being composed of several whorls of distinct floral organs, the flower is one of the most complex organs in the plant, and is vital for the reproduction of angiosperms. Perturbation of the miRNA pathway leads to flower developmental defects indicating its importance for flower development (Wollmann and Weigel, 2010). MiR172 was found to regulate floral organ identity and flowering time by post-transcriptional regulation of members of the *APETALA2* (*AP2*) transcription factor family (Zhu and Helliwell, 2011). MiR172-mediated repression of AP2 in the flower is crucial for the formation of the two inner whorl organs (Aukerman and Sakai, 2003; Chen, 2004; Zhao *et al.*, 2007). Overexpression of miR172 showed floral homeotic phenotypes similar to those of *ap2* loss-of-function (carpels instead of sepals and lack of petals) (Aukerman and Sakai, 2003). MiR159 is required for normal anther development by repressing GAMYB-like transcription factors (Allen *et al.*, 2007) and act as a molecular switch that restrict the expression of *MYB33* and *MYB65* to anthers (Alonso-Peral *et al.*, 2010). Overexpression of miR159 disrupts anther development and leads to male sterility in *Arabidopsis* (Achard *et al.*, 2004). MiR167 represses the *ARF6* and *ARF8* transcription factors which are required for fertility of both ovules and anthers (Wu *et al.*, 2006). Overexpression of miR167 causes defects in anther dehiscence and failure to release pollen (Wu *et al.*, 2006). MiR160 negatively regulates ARF10, ARF16 and ARF17 and is required for normal flower formation and fertility (Mallory *et al.*, 2005; Liu *et al.*, 2010). The *floral organs in carpel* (*foc*) loss-of-function mutant of miR160 produced irregularly shaped flowers, with floral organs inside the siliques, and had aberrant seeds (Liu *et al.*, 2010). MiR166/165 functions to negatively regulate the HD-ZIP III genes in various floral organs and are crucial for normal organ polarity, and vascular development (Kim *et al.*, 2005; Williams *et al.*,

2005). The miR166a gain-of-function mutants of miR166 *meristem enlarged1* (*men1*) and *jabba-1D* (*jab-1D*) have fascinated inflorescence stems and defective vascular differentiation and radial patterning (Kim *et al.*, 2005; Williams *et al.*, 2005). MiR319 regulates petal growth and development by regulating the TEOSINTE BRANCHED/ CYCLOIDE A/PCF (TCP) transcription factors *TCP2*, *TCP3*, *TCP4*, *TCP10*, and *TCP24* (Palatnik *et al.*, 2007; Nag *et al.*, 2009). The *Arabidopsis miR319a*^{129} loss-of-function mutants produced flowers with narrower and shorter petals, and defective anthers due to elevated levels of *TCP4* (Nag *et al.*, 2009). MiR164 play a key role in floral boundaries formation by regulating the expression of the CUC1 and CUC2 boundary genes (see below) (Mallory *et al.*, 2004*a*; Baker *et al.*, 2005; Sieber *et al.*, 2007). The *early extra petals1* (*eep1*) miR164c loss-of-function mutants produced flowers with extra petals in early-arising flowers(Baker *et al.*, 2005).

A.7. Flower boundaries are essential for normal formation of whorls and floral-organs

The production of plant lateral organs depends on the formation of a narrow domain of non-dividing cells or boundary that separates the organ primordium from the meristem. In addition, normal lateral organ architecture requires proper organ-organ boundary formation that separates distinct tissues (Breuil-Broyer *et al.*, 2004; Aida and Tasaka, 2006*a*; Rast and Simon, 2008). The boundary cells display unique morphological characteristic: their epidermal cells have a saddle-shaped surface and they are strongly elongated along the boundary compare to the to the meristem and primordia, whose epidermal cells show a fairly round shape with a flat or convex surface (Aida and Tasaka, 2006*a*). It was found that formation of boundaries is regulated by specific boundary genes that are expressed in the cells that will form the boundary. Accordingly, misexpression of these genes can lead to growth arrest or abnormal development (Aida *et al.*, 1997; Takeda *et al.*, 2004; Brewer *et al.*, 2004; Aida and Tasaka, 2006*a*). In *Arabidopsis*, several gene families are involved in the specification of meristem–organ and organ–organ boundaries. Misexpression of those genes lead to either floral organ fusions as can be seen in *cuc1 cuc2* double mutants who produced flowers with fused sepals and stamens (Aida *et al.*, 1997) or to loss of floral organs as in loss-of-function mutant of *PETAL LOSS* (*ptl*) and *HANABA TARANU* (*han*) which resulted in flowers with fewer petals (Griffith *et al.*, 1999;

Zhao *et al.*, 2004). In the past decade more and more regulatory boundary genes have been discovered, revealing the genetic pathway controlling both floral organ initiation and boundaries formation allowing normal flower organogenesis (Li *et al.*, 2010; Huang *et al.*, 2012; Lampugnani *et al.*, 2013). Among them, the *RABBIT EARS* (*RBE*) which promotes both intra- and inter- perianth whorls separation (Takeda *et al.*, 2004; Krizek *et al.*, 2006). Lately, it has been discovered that *RBE* negatively regulates *MiR164c* and function to fine-tune MIR164 expression, and by that regulates the expression of *CUC1* and *CUC2* boundary genes (Huang *et al.*, 2012). The *Arabidopsis CUC1* and *CUC2* are functionally redundant miR164-regulated *NAM* genes that promote boundary formation and maintenance throughout vegetative and reproductive development (Aida *et al.*, 1997; Takada *et al.*, 2001). Accordingly, they are expressed between the meristem and the new lateral organ, at the base of the outgrowing teeth defining the leaf sinuses, between the inflorescence meristem and the new flower meristem, and between floral-organ primordia (Ishida *et al.*, 2000; Takada *et al.*, 2001; Nikovics *et al.*, 2006). Consistent with their requirement for boundary formation, *cuc1 cuc2* double mutants develop fused cotyledons, and produce flowers with fused sepals and stamens and with fewer petals (Aida *et al.*, 1997). Similar phenotypes have also been observed in plants overexpressing miR164 (Mallory *et al.*, 2004*a*; Laufs *et al.*, 2004). Gain-of-function of either *CUC1* or *CUC2* leads to extra floral organ formation and variable growth-suppression phenotypes, which have been suggested to be caused by repression of cell division (Takada *et al.*, 2001; Mallory *et al.*, 2004*a*; Laufs *et al.*, 2004; Baker *et al.*, 2005; Nikovics *et al.*, 2006; Sieber *et al.*, 2007).

A.8. Objectives

The miRNA pathway plays important roles in flower development but little is known on their function in tomato, one of the most important agricultural crops. Since fruit initiate from fertilized flowers, better understanding of flower development of this crop is essential to improve its yield. The main goal of this work is to improve our understanding on the roles of the miRNA pathway in tomato flower development.

Specific objectives are:

1.1. To reveal processes and genes which are regulated by miRNAs during flower development.

1.2. To characterize the sly-miR164 target genes in the flowers.

1.3. To analyze the function of *SlNAM2* in flower development.

1.4. To characterize the biological role of *SlNAM2* regulation by sly-miR164 in the flower.

B. Materials and Methods

B.1. Plant material and growth conditions

Tomato (*Solanum lycopersicum*) cv. M82 lines *35S:LhG4*, *FIL:LhG4*, *OP:GUS* (Lifschitz *et al.*, 2006), *650:LhG4*, *BLS:LhG4*, *OP:mRFP* (Shani *et al.*, 2009), *AP1:LhG4*, *AP3:LhG4* (Fernandez *et al.*, 2009) and *OP:MIR164* (Alvarez *et al.*, 2006) have been described elsewhere. The tomato plants were grown under greenhouse conditions with temperatures ranging between 15 and 25 °C in a tuff–peat mix with nutrients, using 4-liter pots. Germination and seedling growth took place in a growth chamber with a 16 h light period and 8 h dark period (photosynthetic photon flux density: 50–70 µmol $m^{-2}s^{-1}$) at a constant temperature of 24°C. For crosses, closed flowers were emasculated by removal of the petals and stamens and hand-pollinated with the pollen of an appropriate homozygous driver line.

B.2. Total RNA extraction and small-RNA blot analyses

Total RNA was isolated from different tomato tissues with Bio-TRI RNA reagent (Bio-Lab, Jerusalem, Israel) according to the manufacturer's protocol. After addition of isopropanol, the RNA extract was incubated overnight at -20 °C to enhance the precipitation of low-molecular-weight RNAs. Following an ethanol wash, RNA was resuspended in RNase-free water and kept at -80 °C until use. Small-RNA gel-blot analysis of 5 µg total RNA was performed as described previously (Talmor-Neiman *et al.*, 2006). For the detection of sly-miR164 and *U6* small nucleolar RNA, a radiolabeled oligo probe that is complementary to the corresponding small RNA was used. For the detection of the *SlNAM2* siRNAs, a 353-bp fragment from the 3' untranslated region (UTR) of *SlNAM2* was amplified by RT-PCR from tomato flower cDNA with the primers SlNAM2IR_ClaI-PstI_fwd and SlNAM2IR_HindIII-EcoRI_rev (all primer sequences are given in Table 1) and then cloned into pGEM-T Easy (Promega, Madison, WI, USA) so that it was in the antisense orientation relative to the T7 promoter. Then a radiolabeled RNA probe was transcribed using the RiboScribe T7 probe synthesis kit (Epicentre Biotechnologies, Madison, WI, USA) in the presence of [α-^{32}P]UTP.

B.3. Target prediction and validation by cleavage-site mapping

Sly-miR168 and sly-miR164 targets were predicted by psRNATarget (http://plantgrn.noble.org/psRNATarget/) (Dai and Zhao, 2011) against the current version of the publicly available genome [SGN ITAG release 2.3 predicted cDNA (SL2.40)]. For target validation, total RNA was extracted from tomato flowers as described above, and enriched for poly(A) mRNA using the Oligotex mRNA Mini Kit (Qiagen, Valencia, CA, USA). A modified procedure for RNA ligase-mediated rapid amplification of cDNA ends (5' RLM-RACE) was performed with the GeneRacer Kit (Invitrogen, Carlsbad, CA, USA) as described previously (Talmor-Neiman *et al.*, 2006). For validation of sly-miR168 targets, cDNA was amplified with the GeneRacer-5' primer and with SlAGO1-1_RACE/ SlAGO1-2_RACE primers, followed by nested PCR using GeneRacer-5'-nested primer and SlAGO1-1_RACE_nested/SlAGO1-2_RACE_nested primers, respectively. For validation of sly-miR164 targets, cDNA was amplified with the GeneRacer-5' primer and with SlNAM2_RACE, SlNAM3_RACE, SlNAC1_RACE and GOBLET_RACE primers, followed by nested PCR using GeneRacer-5'-nested primer and SlNAM2_RACE_nested, SlNAM3_RACE_nested, SlNAC1_RACE_nested and GOBLET_RACE_nested primers, respectively. The PCR conditions used for both amplification steps were as recommended by the manufacturer. The amplified products were gel-purified, cloned into pGEMT-easy vector (Promega) and sequenced. For transgenic *SlNAM2*, total RNA was extracted from young tomato leaves as described above, and 6 µg DNA-free total RNA was used to produce the RLM-RACE cDNA. The cDNA was subjected to amplification procedure with the GeneRacer-5' primer and the transgene-specific primer OCS_rev followed by nested PCR with primer pair GeneRacer-5'-nested and SlNAM2_RACE_nested. Amplification of the intact transgenic transcript was performed by RT-PCR with the primer SlNAM2_Exon_557_fwd found upstream of the sly-miR164 cleavage site and OCS_rev.

B.4. Plasmids constructions

For the reporter construct P0HA [P0 C-terminally fused to a hemagglutinin (HA) tag], the coding region of BWYV P0 was PCR-amplified with primers

BWYV_P0_SalI_fwd, which contains a *Sal*I site at the 5' end, and BWYV_P0_BamHI-HA_rev, which contains a *Bam*HI site, a stop codon and 27 bp encoding YPYDVPDYA HA tag. After sequence verification, the amplified fragment was cloned into the *Sal*I/*Bam*HI sites of the OP-TATA-BJ36 shuttle vector between an *OP* array (Moore *et al.*, 1998) and *Agrobacterium tumefaciens* octopine synthase terminator (OCS) to generate OP-P0HA. The *Not*I fragment of the OP-P0HA vector was then mobilized into the binary vector pART27 (Gleave, 1992) to generate pART27-OP:P0HA. For the pART27-35S:3xFLAG-SlAGO1-1 construct, the coding region of SlAGO1-1 was PCR-amplified from tomato flower cDNA with the primers FLAG_SlAGO1-1_XhoI_fwd, which contains a *Xho*I site at its 5' end, a start codon and 24 bp encoding DYKDDDDK FLAG tag and SlAGO1-1_XhoI_rev, which contains a *Xho*I site at its 3' end. The amplified fragments were cloned into the *Xho*I site of the OP-TATA-BJ36 vector which served as a template for a second PCR with primers 3XFLAG_XhoI_fwd, which contains a *Xho*I site at its 5' end, a start codon and 66 bp encoding DYKDHDGDYKDHDIDYKDDDDK 3XFLAG tag, and SlAGO1-1_XhoI_rev. The amplified fragment was cloned into the *Xho*I site of the pART7(Gleave, 1992) shuttle vector to generate pART7-35S:3xFLAG-SlAGO1-1. After sequence verification, the *Not*I fragment of the pART7-35S:3xFLAG-SlAGO1-1 vector was mobilized into the binary vector pART27 to generate pART27-35S:3xFLAG-SlAGO1-1. A similar strategy was used to generate the pART27-35S:3xFLAG-SlAGO1-2 construct except that FLAG_SlAGO1-2_XhoI_fwd and SlAGO1-2_KpnI_rev primers were used for the first PCR amplification and 3XFLAG_XhoI_fwd and SlAGO1-2_KpnI_rev for the second PCR amplification. For the *SlNAM2* reporter construct, the coding region of *SlNAM2* was cloned by RT-PCR from the flower cDNA with the primers XhoI-U218896_fwd and BamHI-U218896_rev, which contained *Xho*I and *Bam*HI sites at their 5’ ends, respectively. The amplified fragment was restricted with *Xho*I/*Bam*HI and cloned into the respective sites of the OP-TATA-BJ36 shuttle vector between an *OP* array and OCS terminator to generate OP:SlNAM2. To generate OP:mSlNAM2, six silent mutations in the *SlNAM2* sly-miR164 target site were inserted using two-step PCR mutagenesis. Firstly, the 164-mutant-target_fwd and 164-mutant-target_rev primers were used in conjunction with BamHI-U218896_rev and XhoI-U218896_fwd, respectively, to insert six substitutions (lowercase letters in Table 1) into the *SlNAM2*-coding region. Then, the amplified products were assembled by using them as a template for PCR

with the primer pair XhoI-U218896_fwd and BamHI-U218896_rev. The amplified fragment was restricted with *Bam*HI/*Xho*I and cloned into the identical sites of OP:SlNAM2, replacing the respective wild-type *SlNAM2* fragment to generate OP:mSlNAM2. Following sequence validation, the *Not*I fragments of OP:SlNAM2 and OP:mSlNAM2 were mobilized into the pART27 binary vector to generate pART27-OP:SlNAM2 and pART27-OP:mSlNAM2, respectively. For the SlNAM2 RNA interference (RNAi) reporter construct, a 353-bp fragment from the 3' UTR of *SlNAM2* was cloned by RT-PCR from the flower cDNA with the primers SlNAM2IR_ClaI-PstI_fwd and SlNAM2IR_HindIII-EcoRI_rev, each containing two indicated restriction sites at their 5' end. The amplified fragment was restricted with either *Pst*I/*Eco*RI or *Cla*I/*Hind*III and cloned in sense and antisense orientation, respectively, around the first intron of the *Arabidopsis thaliana AKT1* gene to generate max2intpFLAP-SlNAM2IR. Following sequence validation, the *Xho*I fragment of the max2intpFLAP- SlNAM2IR was mobilized into the *Xho*I site of the OP-TATA-BJ36 shuttle vector to generate OP:SlNAM2IR. Following orientation validation, the *Not*I fragment of the OP:SlNAM2IR vector was mobilized into the binary vector pART27 to generate pART27-OP:SlNAM2IR. For the pART27-35S:GFP-SlNAM2_3'UTR, a 353-bp fragment from the 3' UTR of *SlNAM2* that was used for the RNAi construct was cloned by RT-PCR from the flower cDNA with the primers SlNAM2IR_ClaI-PstI_fwd and SlNAM2IR_HindIII-EcoRI_rev and cloned into the *Cla*I/*Hind*III sites of the pART7-GFP shuttle vector to generate C-terminal (pART7-35S:GFP-SlNAM2_3'UTR) translational fusion with GFP under the control of the cauliflower mosaic virus (CaMV) 35S promoter and OCS terminator. The *Not*I fragment of pART7-35S:GFP-SlNAM2_3'UTR was mobilized into the binary vector pART27 to generate pART27-35S:GFP-SlNAM2_3'UTR.

B.5. Agroinfiltration of Nicotiana benthamiana leaves

Agrobacterium strain GV3101 cultures harboring the binary plasmids (for validating SlAGO1s decaying by P0HA: pART27-OP:P0HA, pART27-35S:LhG4, pART27-35S:3xFLAG-SlAGO1-1, and pART27-35S:3xFLAG-SlAGO1-2 and for validating the downregulation of *SlNAM2* by SlNAM2IR: pART27-OP:mSlNAM2, pART27-35S:LhG4, pART27-35S:GFP-SlNAM2_3'UTR and pART27-OP:SlNAM2IR) were mixed as indicated to a final A_{600} of 0.4 and infiltrated into young leaves of 3-week-

old greenhouse-grown *Nicotiana* plants as described previously (Arazi *et al.*, 2005). For Western blot analysis, leaf patches were collected 4 days post-infiltration.

B.6. Protein extraction and western blot analysis

Total protein extracts were prepared from 100 mg of 3-week-old tomato seedlings or from 100 mg *Nicotiana* leaf patches that were ground in 300 µl ESB buffer (75 mM Tris-HCl pH 6.8, 9 M urea, 4.5% v/v SDS, 7.5% v/v β-mercaptoethanol). The mixtures were boiled for 10 min and immediately cooled on ice. The cooled homogenates were centrifuged for 10 min at 10,000 x *g* and the supernatants were transferred to a new tube, quantified using the Qubit Protein Assay Kit (Invitrogen) and equalized with ESB buffer. After equalization, the extracts were mixed with the appropriate volume of 4X SDS-PAGE loading buffer. Equal volumes of total protein extracts were then fractioned by SDS-PAGE on a 12, 8 or 6% polyacrylamide gel for detection of P0HA/GFP, 3XFLAG-SlAGO1 and SlAGO1s, respectively. The fractionated proteins were electroblotted onto BioTrace NT membranes (Pall, Pensacola, FL, USA) and probed with commercial rabbit anti-HA (Santa-Cruz Biotechnology, Santa Cruz, CA, USA) (1:2,000) polyclonal antibodies or mouse anti-FLAG (Sigma-Aldrich, Rehovot, Israel) (1:2,000) monoclonal antibodies, or commercial rabbit anti-AtAGO1 polyclonal antibodies (Agrisera, Vannes, Sweden) (1:2,000), or commercial mouse anti-GFP (Santa-Cruz Biotechnology) (1:2,000) monoclonal antibodies. Antibody–protein interactions were visualized using enhanced chemiluminescence detection (ECL) kit SuperSignal west fempto (Thermo, Rockford, IL, USA) according to the manufacturer's instructions.

B.7. Transformation of tomato plants

The binary vectors pART27-OP:P0HA, pART27-OP:SlNAM2, pART27-OP:mSlNAM2 and pART27-OP:SlNAM2IR were transformed into tomato cv. M82 as described previously (Stav *et al.*, 2010). Transgenic progeny were selected by germinating sterile seeds on selective medium (1X MS medium, 3% w/v sucrose, 100 mg/l kanamycin), where only transgenic seedlings developed a branched root system. Further validation was performed by PCR of genomic DNA with the primer pair BWYV_P0_SalI_fwd and BWYV_P0_BamHI-HA_rev to detect the *OP:P0HA*

transgene and with the primer pairs OCS_rev and SlNAM2_miR164_target_fwd or SlNAM2_mMiR164_target_fwd to detect the *OP:SlNAM2* and *OP:mSlNAM2* transgenes, respectively and with the primer pair pFlap_intron_fwd and SLNAM2IR_ClaI-PstI_fwd to detect the *OP:SlNAM2IR* transgene. The *35S:LhG4* transgene was detected by pART7-35S_fwd and LhG4_156_rev primers.

B.8. Real-time quantitative RT-PCR analyses

Total RNA was extracted from the tested tissues as described above. Total RNA samples were treated with RNase-free DNase (Fermentas Life Sciences, Vilnius, Lithuania) to eliminate genomic DNA contamination. The concentration and integrity of the RNA samples were determined by ND1000 spectrophotometer (Nanodrop Technologies, Montchanin, DE, USA) and by gel analysis, respectively. First-strand cDNA was synthesized from 2–2.4 µg of total RNA using the Superscript first-strand synthesis system for RT-PCR kit and an oligo(dT) primer (Invitrogen) following the manufacturer's instructions. An RT-negative control was used to ensure the absence of genomic DNA template in the samples. For real-time quantitative PCR, 4 µl of diluted cDNA was used in a 10 µl PCR containing 200 nM of each primer and 5 µl Platinum SYBR Green qPCR SuperMix-UDG (Invitrogen). To ensure the specificity of the amplified fragment, the amplicons were verified by sequencing. Furthermore, at the end of each PCR run, the melting temperature of the product was determined to verify the specificity of the amplified fragment. PCR products were analyzed using Rotor Gene Series 6000 software version 1.7 (Qiagen). Two to three independent biological replicates were used for each sample (as indicated), and quantifications were performed in triplicate. The relative expression levels of *SlARF10*, *SlAP2*, *SlREV*, *SlSCL* and *SlSPL6* transcripts were calculated using the $2^{-\Delta\Delta Ct}$ method normalized to *TIP41* as a reference gene; the relative expression levels of *GOBLET*, *SlNAC1*, *SlNAM2* and *SlNAM3* mRNA were calculated using a two-standard curve method normalized to *TIP41* as a reference gene.

B.9. Scanning electron microscopy (SEM), histology, confocal microscopy

The pattern of Red Fluorescent Protein (RFP) expression was detected by visualization of fresh tissue in an Olympus IX81/FV500 laser-scanning confocal

microscope (Olympus Corporation, Tokyo, Japan). For the RFP signal, a 543-nm laser line was used and emission was collected with a BA560IF filter. For chlorophyll autofluorescence, a BA660IF filter was used. For SEM analysis, various tissues were collected and placed in FAA (3.7% formaldehyde, 5% acetic acid, 50% EtOH, by volume) solution until use. Then the FAA was removed and tissues were washed in an increasing gradient of ethanol (50, 70, 80, 90, 95, and 100%). Fixed tissues were critical-point-dried, mounted on a copper plate and gold-coated. Samples were viewed in a Jeol JSM-5610 LV microscope (JEOL Ltd, Tokyo, Japan). For histological analyses, tissues were fixed in FAA until use, then dehydrated in increasing concentrations of ethanol, cleared with histoclear and embedded in paraffin. Sections cut by microtome to 10-µm thickness were placed on microscope slides, and stained with 1% (w/v) Safranin followed by 0.2% (w/v) Fast Green. Slides were examined under bright-field using a Leica light microscope equipped with a camera.

B.10. GUS histochemical analysis

GUS assay was performed according to(Jefferson *et al.*, 1987). Briefly, shortly after harvesting, tomato inflorescences were vacuum-infiltrated for 5 min with GUS assay buffer (1.916 mM X-Gluc, 50 mM $NaPO_4$ buffer pH 7.0, 0.1 mM $K_3Fe(CN)_6$, 0.1 mM $K_4Fe(CN)_6$, 1 mM EDTA, 20% methanol) and then incubated overnight at 37 °C. Tissues were washed in an increasing gradient of ethanol (50, 70, 80, 90, 95, and 100%) for removal of GUS solution and bleaching. Samples were kept in 100% ethanol.

B.11. In-situ hybridization

For the *in-situ* probe, the PCR-amplified SlNAM2 3' UTR fragment, which was used as siRNA probe, was used as a template for *in-vitro* transcription of an antisense cRNA probe with digoxigenin-11-UTP (Roche, Manneim, Germany) using AmpliScribe T7 High Yield Transcription Kit (Epicentre Biotechnologies) according to the manufacturer's protocol. Tomato buds were fixed in FAA, gradually transferred to ethanol and then to K-clear plus (Kaltek, Padova, Italy), and embedded in Paraplast Plus (LaicaBiosystems, Peterborough, UK). Eight-micrometer-thick tissue sections were produced and mounted on Probe On^{TM}Plus slides (Thermo). Slides were treated successively with K-clear plus, an ethanol series, Diethylpyrocarbonate treated double

distilled water, 2 X SSC, Proteinase K (1 µg/mL) in 100 mM Tris-HCl, pH 8.0, and 50 mM EDTA at 37°C, Glycine (2 mg/ml) in PBS, two times with PBS, 4% paraformaldehyde in PBS, two times with PBS, triethanolamine (0.1 M, with stirring), two times with PBS, and increasing ethanol series up to 100% ethanol. For hybridization, slides were incubated with sense or antisense cRNA probes in hybridization buffer (0.3 M NaCl, 10 mM Tris-HCl, pH 8, 10 mM sodium phosphate buffer pH 6.8, 5 mM EDTA, 50% v/v deionized formamide, 10% w/v dextran sulfate, 1 x Denhardt's solution, 200 µg tRNA) overnight at 52°C. Following hybridization, slides were washed successively three times with 0.2 × SSC at 55°C, two times with NTE (0.5 M NaCl, 10 mM Tris-HCl, pH 7.5, and 1 mM EDTA) at 37°C, RNase A (20 µg/ml) in NTE, two times in NTE, and stayed overnight at 4°C in 0.2 x SSC. On the third day, slides were blocked with 1% fresh Boehringer block (Roche) in 100 mM Tris-HCl, pH 7.5, and 150 mM NaCl, and then with 1% BSA solution (1% BSA, 100 mM Tris-HCl, pH 7.5, 150 mM NaCl, and 0.3% Triton X-100). Blocked slides were incubated with anti-digoxigenin antibodies (Roche) for 2 h at room temperature and then washed four times with 1% BSA solution and three times with detection buffer (100 mM Tris-HCl, pH 9.5, and 100 mM NaCl). Then slides were incubated with NBT/BCIP color development substrate (Promega) for 24 hours and then washed with double distilled water followed by increasing ethanol series and then mounted and analyzed.

B.12. Table 1: Primers used in this study

Primer ID	**Primer sequence (5' – 3')[abcd]**
GeneRacer-5'	CGACTGGAGCACGAGGACACTGA
GeneRacer-5'-nested	GGACACTGACATGGACTGAAGGAGTA
SlAGO1-1_RACE	GAAGTGGAAACCTCATTGACTTGCTCGATACA
SlAGO1-2_RACE	CCCTGGACGCAGCGGAAACTTTAGTG
SlNAM2_RACE	GCAAATTCCTTAGCGTTGCGGGATCTTGTAT
SlNAM3_RACE	TCAGCAACTCCAGAGACAATCAAGACCCTGTA
SlNAC1_RACE	TCACACGTAGAGGATGTTGCAGTGGCATT
GOBLET_RACE	TTTCTGAGTCTCCGGCACGGTCCAATTA
SlAGO1-1_RACE_nested	GGCTGAGATGAGGAGCCAGCCTCTGAGTA
SlAGO1-2_RACE_nested	CATGGATGTGTCAGCTGGTCTTCCACAAGTA
SlNAM2_RACE_nested	TGGTTCCAGGTGAACGAAGTCGGAAGA
SlNAM3_RACE_nested	TGAAGGATCTTGAACCCCAAATGAAGCTGGA
SlNAC1_RACE_nested	GTATGCGGTAGATCCGATGGCGGTTG

GOBLET_RACE_nested	CCGCCGGAGAATAACGGAAGCTGGA
BWYV_P0_SalI_fwd	CGCGTCGACATGGCCATGGAATTTCTCG
BWYV_P0_BamHI-HA_rev	CGGGATCC*TCA***GGCATAGTCAGGAACATCGTATGGGTA**TACAAACATTTCGGTGTAGACCGA
3XFLAG_XhoI_fwd	CCGCTCGAG*ATG***GACTACAAAGACCATGACGGTGATTATAAAGATCATGACATCGACTACAAGGATGACGATGACAAG**
FLAG_SlAGO1-1_XhoI_fwd	CCGCTCGAG*ATG***GACTACAAGGATGACGATGACAAG**GTGCGGAAGAGGAGAACTGATG
SlAGO1-1_XhoI_rev	CCGCTCGAGCTAACAATAGAACATCACCCTTTTG
FLAG_SlAGO1-2_XhoI_fwd	GTACCTCGAG*ATG***GACTACAAGGATGACGATGACAAG**GCGAGGAAGAGGAGAAGTGAGTTA
pART7-35S_fwd	AAACCTCCTCGGATTCCATT
LhG4_156_rev	CAACACGGTTCGGGATGTAGT
SlAGO1-2_KpnI_rev	GGGGTACCCCCTAGCAATAGAACATGACCCTC
OCS_rev	GAAACCGGCGGTAAGGATCT
SlNAM2_Exon_557_fwd	TCCTAAAACAGTAAAGAATGATTGG
XhoI-U218896_fwd	CCGCTCGAGGTTGTTTTTG*ATG*ATGATGGA
BamHI-U218896_rev	CGGGATCC*TCA*GTAAGTCCAGAAGCAATCAAGA
164-mutant-target_fwd	TAGCCACGTGCAtTGtTTtagtAATTATGTTACTACTCAAAAGAAT
164-mutant-target_rev	AATTactaAAaCAaTGCACGTGGCTAGGCGATGAAT
SlNAM2_miR164_target_fwd	CTGCTTCTCCAATTATGTTACTACTC
SlNAM2_mMiR164_target_fwd	TTGTTTTAGTAATTATGTTACTACTCAAAAGA
UBI3_rev	TCCCAAGGGTTGTCACATACATC
UBI3_fwd	AGAAGAAGACCTACACCAAGCC
SlNAM2IR_ClaI-PstI_fwd	CCATCGATTGCACTGCAGTGCAGATCTTGATTGCTTCTGGACTTACTG
SlNAM2IR_HindIII-EcoRI_rev	CCCAAGCTTGGGGGAATTCCGTAAGCCAACCAACCTGATCTC
miR164 probe	TGCACGTGCCCTGCTTCTCCA
U6 probe	AGGGGCCATGCTAATCTTCTC
pGEM-T7	TAATACGACTCACTATAGGG
pFlap_intron_fwd	AATTTCTTGTTTCCGATCCTCATA
qRT-SlARF10_fwd	CAGGTCCAGCAGTCCTTTCT
qRT-SlARF10_rev	CGCTGGAAACTTGGTGGTAA
qRT-SlAP2_fwd	GTTCTTCACAATGGCAATCCAAT
qRT-SlAP2_rev	TTCTGAGGACCAATTCTGAGGTC
qRT-SlNAM2_fwd	CCACCATTGACAGATTCATCG

qRT-SlNAM2_rev	GGTGAACGAAGTCGGAAGAG
qRT-GOBLET_fwd	TCGATTCCTCTCCGTATAGCAC
qRT-GOBLET_rev	GTCGAAGACAGAAGTTGGATCG
qRT-SlNAC1_fwd	CGACCAAACAAACCCTAACAAC
qRT-SlNAC1_rev	TGGTTAGGGGTGAAAATGGAG
qRT-SlNAM3_fwd	ACTGCTACTGCTTCGAAATCCA
qRT-SlNAM3_rev	TGAATGGAGCTATTTGGTTACAAGA
qRT-SlREV_fwd	AAACCTTGGCAGAGTTCCTTTCT
qRT-SlREV_rev	TCAGCAATCTTTGTTGGCTCTAA
qRT-SlSCL_fwd	CAACAACAAGCGATTATTGACCA
qRT-SlSCL_rev	GCAGCCCTATAGAAAGGCTTACC
qRT-SlSPL6_fwd	AAACAAGATCCGTCCAAAGTTCA
qRT-SlSPL6_rev	TTGGTGAAACGTCTGTTGAATTG
qRT-TIP41_fwd	ATGGAGTTTTTGAGTCTTCTGC
qRT-TIP41_rev	GCTGCGTTTCTGGCTTAGG

[a]Added restriction enzyme sites are underlined.

[b]lowercase letters indicate substituted nucleotides

[c]Italics letters indicate stop or start codon.

[d]Bold letters indicate TAG-coding sequence.

C. Results

C.1. Tomato encodes two AGO1 homologs that are sensitive to BWYV P0

The first objective of this work was to reveal processes and genes which are regulated by miRNAs during flower development. This can be done by profiling miRNA-pathway mutants (Nodine and Bartel, 2010) and VSRs transgenic plants (Jay *et al.*, 2011), which their phenotype is associated with upregulated levels of miRNA-target transcripts, as was demonstrated for *Arabidopsis*. However, up to date no tomato miRNA-pathway mutants have been described. AGO1 is a key component of miRNA as well as transgene and viral RNA-induced silencing complexes (RISCs) (Baumberger and Baulcombe, 2005). Consistent with that, *ago1* loss-of-function mutants have reduced miRNA levels and as a result miRNA target genes were upregulated and they exhibit severe developmental phenotypes (Bohmert *et al.*, 1998; Lynn *et al.*, 1999; Kidner and Martienssen, 2004, 2005). With this in mind, AGO1 was chosen as a target for interfering with the tomato miRNA pathway. To generate an *ago1*-loss-of-function mutant in tomato and interfere with its-miRNA pathway, the first step was to determine which AGO1-like proteins are encoded by the tomato genome. A BLASTP query of the current version of the publicly available genome [SGN ITAG release 2.3 predicted proteins (SL2.40)] with the *Arabidopsis* AGO1 protein sequence revealed two phylogenetically related ORFs which were 81% identical to each other and highly similar (>90%) to *benthamiana*AGO1-like proteins (Jones *et al.*, 2006). Accordingly, they were named SlAGO1-1 (Solyc06g072300) and SlAGO1-2 (Solyc03g098280) (Fig. 2A). *SlAGO1-1* and *SlAGO1-2* are predicted to encode 1054 aa (117 kDa) and 980 aa (109 kDa) proteins, respectively. Analysis of published RNA sequencing data (Tomato Genome Consortium, 2012) indicated that the transcripts of both are present in vegetative as well as in reproductive organs, with *SlAGO1-2* around 1.4- to 4.0-fold more abundant than *SlAGO1-1*. Moreover, their expression patterns were quite similar, supporting their functional redundancy (Fig. 2B). The *Arabidopsis AGO1* is guided to cleavage by ath-miR168 (Rhoades *et al.*, 2002) and this negative regulation is required for AGO1 homeostasis (Vaucheret *et al.*, 2006). Hence, the next question was whether *SlAGO1-1* and *SlAGO1-2* undergo miR168-guided cleavage. To identify the different members of the miR168 family in tomato, BLASTN with known miR168 sequences versus our tomato deep-sequenced

small RNA data set (Stav *et al.*, 2010) and the publicly available tomato small RNA sequences (Tomato Functional Genomics Database) revealed a single conserved 21-nt miR168 sequence (sly-miR168a) (Fig. 2C), which is encoded by two independent genomic loci that can fold into a pre-miRNA-like hairpin structure (Fig. 2D). In addition, the specific sly-miR168* strand encoded by each hairpin was identified in our small RNA data set, validating their functionality as sly-miR168a precursors (Fig. 2D). To confirm that *SlAGO1-1* and *SlAGO1-2* are subjected to sly-miR168a cleavage *in vivo*, mRNAs from flowers were isolated and followed by RLM-RACE analysis to detect their 3' cleavage products. A single 5' RACE product of the expected size was amplified for each and the sequence of several inserts revealed that their 5' ends all terminate at a position that pairs with the 10^{th} sly-miR168a nucleotide, thus indicating targeting by this miRNA (Fig. 2E).

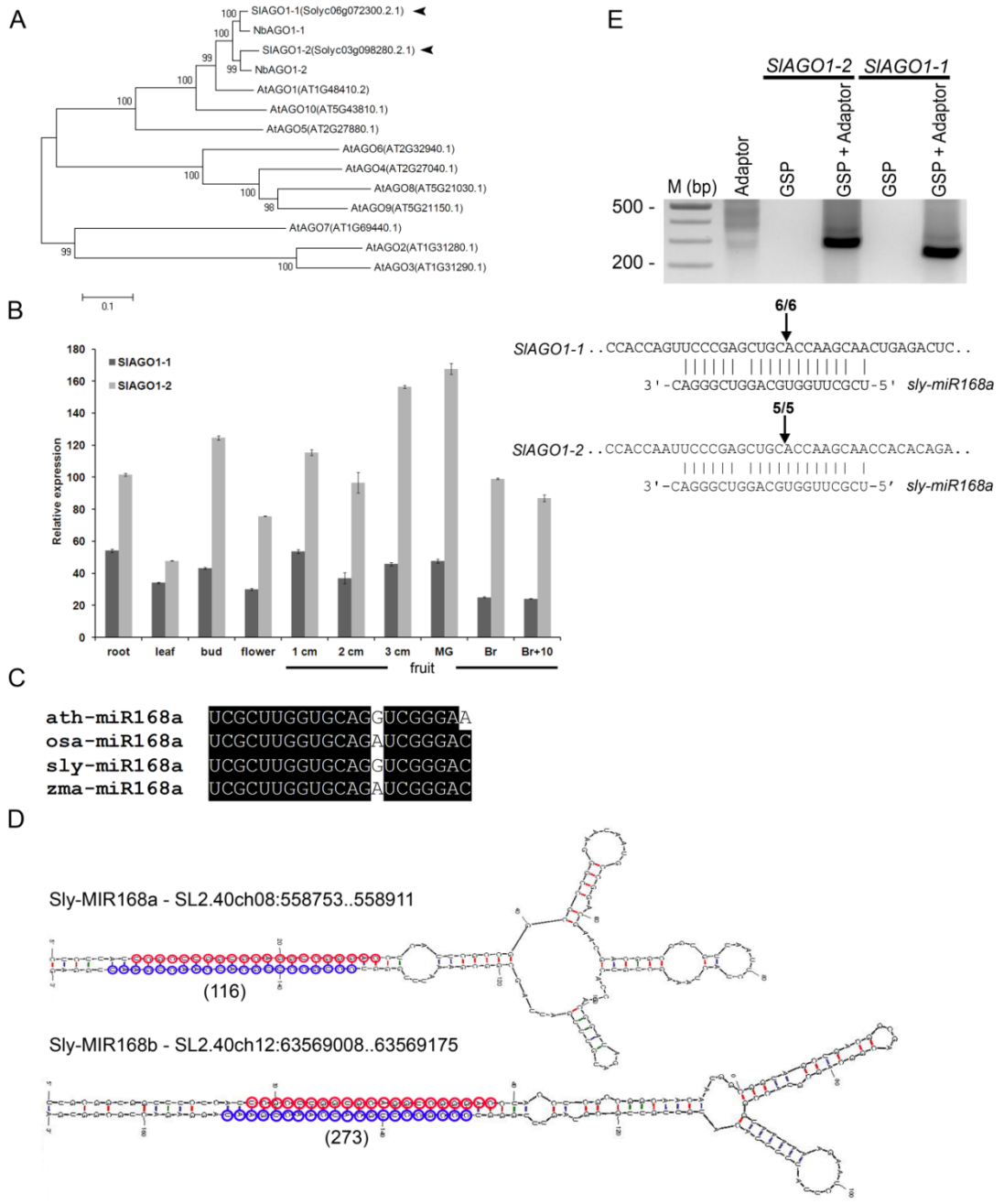

Fig. 2. The tomato *AGO1* homologs are targeted by sly-miR168a. (A) An unrooted phylogenetic tree based on the *Arabidopsis* AGO proteins and the tomato AGO1-like proteins (arrowheads) was constructed by the neighbor-joining method with 100 bootstrap sampling (MEGA program, version 4.0) (Tamura *et al.*, 2007) (B) Accumulation of SlAGO1s in different tissues of tomato cv. Heinz based on published RNA-seq data from (Tomato Genome Consortium, 2012). Data are means ± SE of normalized expression of two independent biological samples. MG – mature green; Br – breaker. (C) Nucleotide sequence alignment of *Arabidopsis* (ath), rice (osa), maize (zma) and tomato (sly) miR168 members. Identical nucleotides are shaded in black. (D) Hairpin secondary structures of sly-miR168 precursors. The position of each precursor in the tomato genome is indicated. Mature miR168 and matching miRNA* sequences are marked by red and blue circles, respectively, and the abundance of the miRNA* in our small RNA data set is indicated below. (E) Experimental validation of Sly-miR168 cleavage site in *SlAGO1-1* and *SlAGO1-2* mRNAs by RLM-RACE. Upper panel, ethidium bromide-stained agarose gel showing the 5' RACE products. The

GeneRacer 5’ primer (Adaptor) and SlAGO1 3’ primer (GSP) used for each RACE reaction are indicated above. Lower panel, alignment of sly-miR68 with their target mRNAs. The arrows and numbers indicate the positions of cleavage sites inferred from 5’ RACE and fraction of sequenced clones, respectively.

It has been suggested that the suppressor of silencing P0 prevents the assembly of small RNA-containing RISCs, resulting in the degradation of AGO1 (Baumberger *et al.*, 2007; Bortolamiol *et al.*, 2007; Csorba *et al.*, 2010). To test the sensitivity of the tomato AGO1-like proteins to P0, plasmids expressing FLAG-tagged SlAGO1-1 and SlAGO1-2 under the 35S promoter were agroinfiltrated into *benthamiana* leaves alone or together with a responder plasmid that, upon transactivation by *LhG4* (Moore *et al.*, 1998), expresses P0HA. In addition, a driver plasmid constitutively expressing *LhG4* was included in all samples (Fig. 3A). Four days post-infiltration, the expression levels of 3xFLAG-SlAGO1-1/2 and P0HA proteins were analyzed by immunoblotting. This analysis indicate that the level of each 3xFLAG-SlAGO1 protein was significantly lowered in leaf extracts that co-expressed P0HA compared to control extracts that did not express P0HA, demonstrating that SlAGO1-1 and SlAGO1-2 are sensitive to P0-mediated destabilization (Fig. 3B). As *SlAGO1-1/2* and *AtAGO1* transcripts are cleaved by miR168 and encode similar protein products that are destabilized in the presence of P0, it is likely that these genes are homologs.

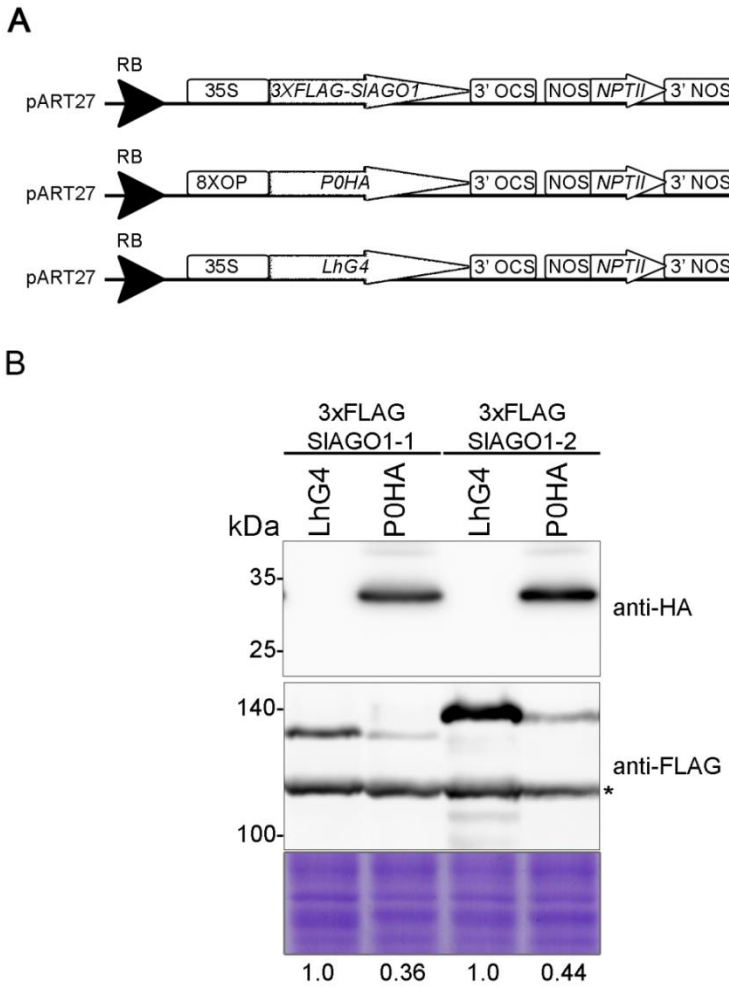

Fig. 3. SlAGO1-1 and SlAGO1-2 are destabilized in the presence of P0HA. (A) Schematic representation of the binary plasmids used in b. (B) *benthamiana* leaves were infiltrated with *Agrobacterium* mixtures harboring the indicated pART27-35S:3xFLAG-SlAGO1 plasmid and the driver plasmid pART27-35S:LhG4 with (P0HA) or without (LhG4) bacteria harboring the P0HA responder plasmid (pART27-pOp-P0HA), and protein samples were taken 4 days post-infiltration. P0HA (upper panel) and 3x-FLAG-SlAGO1 proteins (lower panel) were detected by Western blotting in 5.7 µg total protein extract probed with anti-HA and anti-FLAG commercial antibodies, respectively. 3xFLAG-SlAGO1-1 and 3xFLAG-SlAGO1-2 expression was normalized to an anti-FLAG cross-reacting band (marked by * and levels are indicated at the bottom) that together with Coomassie Blue staining served as a loading control. The positions of molecular-mass standards (kDa) are indicated on the left.

C.2. Constitutive expression of P0HA arrests seedling growth and increases levels of certain miRNA-targeted mRNAs

The sensitivity of both SlAGO1s to P0 suggested a potential strategy to downregulate both proteins *in planta* by stable expression of P0HA, thereby revealing developmental processes that depend on AGO1-mediated silencing in tomato. Nevertheless, it has been shown that strong expression of P0 arrests transgenic

seedling growth (Bortolamiol *et al.*, 2007). Thus, to stably express P0 in tomato while preventing its possible lethality during transgenic explant regeneration, the two-component OP/LhG4 transactivation system (Moore *et al.*, 1998) was used. Seven independent transgenic tomato plants were regenerated and examined for the presence of the *OP:P0HA* responder transgene using PCR and genomic DNA (Fig. 4). A homozygous responder line *OP:P0HA-16*, which drove strong P0HA expression upon activation, was then selected for further use (data not shown).

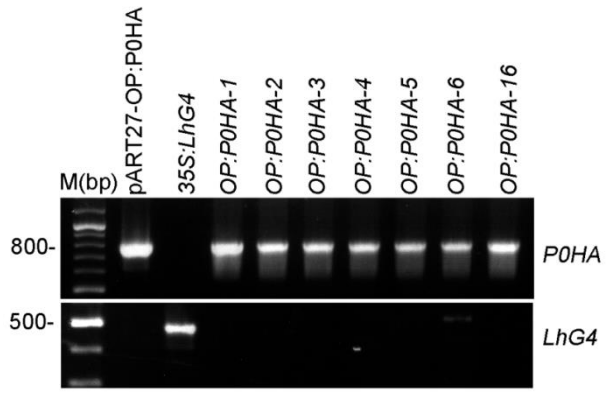

Fig. 4. Transgenic plant validation. Genomic DNA PCR analysis of representative tomato *OP:P0HA* reporter lines and *35S:LhG4* driver line. Specificity of primers used is indicated on the right.

To test the effect of constitutive expression of *P0HA* on tomato, the *OP:P0HA-16* (henceforth be called *OP:P0HA*) plants were crossed (>>) with a *35S:LhG4* driver line in which the *LhG4* transgene is under the control of the strong constitutive *35S* promoter (Fig. 3A, 4). Phenotypic analysis of the *OP:P0HA* responder line indicated that its growth and development are identical to that of the parental M82 tomato (data not shown). In contrast, all the *35S>>P0HA* F1 progeny displayed pleiotropic developmental phenotypes. These included lagging germination, crooked hypocotyls and abnormal-looking succulent hairy cotyledons (Fig. 5A-F). In addition, their development was arrested at the true leaf primordium stage (Fig. 5G-H) and 4 weeks post-germination, they shriveled up and died, reminiscent of the phenotype of the *Arabidopsis 35S:P0* seedlings that lack a functional AGO1 due to strong expression of P0 (Bortolamiol *et al.*, 2007). In agreement, Western blot analysis showed that the P0HA protein accumulates and a specific anti-AtAGO1 cross-reacting ~137 kDa protein band, most likely representing both SlAGO1s, decreases in the abnormal *35S>>P0HA* seedlings (Fig. 5I). In *Arabidopsis*, downregulation of AGO1 by P0

differentially modifies the levels of miRNA-target transcripts (Bortolamiol *et al.*, 2007). Consistent with this, six miRNAs which have known functions in *Arabidopsis* flower development were chosen, and their putative miRNA-target genes level were determined. Quantification of those miRNA-target mRNAs in *35S>>P0HA* versus control seedlings revealed significant upregulation of certain putative targets (*SlARF10, SlSPL6, Solyc03g115850*), whereas the levels of others (*SlAP2, SlREV, SlSCL*) were not different from controls (Fig. 5J). The pleiotropic developmental phenotypes, lethality, destabilization of SlAGO1 proteins and elevated accumulation of miRNA-target mRNAs, strongly suggested that P0HA perturbs the SlAGO1-mediated silencing pathways in *35S>>P0HA* seedlings.

C.3. Stage-specific expression of P0HA differentially affects compound leaf development

The severe growth arrest phenotype of the *35S>>P0HA* seedlings hampered further analysis of the effects of SlAGO1 downregulation on tomato development beyond germination (Fig. 5). To validate that the P0HA system is sensitive enough and can interfere with the miRNA pathway when expressed under less potent and tissue specific promoters, several tissue-specific driver lines (promoter*:LhG4*) which have been previously characterized and provide different temporal and/or spatial specificities were chosen for further investigation (Alvarez *et al.*, 2006; Shalit *et al.*, 2009; Shani *et al.*, 2009; Fernandez *et al.*, 2009). Therefore, the requirement of AGO1-mediated silencing for the different phases of compound leaf development was studied by crossing the *OP:P0HA* responder line to *FIL:LhG4*, *BLS:LhG4* and *650:LhG4* driver lines, which have been shown to drive comparable expression in different developmental windows and at distinct locations of the leaf primordium (Shani *et al.*, 2009). The *FIL* (*FILAMENTOUSFLOWER*) promoter drives expression throughout young leaf primordia soon after they initiate from the SAM, but not in the SAM (Lifschitz *et al.*, 2006; Shani *et al.*, 2009). Both *BLS* and *650* promoters initiate expression later than *FIL* (starting from the P4 stage) and drive comparable expression in initiating leaflets, and distal and abaxial domains of the P5 primordia, respectively (Shani *et al.*, 2009). Upon germination, the effect of *P0HA* expression was notable on *FIL>>P0HA* and *650>>P0HA* cotyledons. The *FIL>>P0HA* cotyledons were slightly epinastic, and the *650>>P0HA* cotyledons were reddish,

particularly along the mid vein and on the abaxial side (Fig. 6). No obvious phenotypes were observed among *BLS>>P0HA* cotyledons.

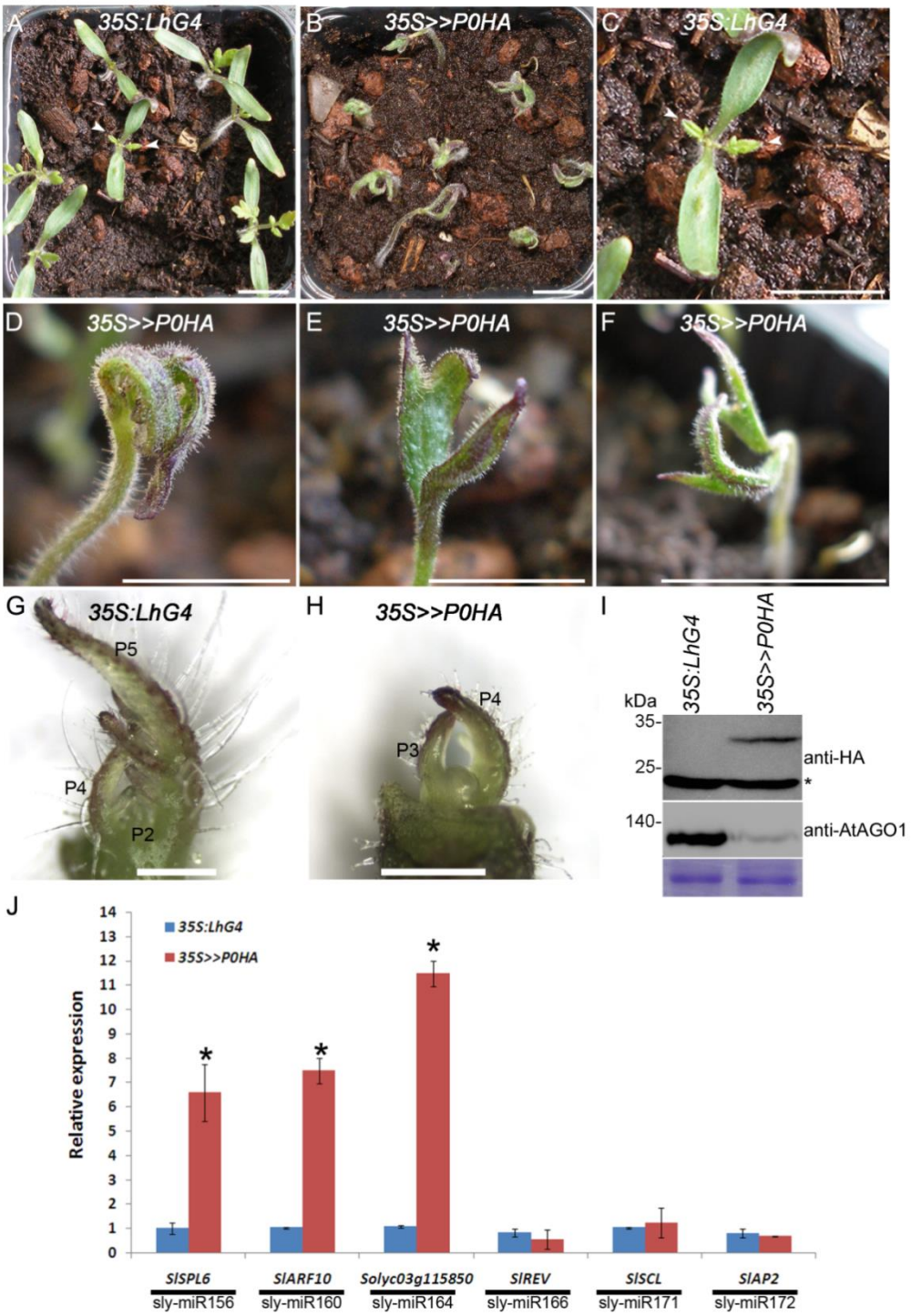

Fig. 5. Phenotypic and molecular characterization of *35S>>P0HA* seedlings. (A-F) Phenotypes of representative control (*35S:LhG4*) and 35S>>P0HA 3-week-old seedlings. Arrowheads indicate the first true leaves. Scale bars = 1 cm. (G,H) Control (*35S:LhG4*) and 35S>>P0HA shoot apices. Scale bars = 500 µm. (J) Quantitative RT-PCR analysis of miRNA-target transcripts in 12-day-old seedlings of the indicated genotypes. Primers were designed around the corresponding miRNA's complementary site. *TIP41* expression values were used for normalization. Data are means ± SE of two biological replicates, each

measured in triplicate. Asterisks indicate statistically significant difference as determined by Student's *t* test ($P \leq 0.05$).

Fig. 6. Effects of leaf-specific P0HA expression on cotyledon development. Control (*FIL:LhG4*) and P0HA-expressing genotypes are indicated. Scale bar = 5 mm.

In comparison to the control plants, *FIL>>P0HA* plants produced abnormal compound leaves with irregularly arranged leaflets along the rachis that had strap- or filament-like shapes (Fig. 7A), reminiscent of the tentacle-like bladeless leaves of *Arabidopsis ago1-3* (Bohmert *et al.*, 1998). This contrasts with *BLS>>P0HA* and *650>>P0HA* leaves which showed only slight deviation from the wild-type phenotype. The *BLS>>P0HA* leaflet blades had a wrinkled instead of smooth surface with patches of dark and pale green, and the *650>>P0HA* leaf vasculature had a clear reddish color (Fig. 7A).

To determine the basis for the *FIL>>P0HA* leaf phenotype, a comparison was made between the control and *FIL>>P0HA* leaves of early developmental stages. As shown in Fig. 7B, starting from the P2–P3 stage primordia, a pronounced alteration in *FIL>>P0HA* primordium morphology was observed, being smaller than the control primordia. At the P4 stage, initiating primary leaflets showed changeable growth orientations, uncovering the reason for the irregular leaflet arrangement observed in mature *FIL>>P0HA* leaves. At the P6 stage, the primary leaflets were abnormally flattened and developed cylinder-like appendages on their abaxial side that later grew into tentacle-like filaments (Fig. 7B). Quantitative RT-PCR analysis of *FIL>>P0HA* apices demonstrated a significant increase in selected miRNA-target transcripts, an indication for SlAGO1s downregulation (Fig. 7E). On the other hand, in young *BLS>>P0HA* and *650>>P0HA* leaves, which initiate P0HA expression later than *FIL>>P0HA*, no deviating phenotypes were observed in the P1–P5 stage leaf primordia (data not shown). The adaxial-abaxial polarity in the *FIL>>P0HA* and *BLS>>P0HA* leaflets was also investigated. The adaxial epidermis of the wild-type smooth terminal leaflet blade (here represented by *FIL:LhG4*) was characterized by

relatively uniform pavement cells, and the abaxial epidermis was characterized by diverse size pavement cells interspersed with stomatal cells (Fig. 7C).

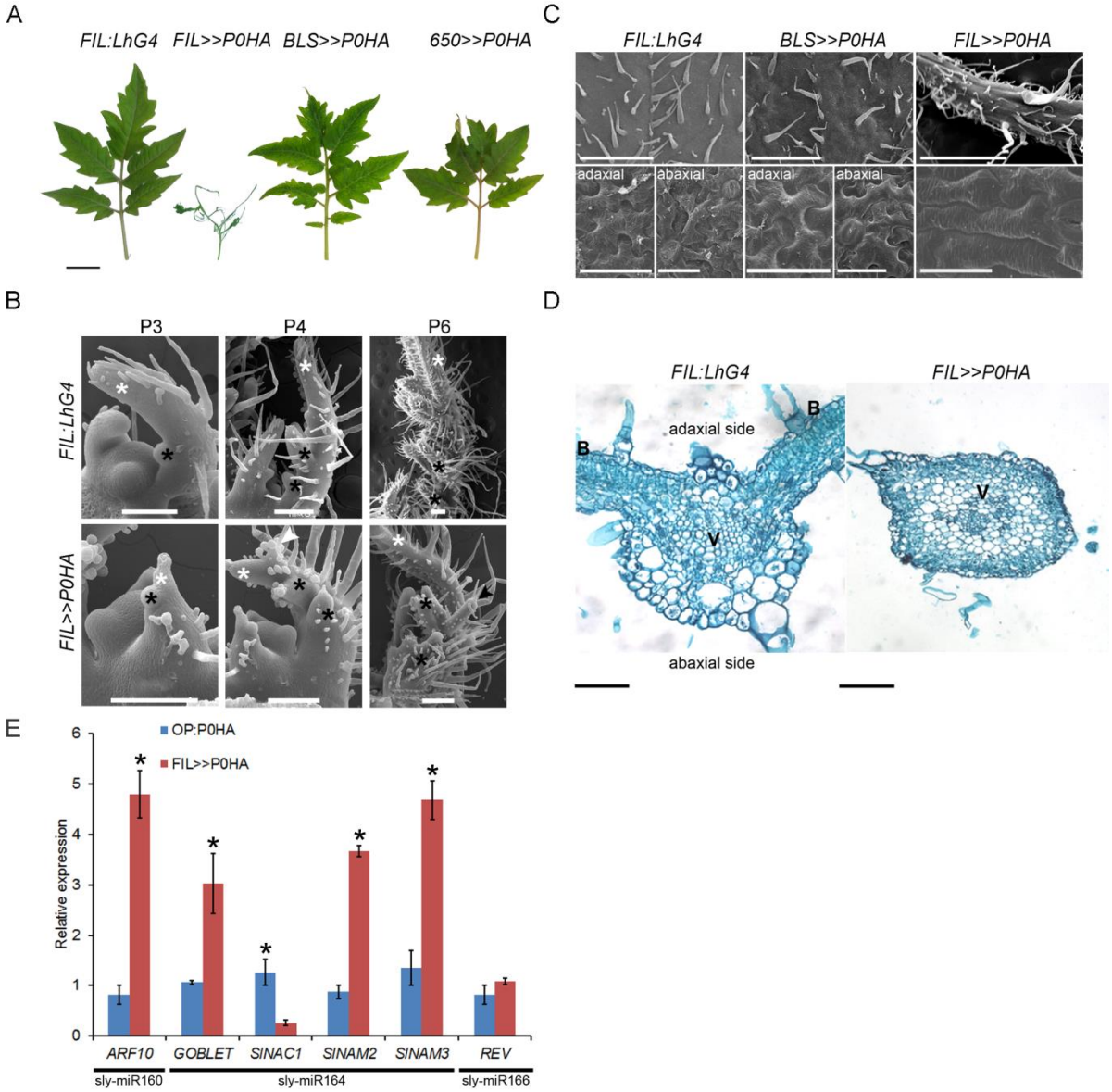

Fig. 7. Phenotypic and molecular characterization of control (*FIL:LhG4*) and indicated genotype leaves. (A) Representative fully expanded 3rd leaf. Scale bar = 2 cm. (B) Comparison of representative P2–P6 stages of early leaf development between control and *FIL>>P0HA* plants. Note the ectopic outgrowth on the abaxial side of the leaflets (arrowhead). The terminal and primary leaflets are indicated by white and black asterisks, respectively. Scale bars = 200 µm. (C) An emerging 3rd leaf's terminal leaflet blade epidermal patterns. Upper panel, global view of the adaxial blade surface around the midvein. Scale bars = 1 mm. Lower panel, magnified views of the abaxial and adaxial blade surfaces around the midvein. Scale bars = 25 µm. (D) Light micrographs of transverse sections of fully expanded 3rd leaf terminal leaflet of the indicated genotypes. V – vascular bundle; B – blade. Scale bars = 100 µm. (E) QRT-PCR analysis of selected miRNA-target transcripts from the indicated genotypes in apices collected from a 1-month-old seedling. Primers were designed around the corresponding miRNA complementary site. *TIP41* expression values were used for

normalization. Data are means ± SE of two biological replicates, each measured in triplicate. Asterisks indicate statistically significant difference compared to control as determined by Student's *t* test ($P \leq 0.05$)

The *BLS>>P0HA* terminal leaflets had a wrinkly instead of smooth blade that was covered with adaxial and abaxial epidermal pavement cells that differed slightly from the wild type (Fig. 7C). In contrast, the epidermal surface of the *FIL>>P0HA* cylindrical leaflets was not composed of either adaxial or abaxial pavement cells but instead of long rectangular epidermal cells that could not be characterized as adaxial or abaxial (Fig. 7C). A similar epidermal cell phenotype has been previously observed in *Arabidopsis ago1-3* null mutant cotyledons showing reduced adaxial/abaxial differentiation (Bohmert *et al.*, 1998). Indeed, transverse sections through the *FIL>>P0HA* leaflets revealed an almost radial structure (Fig. 7D). These leaflets were composed of abnormal vasculature surrounded by uniform parenchyma, mesophyll and epidermal cells, indicating loss of adaxial/abaxial identity, most probably due to SlAGO1 downregulation by P0HA.

C.4. Flower-specific expression of P0HA disturbs organogenesis and induces radialization of petals and anthers

Wild-type M82 tomato flowers are composed of four distinct whorls. The perianth contains five or six sepals alternating with five or six yellow petals. The two inner reproductive whorls contain five or six yellow stamens forming a cone, which encloses two fused carpels that develop a multilocular ovary and a protruding style and stigma. To expose the developmental processes that require miRNAs regulation during tomato flower development, *OP:P0HA* plants were crossed with *AP1:LhG4* and *AP3:LhG4* driver lines that express *LhG4* through the well-characterized *Arabidopsis APETALA1* (*AP1*) and *APETALA3*(*AP3*) flower-specific promoters (Jack *et al.*, 1992; Mandel *et al.*, 1992). First, the detailed expression patterns directed by these promoters in developing tomato flowers were studied by crosses with *OP:mRFP* (Shani *et al.*, 2009) and *OP:GUS* (Lifschitz *et al.*, 2006) reporter lines. As shown in Fig. 8, the expression domains of all promoters were quite similar to their known expression in the *Arabidopsis* flower (Jack *et al.*, 1992; Mandel *et al.*, 1992). The *AP1* promoter was initially expressed throughout young floral primordia (Fig. 8B, C), in accordance with its function as a floral meristem identity gene (Mandel *et*

al., 1992). As the buds developed, mRFP expression directed by *AP1* was mainly confined to the developing sepals and petals (Fig. 8F,I), in accordance with its function in specifying the identity of these organs (Mandel *et al.*, 1992). In addition, weak mRFP signal in the receptacle and distal part of the three inner whorls was detected. In young floral primordia, the more restricted *AP3* promoter showed specific mRFP expression in the distal part of developing sepals (Fig. 8D). In more developed buds, the mRFP signal was detected on the adaxial side of sepals, throughout the developing petals (Fig. 8G), in the stamen vasculature and on the abaxial side of anthers (Fig. 8J,K). These analyses indicated that the *AP1:LhG4* and *AP3:LhG4* driver lines can direct specific expression in the three outer whorls and to some extent in the fourth whorl of the tomato flower.

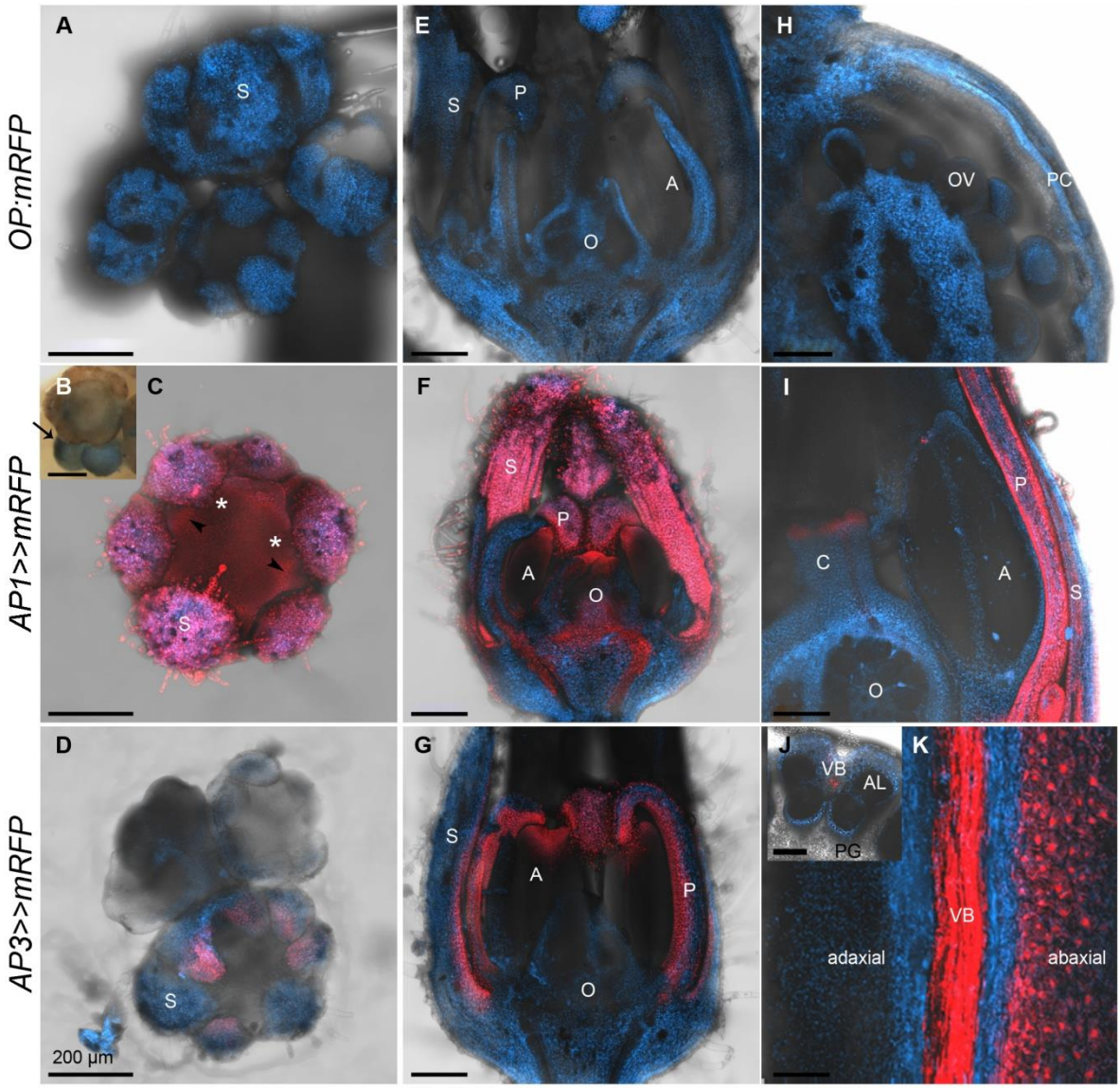

Fig. 8. Characterization of the expression directed by flower-specific driver lines. (A, C-K) Confocal microscope images of developing tomato flowers of controls (*OP:mRFP*) and the indicated genotypes. (A-D) Stage 1–3 buds (tomato flower stages are according to (Brukhin *et al.*, 2003) (B) Whole-mount GUS staining of *AP1>>GUS* inflorescence meristem (marked by an arrow) and stage 2 bud. (E-G) Longitudinal sections of stages 6-7 buds. (H) Longitudinal section of ovary at anthesis. (I) Longitudinal section of stage 8 bud. Transverse (J) and longitudinal (K) sections of anther at anthesis. The red and blue colors represent mRFP and chloroplast fluorescence signals, respectively. Arrowheads indicate the position of the petal primordia and asterisks represents the position of the anther primordia. S – sepal; C – carpel; O – ovary; A – anther; P – petal; ST – stigma; VB – vascular bundle; AL – anther locule; OV – ovule; PG – pollen grains; PC – pericarp. All scale bars = 200 µm.

Next, the *AP1>>P0HA* and*AP3>>P0HA* plants phenotypes were characterized. These plants showed a wild-type phenotype during vegetative growth (data not shown). However they displayed dramatic floral phenotypes within the expression domains of each promoter. Expressing *P0HA* under control of the *AP1* promoter resulted in the development of smaller flowers with deformed organs in all four whorls, in agreement with *AP1* expression in young floral primordia (Fig. 8). The sepals were more succulent and frequently failed to enclose the developing flower (Fig. 9). In the second whorl, most of the flowers produced smaller needle-like petals.

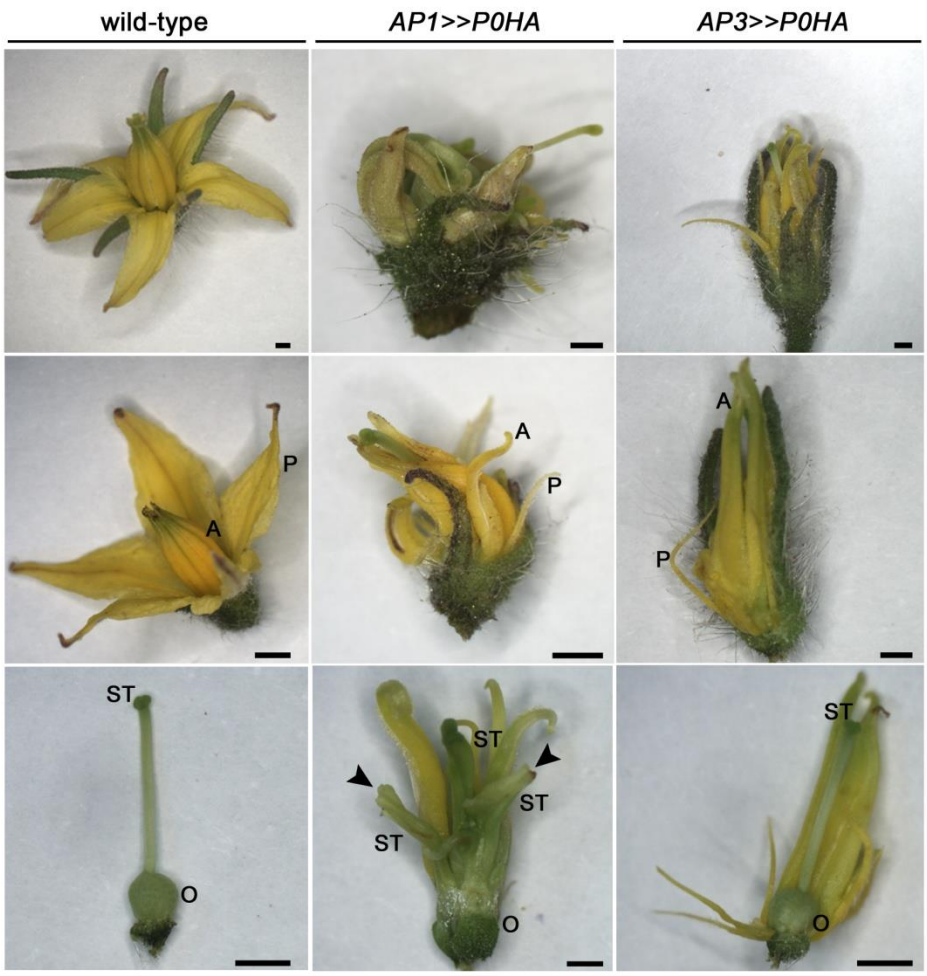

Fig. 9. Phenotypes of *AP1>>P0HA* and *AP3>>P0HA* flowers and fruits. Abnormalities caused by flower-specific *P0HA* expression. The upper panel presents the whole flower, the middle panel presents whorls two and three, and the lower panel presents the pistil. P – petal; A – anther; O – ovary; ST – style. Stigma-less styles are indicated by arrowheads.

The third whorl contained deformed filament-like anthers, some of which were fused (Fig. 9). The fourth whorl contained an abnormal pistil composed of an enlarged ovule-less ovary and numerous styles either tipped or not tipped with stigmatic tissue (Fig. 9). The defects in the reproductive whorls of *AP1>>P0HA* flowers led to sterility. Notwithstanding, very rarely, parthenocarpic fruit did develop (Fig. 10). Consistent with the *AP3* expression pattern (Fig. 8), expressing *P0HA* using this promoter resulted in abnormal phenotypes only in the second and third whorls, while the sepals showed an almost normal phenotype and the pistils developed normally, like the wild-type controls (Fig. 9). The *AP3>>P0HA* petals were filament-like, but unlike the *AP1>>P0HA* petals, their proximal region was flat and encircled the reproductive whorls. The *AP3>>P0HA* stamens were deformed and occasionally

fused as in the *AP1>>P0HA* flowers (Fig. 9). Moreover, these plants set fruit that contained viable

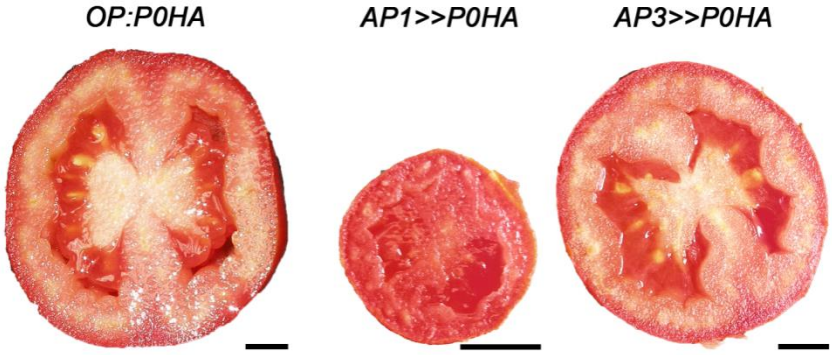

Fig. 10. Cross sections of red fruit of the control (*OP:P0HA*) and indicated genotypes. Scale bar = 1 mm

seeds (Fig. 10). The filament-like phenotypes of petals and anthers suggested that they suffer from an alteration in organ polarity. Additionally, the formation of extra-organs and abnormal floral-organs separation suggested that the boundary morphogenesis was also deformed due to the expression of P0HA. Histological analyses of *AP1>>P0HA* and *AP3>>P0HA* stage 6 buds revealed radial petals compared to the control and an excessive number of abnormal anthers, some of which were fused, radial or both (Fig. 11A-C). Anther radialization was more frequent in *AP3>>P0HA* buds, which is in agreement with the expression of *AP3* promoter in anthers (Fig. 8). SEM examination of *AP1>>P0HA* and *AP3>>P0HA* stage 6 buds supported the above observations, showing filament-like petals and stamens (Fig. 11D-F). In the wild-type tomato flower at anthesis, the petal's adaxial epidermis is composed of cylinder-shaped cells while the abaxial epidermis consists of pavement cells (Fig. 11G). In contrast, the surfaces of the *AP1>>P0HA* and *AP3>>P0HA*filamentouspetals were composed of elongated rectangular epidermal cells with no recognizable abaxial or adaxial identity (Fig. 11H, I). A similar loss of cellular identity and phenotype was observed in the epidermal cells on the outer surface of the *FIL>>P0HA* needle-like leaflets (Fig. 7C), suggesting that *P0HA* expression during petal growth, as in leaflets, disturbed the establishment of proper adaxial-abaxial identity. Quantitative RT-PCR analysis of *AP1>>P0HA* buds demonstrated a significant increase in certain miRNA-target transcripts, validating the perturbation of the miRNA pathway by expressed P0HA (Fig. 11J). *Solyc03g115850,*

a miRNA-target-transcript that was most influenced by P0HA expression, is a NAC gene, which we have predicted as a miR164 target gene. RNA gel blot analysis of miR164 showed that it is present in buds and reach maximum levels in open flowers and ripening fruit (Fig. 12). In plants, miR164 is a conserved and important regulator of the *CUC* genes which are involved in vegetative as well as reproductive organ-boundary formation (Aida *et al.*, 1997; Laufs *et al.*, 2004).This raised the possibility that the perturbation of miR164 by P0HA in *AP1>>P0HA* and *AP3>>P0HA* flowers may contributed to the deformed boundary formation.

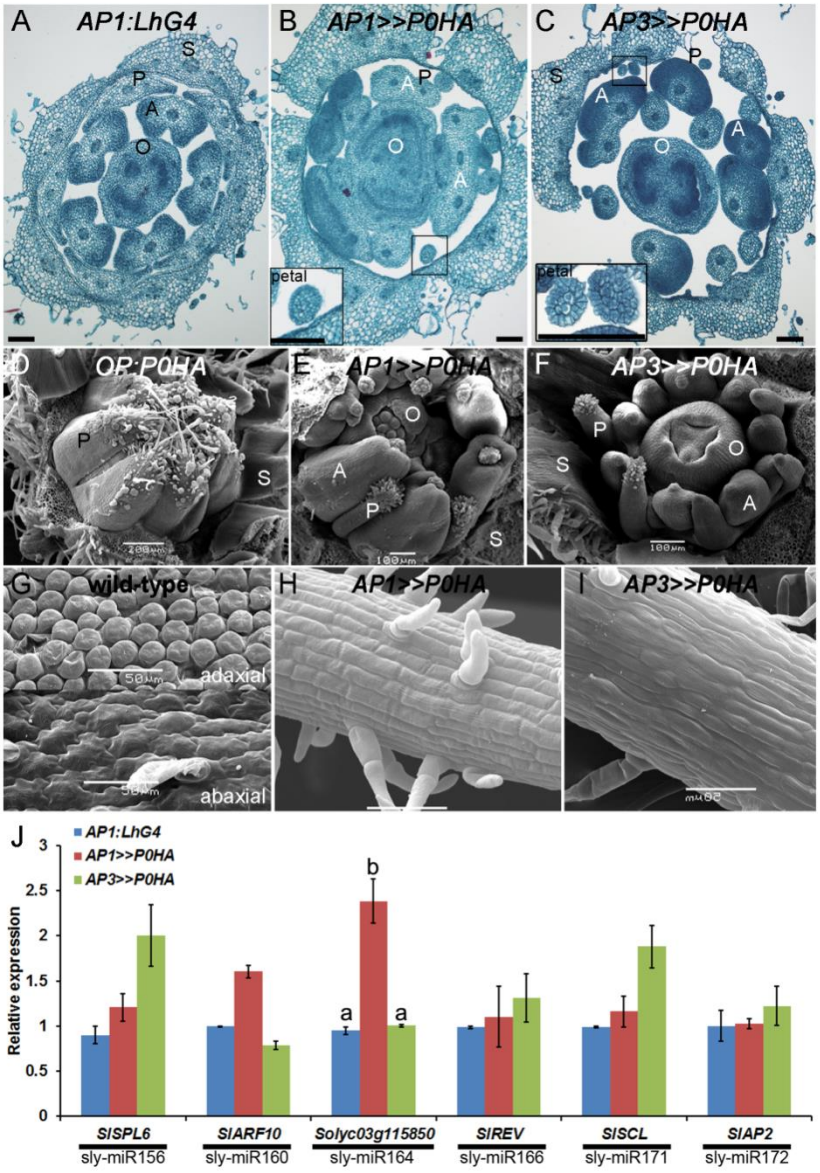

Fig. 11. Microscopic and molecular analyses of *AP1>>P0HA* and *AP3>>P0HA* flowers. (A-C) Transverse sections of 2 mm buds of controls (*AP1:LhG4*) and the indicated genotypes. Insets show representative petals at a higher magnification. Scale bars = 100 µm. (D-F) Scanning electron micrographs of 2 mm buds. The sepals were removed to expose the developing petals and anthers. (G-I) Scanning electron micrographs of the petal epidermis of the wild type and the indicated genotypes. (J) QRT-PCR analysis of selected miRNA-target

transcripts from the indicated genotypes in 2–3 mm buds. Primers were designed around the corresponding miRNA complementary site. *TIP41* expression values were used for normalization. Data are means ± SE of two biological replicates, each measured in triplicate. Different letters indicate statistically significant difference as determined by Student's *t* test ($P \leq 0.01$). Scale bars = 50 μm. S – sepal; P – petal; A – anther; O – ovary

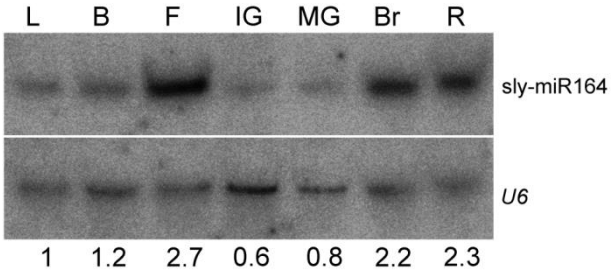

Fig. 12. miR164 expression in tomato. Northern blot analysis of sly-miR164 in the indicated tomato tissues. Sly-miR164 expression was normalized to *U6 snRNA* and levels are indicated below the panel. L – leaves; B – buds; F – flower at anthesis; IG - immature green; MG - mature green; Br – breaker; R – red.

C.5. Sly-miR164 guides the cleavage of four NAC-domain genes in tomato

Perturbation of the miRNA-pathway by P0HA in *AP1>>P0HA* and *AP3>>P0HA* resulted flowers with defective floral-boundaries (Fig. 9, 11). *AP1>>P0HA* produced flowers with extra floral organs, the petals were fully separated and did not enclosed the basal part of the ovary while the anthers were fused (Fig. 9). *AP3>>P0HA* produced flowers with extra and fused anthers (Fig. 9). Moreover, molecular analysis revealed that *Solyc03g115850*, a NAC gene which was predicted as sly-miR164-target gene was upregulated in the P0HA expressing plants (Fig. 5J, 7E, 11J). Since sly-miR164 and its target genes are likely to play important function in tomato flower development as in other plants (Souer *et al.*, 1996; Aida *et al.*, 1997; Weir *et al.*, 2004), they were selected for further analysis. Hence, the next objective of this work was to identify all putative sly-miR164 target genes and to analyze their role in flower development. Because nearly all evolutionarily conserved plant miRNAs are encoded by gene families (Axtell and Bowman, 2008), different members of the tomato miR164 family were first determined. The same strategy as described for miR168 was used, and three putative miR164-like sequences (data not shown) were found, but only the genomic loci encoding the ath-miR164a-identical ones could fold into a pre-miRNA-like hairpin structure (Fig. 13A). In addition, the corresponding sly-miR164*

strand encoded by each hairpin was identified in our small RNA data set, validating their functionality as sly-miR164 precursors (Fig. 13A). An additional query of the tomato genome with sly-miR164 did not identify any novel miR164-like sequences suggesting that the identified sly-miR164 is the only miR164 family member encoded by the tomato genome. To identify gens that are subjected to sly-miR164-guided cleavage in flowers, candidate mRNA targets were predicted (for further details see material and methods) and their cleavage was validated by RLM-RACE. This analysis identified and confirmed that four mRNA targets — *Solyc03g115850, Solyc06g069710, Solyc07g066330* and *Solyc07g062840* were guided to cleavage by sly-miR164 in tomato flowers (Fig. 13B). During this work, the miR164-target gene, *Solyc07g062840* was identified as *GOBLET* (GOB). *GOB* was found to be required for the formation of boundaries between leaflets in compound tomato leaves and in flowers is required for the formation of boundaries between sepals and carpels (Berger *et al.*, 2009). Sequence analysis of their putative open reading frames indicated that they encode NAC-domain proteins. In addition, this analysis revealed that they all contain the signature motifs LPPLxD and [E/x][H/x]VxCFS[N/x] in their C-terminal region, which predict the involvement of NAC-domain proteins in developmental programs (Fig. 14) (Ooka *et al.*, 2003). Phylogenetic reconstruction of the corresponding tomato and *Arabidopsis* NAC-domain proteins indicated that Solyc07g066330 (SlNAC1) encodes a homolog of *Arabidopsis* miR164-regulated NAC1, which has been found to mediate auxin signaling and promote lateral root development (Xie *et al.*, 2000; Guo *et al.*, 2005); the related Solyc03g115850 (SlNAM2) and Solyc06g069710 (SlNAM3) proteins (60%/70% identity/similarity), which belong to the same group as the CUC proteins, were distantly related to ORESARA1 (ORE1) which has been found to positively regulate aging-induced cell death in *Arabidopsis* leaves (Fig. 13C)(Kim *et al.*, 2009) and to ANAC100 clade that was recently found to negatively regulate cell expansion in rose petals (Pei *et al.*, 2013).

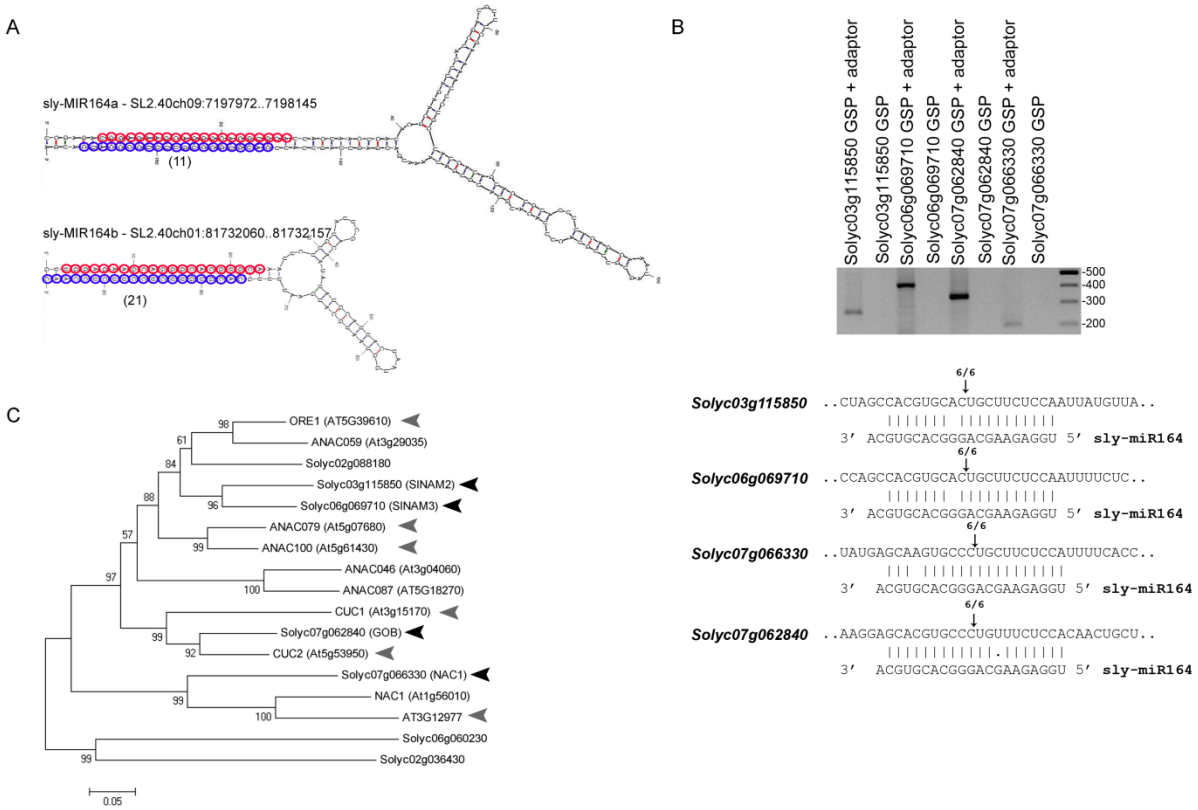

Fig. 13. Characterization of sly-miR164 and its target genes in tomato. (A) Hairpin secondary structures of sly-miR164 precursors. The position of each precursor in the tomato genome is indicated. Mature sly-miR164 and matching sly-miR164* sequences are marked by red and blue circles, respectively, and the abundance of sly-miR164* in the seedling small RNA data set is indicated below. (B) Experimental validation of sly-miR164 cleavage site in *Solyc03g115850, Solyc06g069710, Solyc07g066330* and *Solyc07g062840* mRNAs by RLM-RACE. Upper panel, ethidium bromide-stained agarose gel showing the 5' RACE products. The GeneRacer 5’ primer (Adaptor) and GSP used for each RACE reaction are indicated above. Lower panel alignment of sly-miR164 with its target mRNAs. Arrows and numbers indicate the inferred cleavage sites and the fractions of cloned PCR products terminating at this position, respectively.(C) An unrooted phylogenetic tree of NAM family proteins from *A. thaliana* and tomato, which contain at least one of the motif signatures LPPLxD and [E/x][H/x]VxCFS[N/x]. The phylogenetic tree was constructed by the neighbor-joining method with 100 bootstrap sampling (MEGA program, version 4.0) (Tamura *et al.*, 2007). Black and gray arrowheads mark the proteins encoded by sly-miR164 and ath-miR164 - targeted genes, respectively.

Fig. 14. Sequence alignment of sly-miR164-targeted NAC transcription factors. The multiple alignment was generated with the computer program CLUSTALW (Thompson *et al.*, 1994). The conserved NAC domain is marked by asterisks. The sequences that match the LPPLxD and [E/x][H/x]VxCFS[N/x] motif signatures are boxed.

C.6. Flower-specific silencing of sly-miR164 target genes disturbs whorl and sepal separation

To investigate the involvement of the sly-miR164-targeted *NAM* genes in flower development, sly-miR164 was overexpressed in the flower primordia by transactivation of the previously characterized M82 tomato *OP:MIR164* responder line(Alvarez *et al.*, 2006) with the available flower-specific *AP1:LhG4* driver line, which drives expression throughout young floral primordia (Fig. 8). First, sly-miR164 overexpression was validated by northern analysis of young *AP1>>MIR164* buds revealing a threefold increase in its levels compared to control buds (Fig. 15A). This increase was consistent with the significant reduction in the accumulation of *GOB* (70%) and that of *SlNAC1*, *SlNAM2* and *SlNAM3* (~95%) in these buds, further corroborating their targeting by sly-miR164 (Fig. 15B). Phenotypic analysis of silenced *AP1>>MIR164* flowers revealed elongated sepals that were fused to each other at various points (Fig. 15C). Moreover, failure of these sepals to peel away from the flower suggested the occurrence of partial fusion between the first and second whorls (Fig. 15C). Indeed, transverse sectioning of young *AP1>>MIR164* buds at the base of the style showed that the three outer whorls and their organs were not separated at that stage, whereas in control buds they were completely separated (Fig. 15D). Accordingly, longitudinal sectioning of fully developed *AP1>>MIR164* flowers showed that the three outer whorls and in addition the fourth whorl separated later than in controls (Fig. 15D). Together, these phenotypes indicated that sly-miR164 target genes are required for the normal formation of flower sepal and interwhorl boundaries. The *gob-3* loss-of-function tomato mutant has been shown to produce flowers with increased sepal fusions and fewer locules, and to set fruit with fused outer floral organs, suggesting that *GOB* is central to the formation of tomato-flower boundaries (Blein *et al.*, 2008; Berger *et al.*, 2009). Thus, it is highly likely that the reduced levels of *GOB* in *AP1>>MIR164* flower primordia are responsible for at least some of the defective boundary phenotypes. Nevertheless, since *GOB* silencing in *AP1>>MIR164* flowers was driven by a heterologous promoter and was not complete as in the *gob-3* loss-of-function mutant flowers, the *AP1>>MIR164*

defective flower-boundary phenotypes might be the result of downregulation of *GOB* and either one or a combination of the other sly-miR164 target genes.

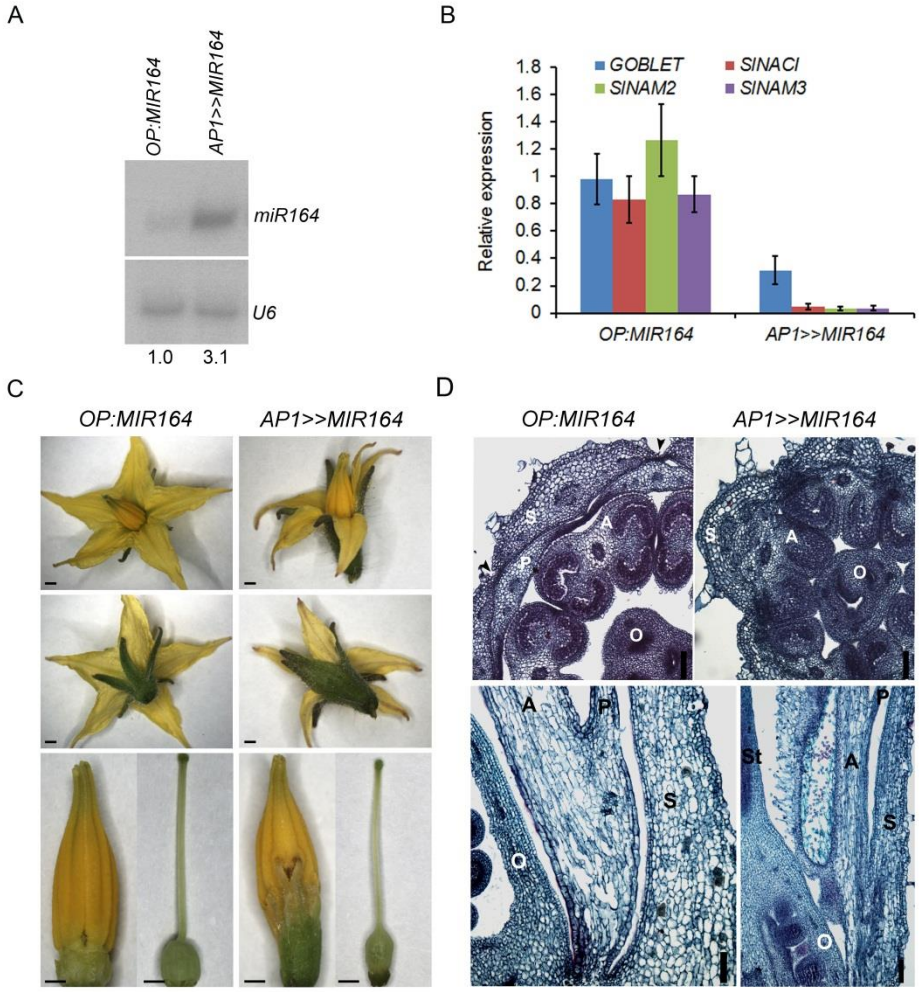

Fig. 15. Flower specific miR164 overexpression leads to sepal and whorl fusions. (A) Northern blot analysis of sly-miR164 in stage 8 buds from the indicated genotypes (tomato flower stages are according to (Brukhin *et al.*, 2003)). MiR164 expression was normalized to *U6 snRNA* and levels are indicated below the panel. (B) Quantitative RT-PCR analysis of *GOBLET*, *SlNAC1*, *SlNAM2* and *SlNAM3* in stage 8 buds of the indicated genotypes. Primers were designed around the corresponding sly-miR164- complementary site. *TIP41* expression values were used for normalization. Data are means ± SD of three biological replicates, each measured in triplicate. (C) Flower phenotypes of the indicated genotypes. The upper panel presents a whole flower; the middle panel presents a side view of the whole flower and the lower panel presents isolated anthers and pistil after removal of the sepals and petals. Scale bars = 1 mm. (D) Transverse and longitudinal sections of control (*OP:MIR164*) and *AP1>>MIR164* stage 10 buds (upper panel) and flowers before anthesis (lower panel). Black arrowheads indicate the sepal–sepal boundary. S – sepal; P – petal; A – anther; O – ovary; St – style. Scale bars = 100 µm.

C.7. SlNAM2 is expressed in floral boundaries

Overexpression of sly-miR164 at early stages of flower development uncovered the function of sly-miR164 target genes and their requirement for proper floral-boundary morphogenesis (Fig. 15). Since *SlNAC1* probably represents a homolog of *Arabidopsis NAC1* (Fig. 13C), which has not been implicated in flower-boundary formation (Guo *et al.*, 2005), its contribution to the boundary-defective phenotype was less likely. In addition, *SlNAM2* was much more abundant than *SlNAC1* and *SlNAM3* in developing flowers (Fig. 16). Thus, to examine the possible involvement of *SlNAM2* in flower-boundary establishment, its spatial expression in young buds was determined by *in-situ* hybridization.

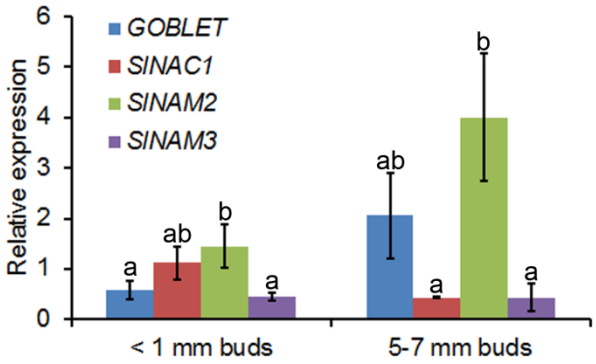

Fig. 16. Quantitative RT-PCR analysis of sly-miR164-targeted genes in developing flowers. Primers were designed around the corresponding miR164 complementary sites. *TIP41* expression values were used for normalization. Data are means ± SD of three biological replicates, each measured in triplicate. Different letters indicate statistically significant differences as determined by Student's *t* test ($P \leq 0.05$).

Longitudinal and successive transverse sections of stage 8 buds showed spatial separation of the whorls and their corresponding floral organs (Fig. 17A–E). A transverse section of a relatively proximal part of a young bud showed completely fused whorls (Fig. 17B). At that same location, stripes of *SlNAM2* mRNA were expressed at the boundary between the first and second whorls prior to their separation (Fig. 17F). In a more distal plane, the first and the fourth whorl are clearly separated from the second and third, respectively, but the perianth organ primordia are still laterally fused (Fig. 17C). At that position, stripes of *SlNAM2* mRNA were detected at the boundaries between the second and the third and the third and the fourth whorls. In addition, *SlNAM2* mRNA marked the lateral margins of the sepals

and surrounded the stamen filaments (Fig. 17G). At a more distal plane, all whorls were separated (Fig. 17D) and *SlNAM2* mRNA was detected between the fused sepals (Fig. 17H). In the most distal section of the ovary, the sepals, which protect the bud, were the only organs that remained fused to each other (Fig. 17E) and that fusion was marked by *SlNAM2* mRNA (Fig. 17I). In accordance with its strong sly-miR164-mediated silencing in *AP1>>MIR164* buds (Fig. 15B), *SlNAM2* expression was not detected in them, further confirming the authenticity of the wild-type *in-situ* signal (Fig. 17J–M). Taken together, the *SlNAM2* transcript was expressed at the boundaries between adjacent sepals and whorls suggesting that it might be involved in their separation. However, no significant *SlNAM2* mRNA signal could be detected before the fusion of carpels (bud stages 1–6; data not shown), indicating that it is poorly expressed at the time of whorl-boundary formation. *GOB* is expressed in the boundaries between floral meristem and floral-organ primordia (Blein *et al.*, 2008). This implicates *GOB* rather than *SlNAM2* in whorl boundary formation and raises the possibility that *SlNAM2* is involved in floral-boundary maintenance.

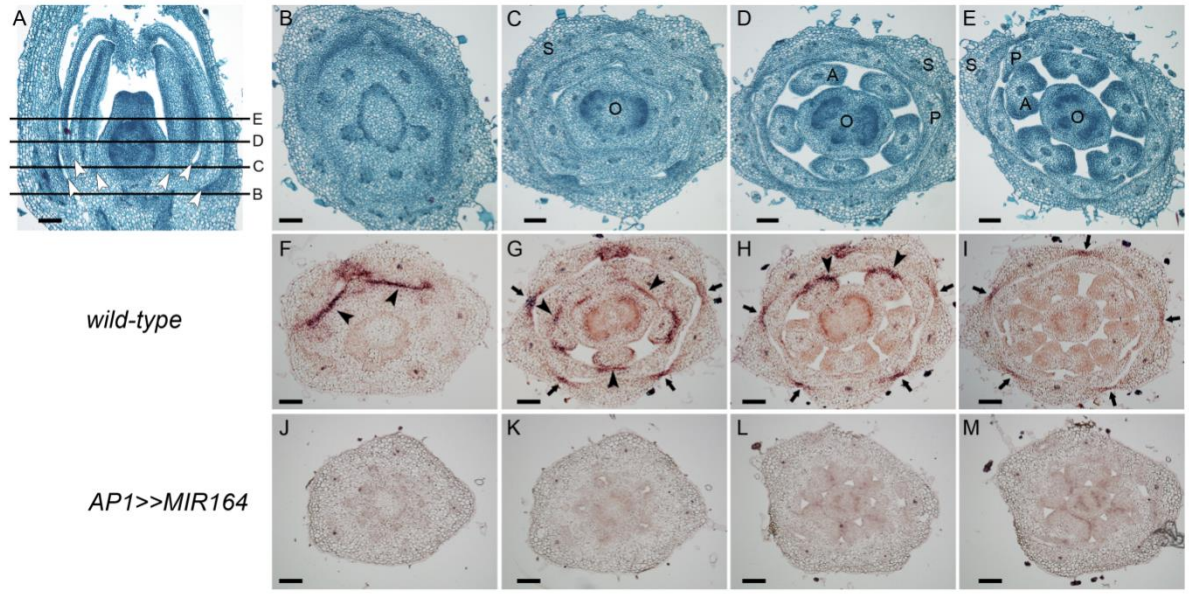

Fig. 17. Expression pattern of *SlNAM2* in tomato bud. (A) Longitudinal section of wild-type flower buds at stage 8. The lines mark the positions of the cross sections shown in B–E. Arrowheads mark the points of separation between corresponding whorls. (B–M) Successive transverse sections from the base upward. (B–E) Safranin-Fast Green differential staining. (F-M) *In-situ* hybridization with *SlNAM2* antisense probe in the indicated genotypes. Arrowheads and arrows mark *SlNAM2* signal between whorls and around floral organs, respectively. S – sepal; P – petal; A – anther; O – ovary. Scale bars = 100 µm.

C.8. Accumulation of SlNAM2*-encoding transcript is associated with growth-repression phenotypes*

Cell proliferation is greatly reduced in the organ–meristem and organ–organ boundaries (Breuil-Broyer *et al.*, 2004). This process is mediated by the activity of regulatory boundary genes (Aida and Tasaka, 2006*a*) and plays a role in organ morphogenesis (Nikovics *et al.*, 2006). While loss-of-function mutations in these genes result in overgrowth of the boundary region, manifested as organ fusions, over accumulation of these genes due to gain-of-function or ectopic expression usually represses growth, manifested as smaller and occasionally multiple organs and extra and elaborate lobing of cotyledons, leaves and floral organs (Hiratsu *et al.*, 2002; Brewer *et al.*, 2004; Baker *et al.*, 2005; Berger *et al.*, 2009; Busch *et al.*, 2011; Huang *et al.*, 2012). Since *SlNAM2* is expressed at flower boundaries, raised the question whether it has similar boundary gene activity and can suppress growth when accumulated. To investigate this, two homozygous tomato responder lines were generated that are able to express wild-type (*SlNAM2*) and sly-miR164-resistant (*mSlNAM2*) versions of the gene upon transactivation (for further details see Material and methods, and Fig. 18). Both were crossed with the strong constitutive *35S:LhG4* and flower-specific *AP1:LhG4* driver lines to generate corresponding transactivated F1 progeny plants. Inactivated *OP:SlNAM2* and *OP:mSlNAM2* responder plants were morphologically identical to the driver lines and wild-type M82 tomato (data not shown). However, *35S>>mSlNAM2* plants and to a much lesser extent *35S>>SlNAM2* plants showed various growth-repression-associated phenotypes. Compared to control tomato cotyledons which are oval and entire, the *35S>>mSlNAM2* cotyledons were abnormally shaped, smaller and lobed, and occasionally three instead of two cotyledons were produced (Fig. 19A–C). A similar but less pronounced phenotype was observed in *35S>>SlNAM2* cotyledons, which were larger than *35S>>mSlNAM2* (Fig. 19B). Reminiscent multiple and serrated cotyledon phenotypes have also been reported as a result of expression of the *GOB*sly-miR164-resistant mutant gene *Gob-4d* under its native or leaf-specific *FIL* promoter, respectively (Berger *et al.*, 2009). In addition, mature *35S>>mSlNAM2* plants were dwarf whereas the *35S>>SlNAM2* plants were no different from controls (Fig. 19D). Moreover, examination of *35S>>mSlNAM2* flowers revealed a reduction in flower size and wrinkled and slightly lobed petals (Fig. 19E). Also, compared to

control and *35S>>SlNAM2*, dramatic growth repression was observed in the two inner whorls of *35S>>mSlNAM2* flowers, including shorter stamens and style (Fig. 19F, H). Moreover, the pistil was very wide as a result of extra carpel formation (Fig. 19G). QRT-PCR analysis of control and transgenic flowers revealed relatively mild accumulation of *SlNAM2* in *35S>>SlNAM2* compared to controls, and consistent with *mSlNAM2* resistance to sly-miR164 cleavage, a much higher accumulation of SlNAM2-encoding transcript was detected in *35S>>mSlNAM2* flowers (Fig. 19I).

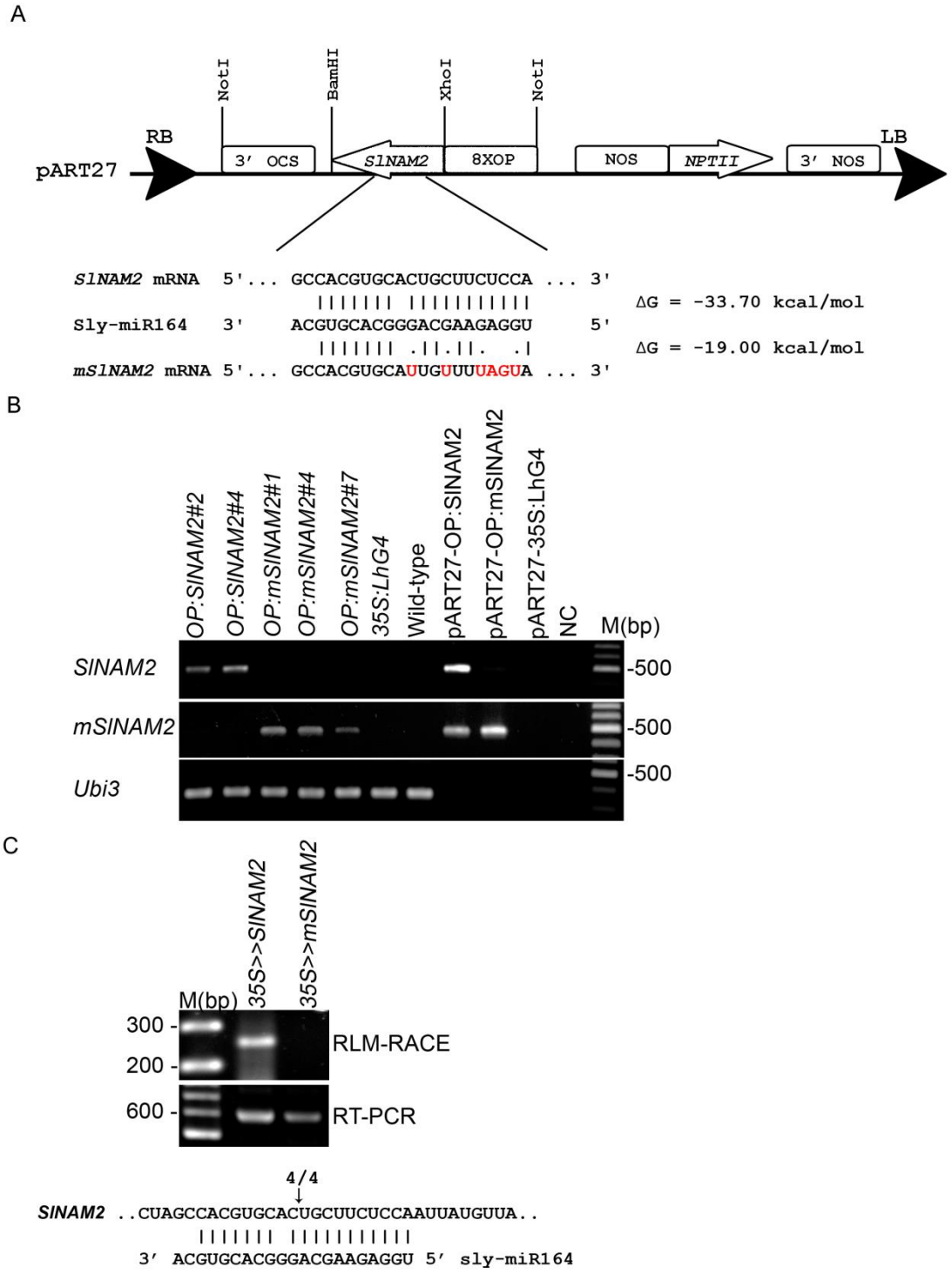

Fig. 18. Generation of *OP:SlNAM2* and *OP:mSLNAM2* responder lines. (A) Schematic representation of the responder binary constructs. The sly-miR164 complementary sequence in *SlNAM2* mRNA, the sly-miR64 sequence, the silent mutations (in red) introduced in *mSlNAM2* and the minimum free energy hybridization values as determined by RNAhybrid (Rehmsmeier *et al.*, 2004) are shown in the expanded region. (B) Genomic DNA PCR analysis of representative tomato *OP:SlNAM2* and *OP:mSlNAM2* reporter lines. The *OP:SlNAM2#4* and *OP:mSlNAM2#7* lines were used for further analysis.(C) Cleavage analysis of *SlNAM2* and *mSlNAM2* transgenic transcripts. The miRNA-mediated cleavage site was determined by RLM-RACE of total *35S>>SlNAM2* and *35S>>mSlNAM2* leaf RNA using a transgene-specific RACE primer for the 3' OCS. The presence of an intact transgenic

transcript was verified by RT-PCR. Below, arrow marks the position of the inferred cleavage site in the transgenic *SlNAM2* transcript, and the number above it indicates the fraction of cloned PCR products terminating at this position.

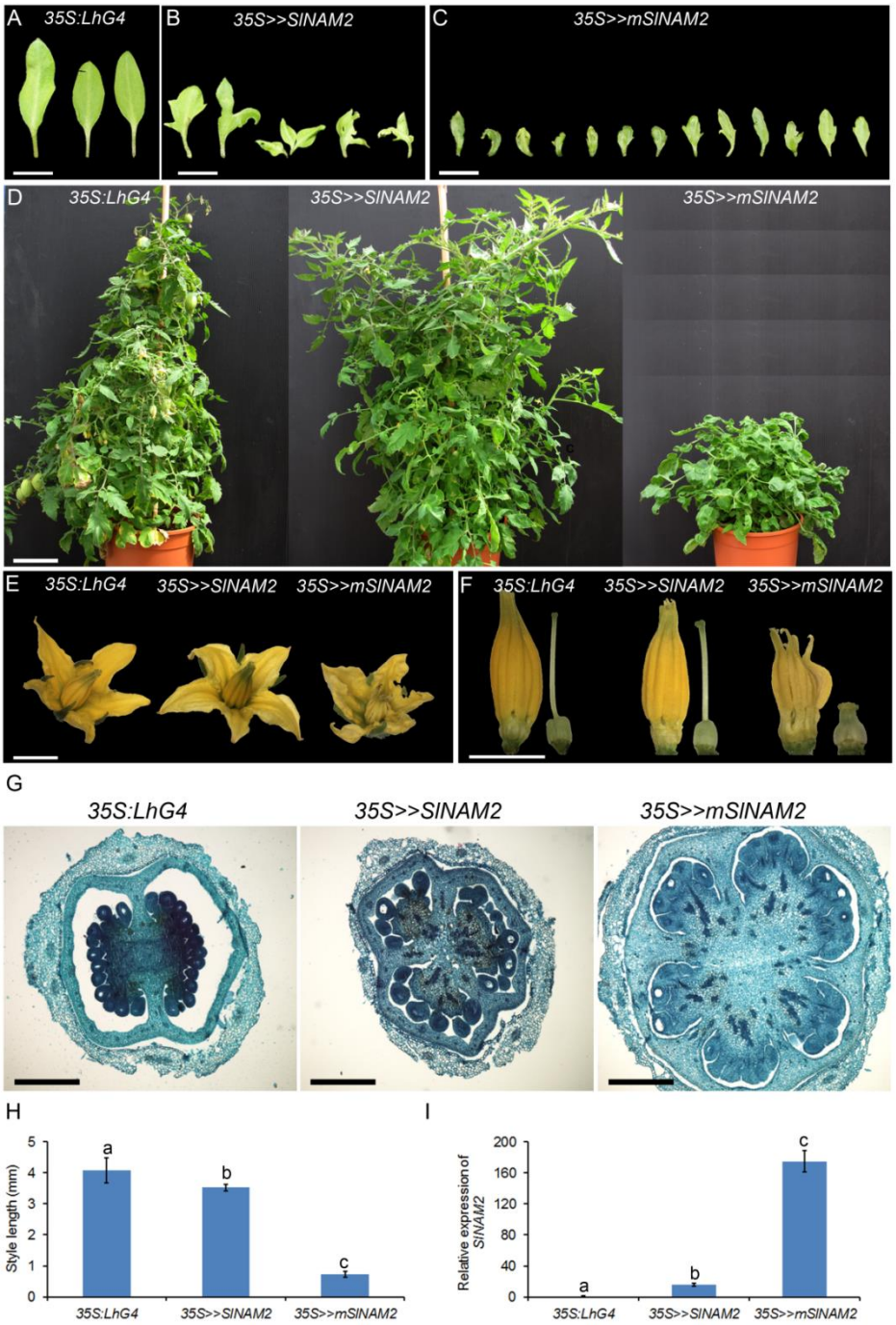

Fig. 19. Phenotypic and molecular characterization of *35S>>SlNAM2* and *35S>>mSlNAM2* plants. (A–C) Phenotypes of isolated cotyledons 11 days after sowing from control (*35S:LhG4*) and transactivated (*35S>>SlNAM2* and *35S>>mSlNAM2*) tomato seedlings. Multiple cotyledons were separated. (D) Four-month-old plants of the indicated genotypes. (E) Representative flower at anthesis of the indicated genotypes. (F) Stamen and pistil phenotypes of the indicated genotypes. (G) Transverse sections of the ovary of the indicated genotypes. (H) Style lengths of the indicated genotypes. Data are means ± SD (n=10). Different letters indicate statistically significant difference as determined by Student's *t* test ($P \leq 0.01$). (I) QRT-PCR analysis of SlNAM2-encoding transcripts in the flowers of

indicated genotypes. Primers were designed around the corresponding sly-miR164 complementary site. *TIP41* expression values were used for normalization. Data are means ± SD of two biological replicates, each measured in triplicate. Different letters indicate statistically significant difference as determined by Student's *t* test ($P \leq 0.01$). Scale bars A–C = 1 cm; D = 10 cm; E, F = 5 mm; G = 500 μm.

Similarly, high accumulation of SlNAM2-encoding transcript in *AP1>>mSlNAM2* buds (Fig. 20A) was associated with significantly smaller sepals and styles and slightly lobed petals compared with the organs of control *OP:SlNAM2* flowers (Fig. 20), whereas less accumulation in *AP1>>SlNAM2* buds resulted in milder organ phenotypes (Fig. 20). Together, these results demonstrated a positive correlation between the accumulation levels of SlNAM2-encoding transcript and abnormalities typically observed in plants overexpressing boundary genes, suggesting similar activity for *SlNAM2*.

C.9. SlNAM2 *accumulation rescues the fusion phenotypes of AP1>>MIR164 flowers*

Since *SlNAM2* is expressed at floral whorl and organ boundaries (Fig. 17) and can suppress growth when accumulated (Fig. 19,20), the next step was to determine whether SlNAM2 growth-suppression activity can define floral boundaries. To that end, *AP1>>MIR164* mutant flowers, which had fused sepals and abnormal whorl separation, were complemented with SlNAM2, and the resulting phenotype was analyzed. This was done by expressing *mSlNAM*2 in the background of *AP1>>MIR164* plants (*AP1>>MIR164 >>mSlNAM2*). As a control, *SlNAM2* was expressed on the same genetic background (*AP1>>MIR164 >>SlNAM2*). As expected, analysis of *AP1>>MIR164 >>SlNAM2* flowers showed elongated fused sepals and abnormal interwhorl fusion (Fig. 21A–C). This abnormal phenotype was no different from that of *AP1>>MIR164* flowers (Fig. 15C–D). In contrast, the *AP1>>MIR164 >>mSlNAM2* flowers had a wild-type-like phenotype. Although their sepals were slightly shorter than controls they were not fused (Fig. 21A–B) and contained no abnormal interwhorls fusions (Fig. 21A, C). QRT-PCR of young buds revealed accumulation of the sly-miR164-ressistant *mSlNAM2* in *AP1>>MIR164 >>mSlNAM2* whereas the sly-miR164-sensitive *SlNAM2*,

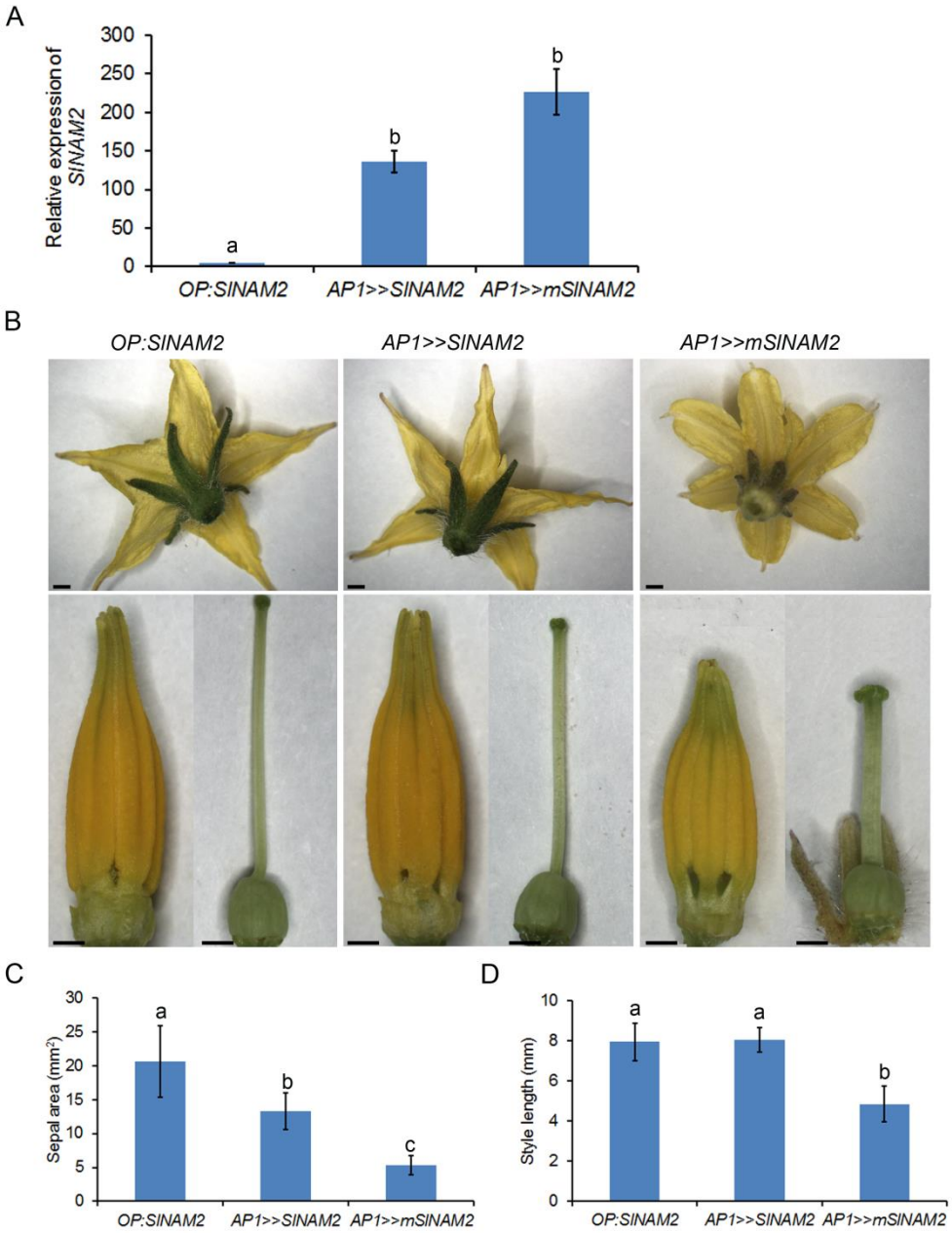

Fig. 20. Phenotypic characterization of *AP1>>SlNAM2* and *AP1>>mSlNAM2* flowers. (A) Quantitative RT-PCR analysis of *SlNAM2* in stage 9 buds. Primers were designed around the corresponding miR164 complementary site. *TIP41* expression values were used for normalization. Data are means ± SD of two biological replicates, each measured in triplicate. Different letters indicate statistically significant difference as determined by Student's *t* test ($P \leq 0.01$). (B) Representative flower at anthesis of the indicated genotypes. The upper panel presents the whole flower and the lower panel presents isolated anthers and pistil after removal of the sepals and petals. Scale bars = 1 mm. (C) Sepal areas of the indicated genotypes. Data are means ± SD ($n \geq 70$). Different letters indicate statistically significant difference as determined by Student's *t* test ($P \geq 0.01$). (D) Style lengths of the indicated genotypes. Data are means ± SD ($n \geq 10$). Letters indicate statistically significant differences as determined by Student's *t* test ($P \geq 0.01$).

SlNAC1, *SlNAM3* and *GOB* were silenced (Fig. 21D and data not shown). These results demonstrated that when accumulated and expressed at early stages of flower development, SlNAM2is able to restore the formation of floral boundaries.

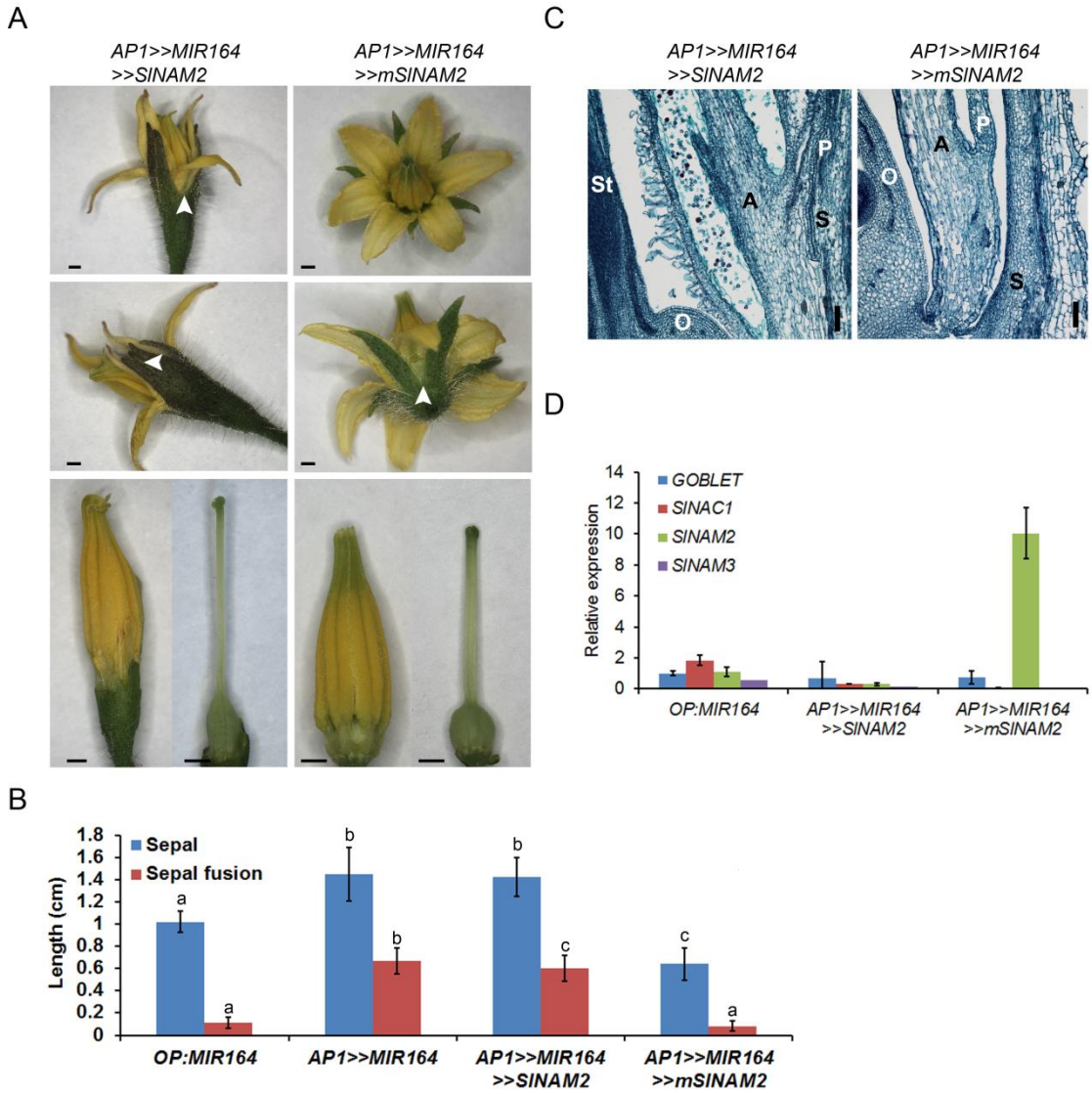

Fig. 21. Restoration of normal flower phenotype upon expression of *mSlNAM2* in miR164-overexpressing flowers. (A) Flower phenotypes of the indicated genotypes. The upper panel presents the whole flower; the middle panel presents a whole flower on its side and the lower panel presents isolated anthers and pistil. Arrowheads mark the points of sepal fusion. Scale bars = 1 mm. (B) Sepal and fusion lengths of the indicated genotypes. (C) Longitudinal section of flowers before anthesis from the indicated genotypes. Scale bars = 100 µm. S – sepal; P – petal; A – anther; O – ovary; St – Style. (D) Quantitative RT-PCR analysis of *GOBLET, SlNAC1, SlNAM2, SlNAM3*in 1–2 mm buds of the indicated genotypes. Primers were designed around the corresponding miRNA's complementary site. *TIP41* expression values were used for normalization. Data are means ± SD of three biological replicates, each measured in triplicate.

C.10. SiRNAs specific for SlNAM2 fail to reduce its transcript levels

To further understand *SlNAM2* function and elucidate its specific contribution to *AP1>>miR164* fusion phenotypes two approaches were taken to downregulate *SlNAM2*. Firstly, transgenic tomato plants were generated that were specifically silenced for this gene by *trans*-activated RNAi. To that end, a responder RNAi construct (OP:SlNAM2IR) that contained a 353 bp fragment from the 3' UTR region of SlNAM2 was constructed (Fig. 22A). The effectiveness of the *trans*-activated RNAi construct was tested by transient expression in *benthamiana* epidermal cells. This was done by coexpressing *OP:SlNAM2IR* with chimeric GFP that contained the *SlNAM2* targeted 3' UTR at its C-terminal, in the presence of a driver plasmid that constitutively expressed *LhG4*. Four days post-infiltration, a significantly lowered GFP expression was observed in *benthamiana* cells that were infiltrated with *OP:SlNAM2IR* compared to control extracts that did not (Fig. 22B) and immunoblotting against GFP confirmed that result (Fig. 22C), demonstrating the usefulness of the *OP:SlNAM2IR* construct. Next, the OP:SlNAM2IR was transformed into M82 tomato and nineteen independent plants were regenerated and transactivated by a cross with the constitutive *35S:LhG4* driver line. Molecular analysis of the F1 progeny for SlNAM2-associated small interfering RNAs (siRNAs) revealed significant levels of siRNAs in the cotyledons of certain transactivated progeny plants (Fig. 22D). However, the transactivated plants produced plants that were morphologically identical to the driver lines and wild-type M82 tomato (data not shown). Molecular analysis of SlNAM2 in the flower verified the resulted wild-type phenotype and revealed that the transcript level was not changed despite the production of the siRNAs, rendering these plants non-informative (Fig. 22E).

Studies have shown that alteration in the miRNA sequence does not always affect the miRNA processing from its precursor (Vaucheret *et al.*, 2004), thus enabling the generation of artificial-miRNA (amiRNA) against a gene of choice by modifying the endogenous miRNA precursors (Alvarez *et al.*, 2006; Niu *et al.*, 2006). Since SlNAM2 and SlNAM3 might have a redundant functionality, an amiRNA was design to downregulate both (Fig. 23).The*pre-MIR164b* was chosen as a backbone, based on previous studies in tomato (Alvarez *et al.*, 2006). The amiRSlNAM designed to directly target *SlNAM2* and *SlNAM3* (Fig. 24A) and has a 5' uridine like most plants miRNAs. Mismatches were introduced into the miRNA complementary

sequence to mimic the predicted stem of the *MIR164b* precursor, assuming that bulges in the *MIR164b* backbone contain essential recognition and processing information (Fig. 24A). The integrated aMIRSlNAM backbone was then synthesis and the aMIRSlNAM was then cloned behind the OP promoter (Fig. 24B).

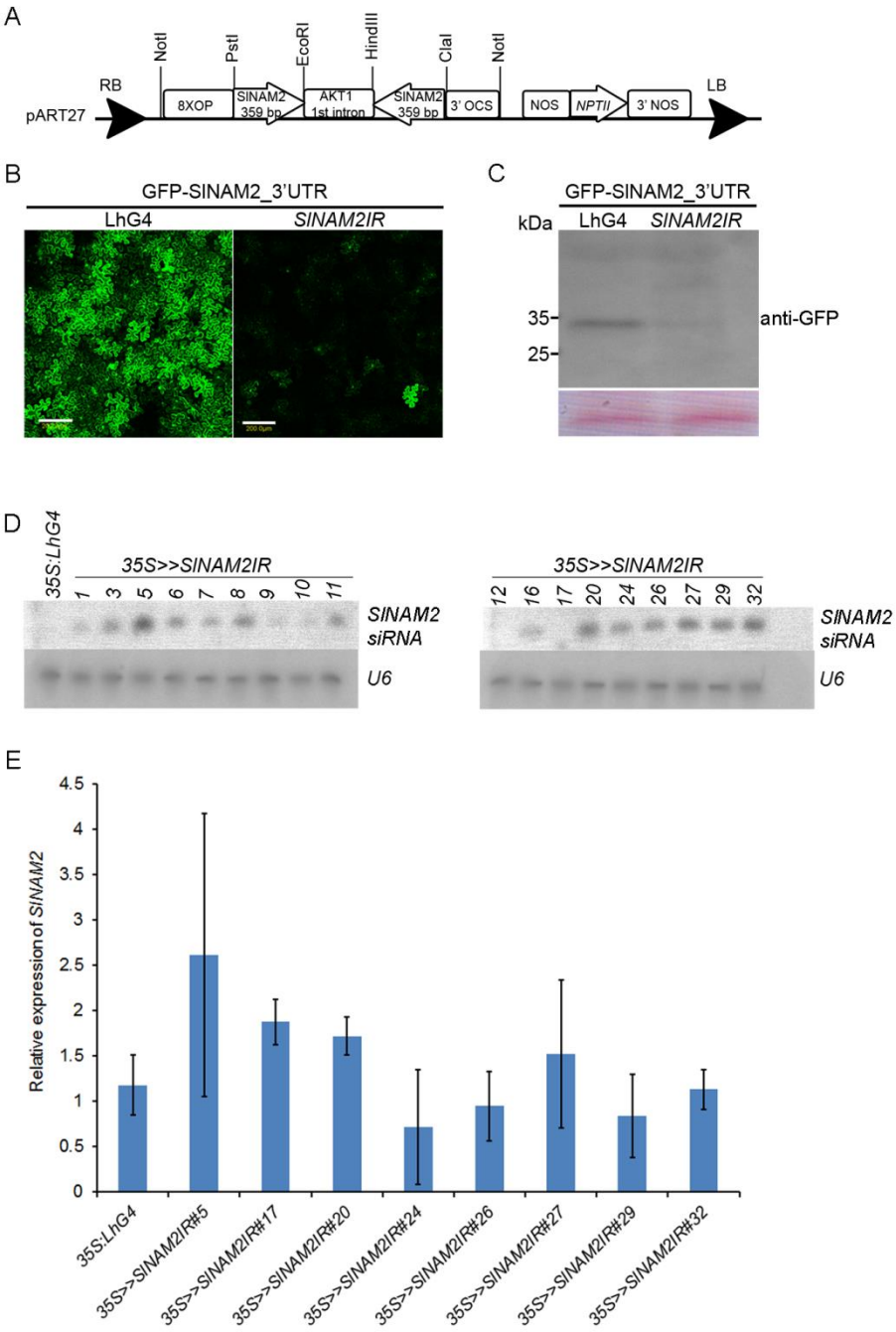

Fig. 22. Construction and molecular analysis of *35S>>SlNAM2IR* plants. (A) Schematic representation of the responder binary construct. (B) Expression of GFP-SlNAM2IR. Indicated constructs were agroinfiltrated into *benthamiana* leaves and the GFP fluorescence was analyzed by confocal laserscanning microscopy. Images of representative leaf epidermal cells were taken four days post agroinfiltration. (C) Western blotting of equal volume of total protein extract probed with anti-GFP commercial antibodies. ponceau staining served as a loading control. The positions of molecular-mass standards (kDa) are indicated on the left.

(D) RNA gel-blot analysis of *SlNAM2* siRNAs in the indicated *35S>>SlNAM2IR* plants (upper panel). The *U6 snRNA* was used as a loading control (lower). (E) QRT-PCR analysis of *SlNAM2* in the flowers of the indicated *35S>>SlNAM2IR* plants. Primers were designed around the corresponding sly-miR164 complementary site. *TIP41* expression values were used for normalization. Data are means ± SD of three technical replicates.

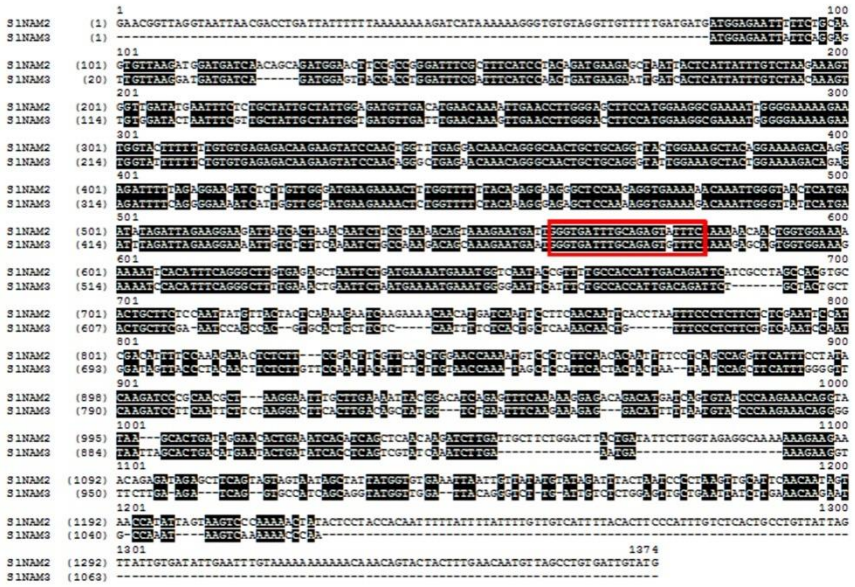

Fig. 23. *SlNAM2* and *SlNAM3* cDNA alignment. The target sites of amiRSlNAM are boxed.

Next, the OP:aMIRSlNAM was transformed into M82 tomato and eight independent plants were regenerated and transactivated by a cross with the constitutive *35S:LhG4* driver line. Molecular analysis of the F1 progeny for amiRSlNAM revealed low levels of mature amiRNAs in the cotyledons of only one transactivated plant (Fig. 24C), the amiRSlNAM* strand was also tested to insure proper loading of the mature strand to the RISCs. Moreover, phenotypic and molecular analyses of its transactivated F1 progeny are under way. In light of the above results the contribution of *SlNAM2* to the fusion phenotype of *AP1>>miR164* flowers and its specific requirement for flower development remains unknown.

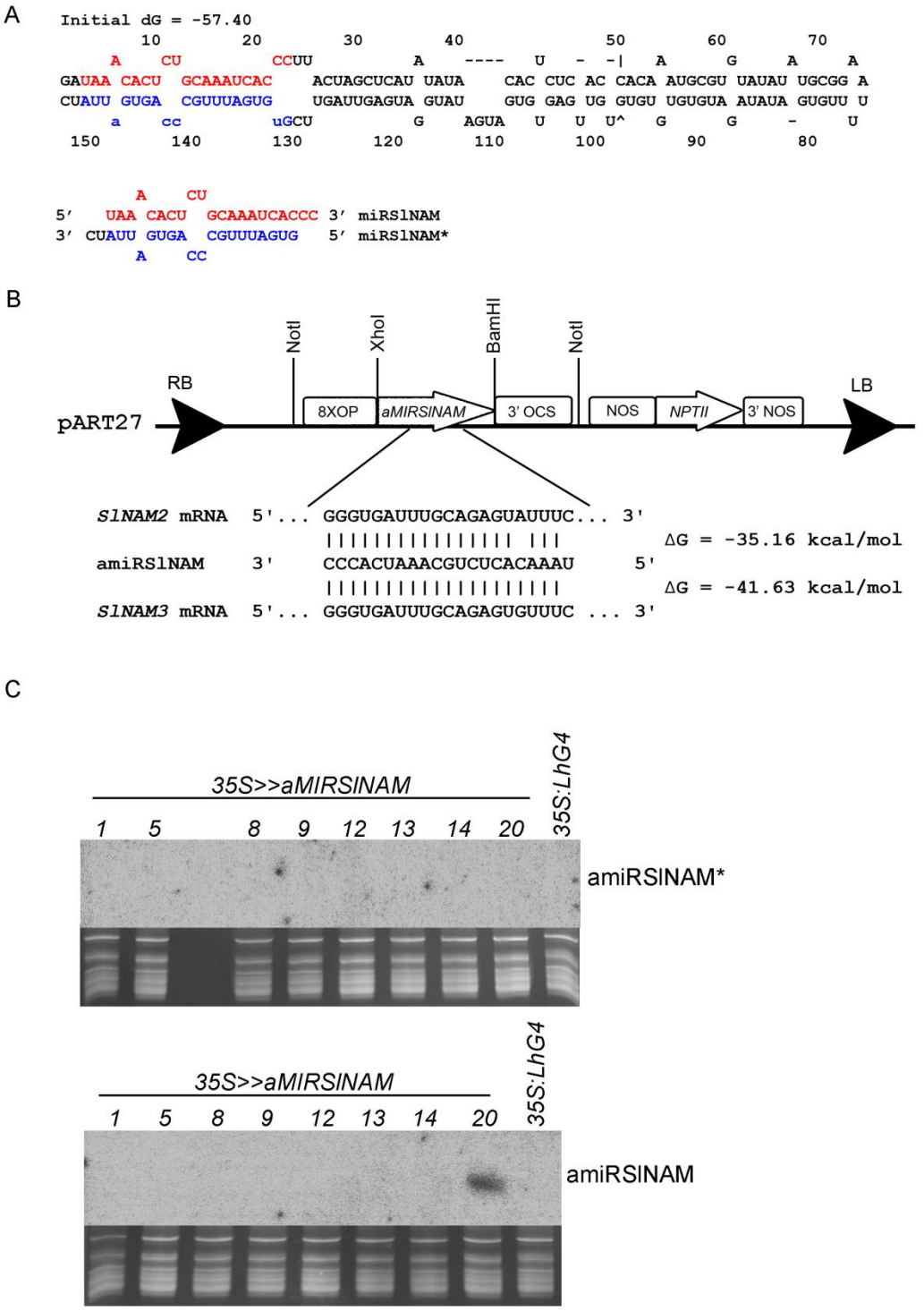

Fig. 24. Construction and employment of *amiRSlNAM*. (A) Predicted folding and dicing of the pre amiRSlNAM backbone. (B) Schematic representation of the responder binary construct. The amiRSlNAM complementary sequence in *SlNAM2* mRNA, the miRSlNAM sequence, the complementary sequence in *SlNAM3* mRNA and the minimum free energy hybridization values as determined by RNAhybrid are shown in the expanded region. (C) RNA gel-blot analysis of amiRSlNAM and amiRSlNAM* in the indicated *35S>>amiRSlNAM* plants (upper panel). The tRNA and 5S rRNA bands were visualized by ethidiumbromide staining of the polyacrylamide gel and served as a loading control.

C.11. The biological significance of SlNAM2 regulation by sly-miR164

Three types of regulatory modes are known to date for miRNAs: spatial restriction, buffering function and temporal regulation(Garcia, 2008). In *Arabidopsis*, the negative regulation by miR164 fine-tunes the levels, as well as patterns of expression of the *CUC1* and *CUC2* transcripts. Precise regulation of *CUC1* and *CUC2* transcript accumulation is crucial for proper control of organ number and boundary formation throughout vegetative and reproductive development (Mallory *et al.*, 2004*a*; Laufs *et al.*, 2004; Baker *et al.*, 2005; Sieber *et al.*, 2007). In tomato, sly-miR164 spatially and quantitatively sharpens and tunes the *GOB* expression domain for proper leaflet separation (Berger *et al.*, 2009). Since *SlNAM2* is directed to cleavage by sly-miR164 (Fig. 13) and is likely to participate in floral-boundary maintenance, the last objective of this work was to understand the biological significance of *SlNAM2* regulation by sly-miR164 and the mode of regulation of the latter. One commonly used approach that was previously used to decipher the miRNA mode of regulation and its regulatory significance, is to express the miRNA-target gene in its native version or in a miRNA-resistant version under his endogenous promoter and to analyze the resulted expression pattern and the resulting biological effects (Sieber *et al.*, 2007). In the absence *of sly-miR164a* and *sly-miR164b* loss-of-function or *SlNAM2* gain-of-function tomato mutants, further investigation was done by using this approach taking advantage of the existing *SlNAM2* and *mSlNAM2* responder lines (*OP:SlNAM2* and *OP:mSlNAM2*). Therefore, to express them at *SlNAM2* native locations, a driver line that will drive *LhG4* expression under *SlNAM2* native promoter was generated. At the time I started this project, the tomato genomic sequence was not available. So, to sequence the *SlNAM2* promoter, a rapid amplification of genomic ends (RAGE) was performed. Using that technique, a fragment of ~1900 bp of *SlNAM2* putative promoter was sequenced, amplified and cloned upstream of the LhG4 activator region to generate the SlNAM2:LhG4 driver construct. Next, the SlNAM2:LhG4 construct was transformed into M82 tomato and eleven independent plants were regenerated. To identify a *SlNAM2:LhG4* driver plant that drive similar global expression pattern to that of *SlNAM2*, the *LhG4* transcript levels in each driver plant was analyzed in leaves and flowers (Fig. 25A). In the leaves, *SlNAM2* is poorly expressed whereas in the flowers it is much more abundant (Fig. 25A). This analysis could not detect any expression of *LhG4* in the leaves and only a weak expression in the flowers of few

transgenic plants (Fig. 25A) suggesting that the expression level driven by the 1.9 Kb putative *SlNAM2* promoter was much lower than that of the endogenous native promoter. To examine the SlNAM2 promoter detailed expression patterns, *SlNAM2:LhG4-4* plants were transactivated by a cross with the *OP:mRFP* (Shani *et al.*, 2009) reporter line. Indeed, a weak mRFP signal was detected in *SlNAM2:LhG4-4* plants, but had different expression domain than that of *SlNAM2* in the flowers (Fig. 25B). Consistent with that, trans-activation of *SlNAM2* and *mSlNAM2* by *SlNAM2:LhG4* did not result any phenotypic deviation from wild-type (data not shown). The above results indicate that the transgenic *SlNAM2:LhG4* drove expression that did not match the endogenous *SlNAM2* promoter not by patterning or by intensity and thus could not be used for answering the above questions. In addition, these results suggest that the promoter of *SlNAM2* may be longer or shorter than 1.9 Kb. Analysis of the *SlNAM2* upstream sequence, following the release of the tomato genome, exposed a repetitive sequence located upstream to the 1.9 kb putative amplified *SlNAM2* promoter, revealing the reason for the failure to amplify a longer promoter fragment by the RAGE technique.

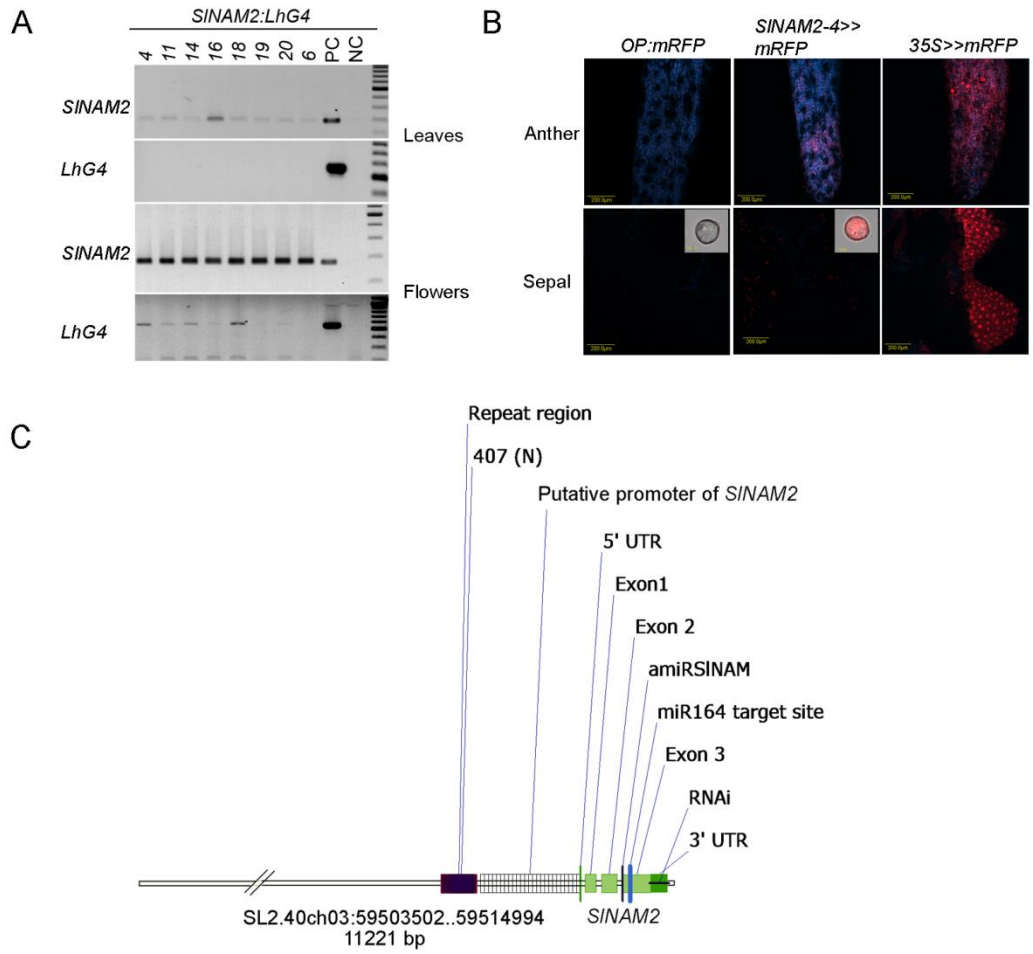

Fig. 25. *SlNAM2* genomic scheme and the expression driven by *SlNAM2:LhG4* trangenic plants. (A) Semi-quantitative analysis of LhG4 transcript in total RNA extracted from the indicated *SlNAM2:LhG4* transgenic line leaves and flowers. Specificity of primers used is indicated on the left. (B) Confocal microscope images of developing tomato flowers of controls (*OP:mRFP*) and the indicated genotypes. (C) Schematic diagram of *SlNAM2* genomic region. Light green boxes represent the ORF; green boxes represent the UTR's; dashed box represent the putative promoter region; the purple box represent the repetitive element. All construct region and cleavage target site are indicated.

D. Discussion

The flower, which contains the reproductive organs, is essential for the development of the fruit. Extensive genetic and molecular research in the last three decades has revealed many of the players, pathways and interactions that are part of the molecular mechanisms underlying flower development (Smyth, 2005; Krizek and Fletcher, 2005; Irish, 2008). Recently, miRNAs were also found to regulate flower morphogenesis and flowering, and accordingly, interfering with the flower miRNA pathway leads to abnormal flower development (Wollmann and Weigel, 2010). Despite the agronomic importance of tomato at the start of this work only one miRNA and its target transcripts have been implicated in tomato flower development (Berger *et al.*, 2009; Buxdorf *et al.*, 2010). The major goal of my Ph.D. was to improve our understanding on the roles of the miRNA pathway in tomato flower development.

D.1. A system to perturb the tomato miRNA pathways

The first objective of this work was to reveal additional processes and genes which are regulated by miRNAs during tomato flower development. In the model plants *Arabidopsis* and moss *Physcomitrella patens*, miRNA pathway null and hypomorphic mutants provided important clues regarding the involvement of the miRNA pathway in certain developmental processes (Bohmert *et al.*, 1998; Lynn *et al.*, 1999; Kidner and Martienssen, 2004, 2005; Yang *et al.*, 2006; Khraiwesh *et al.*, 2010; Nodine and Bartel, 2010). Thus, one way to reveal miRNA-regulated processes and genes was to perturb this pathway in tomato flower and analyze resultant phenotypes. Nevertheless, tomato miRNA-pathway loss-of-function mutants were not described to date. In rice, Wu et al. (2009) succeeded to knock down all four *OsAGO1*s by RNAi. Those plants showed pleiotropic developmental phenotypes correlated with increased accumulation of miRNA target genes. Still, when I started this work, generation of reverse genetics mutants was not straightforward since significant sequence information on the tomato homologs of miRNA pathway components was not available. However, comparative profiling of transgenic *Arabidopsis* plants expressing three different VSRs revealed upregulated transcripts as novel endogenous targets of miRNAs and trans-acting-siRNAs (Jay *et al.*, 2011), supporting the use of VSRs as a means to perturb the miRNA pathway and identify corresponding negatively regulated mRNAs. AGO1 is an essential component of

miRNA-RISC (Baumberger *et al.*, 2007), the effector complex of miRNAs which play key roles in plant development (Chen, 2009). It was found that the Beet western yellows virus P0 VSR suppress silencing by inhibiting the formation of siRNA/miRNA-RISCs (Csorba *et al.*, 2010; Derrien *et al.*, 2012), thus leading to AGO1 degradation (Baumberger *et al.*, 2007; Bortolamiol *et al.*, 2007). This work found that tomato encodes for two AGO1 homologs (SlAGO1s) and both are sensitive to P0 activity (Fig. 3). Therefore, the heterologous expression of P0 silencing suppressor in tomato flowers was chosen as an alternative approach to downregulate SlAGO1s and to perturb its miRNA pathway. Strong transgenic expression of P0 arrests transgenic seedling growth (Bortolamiol *et al.*, 2007) in *Arabidopsis*. In order to prevent P0 possible lethality during transgenic tomato explant regeneration, the two-component OP/LhG4 transactivation system was used to downregulate SlAGO1s (Moore *et al.*, 1998). Accordingly, *35S>>P0HA* seedlings, which contained reduced SlAGO1s levels as a result of P0HA accumulation, showed pleiotropic morphological phenotypes, including post-germination growth arrest (Fig. 5) as well as enhanced accumulation of several miRNA-target transcripts (Fig. 5). Such post-embryonic growth arrest is reminiscent of a fraction of the *Arabidopsis* loss-of-function *ago1* mutant seedlings that developed a single determinate pin-like organ instead of leaves (Lynn *et al.*, 1999; Kidner and Martienssen, 2005). These results indicated that transgenic expression of P0HA can perturb the tomato miRNA pathway. Nevertheless, as both SlAGO1-1 and SlAGO1-2 tomato homologs are sensitive to P0HA, the contribution of each to the abnormal phenotype could not be determined by the P0 approach. To determine the specific contribution of *SlAGO1-1* and *SlAGO1-2*, loss-of-function mutants or specific downregulation is required. In addition, *Arabidopsis* encode for 10 AGO proteins but only mutants of *ago7* and *ago10* showed relatively mild developmental phenotypes (Vaucheret, 2008). Since several AGOs other than AGO1 have been shown to destabilize in the presence of P0 (Baumberger *et al.*, 2007), it is possible that expression of P0 might downregulate their tomato homologs and contribute to the observed P0-mediated phenotypes, as well as yet uncharacterized functions of P0.

D.2. SlAGO1s are required for normal flower development and polarity

The use of transactivated P0 expression also enabled the specific suppression of SlAGO1s at a particular developmental stage or in a particular organ without disturbing prior development or unrelated organs. Two flower specific tomato driver lines (*AP1:LhG4* and *AP3:LhG4*) were available to me during this work (received from Prof. Yuval Eshed, Plant Science Dep. The Weizmann Institute of Science). Characterization of the temporal and spatial expression domains of these driver lines, found that they can direct as early as flower initiation specific expression with certain overlap in the three outer whorls and to some extent in the fourth whorl of the tomato flower. Therefore, these lines were used to drive the flower specific expression of P0HA and perturb its miRNA pathway. The expression of P0HA in the petal primordia produced filament-like almost radial petals (Fig. 11). This phenotype indicated compromised adaxial-abaxial polarity, an organ defect that has been previously reported in several *Arabidopsis ago1* loss-of-function and hypomorphic mutants (Bohmert *et al.*, 1998; Lynn *et al.*, 1999; Kidner and Martienssen, 2004; Yang *et al.*, 2006). Later, this phenotype was associated with the downregulation of miR166/165 that was found to play a role in lateral organ polarity, by regulating subsets of the *HD-ZIP III* transcription factors (Kidner and Martienssen, 2004; Jones-Rhoades and Bartel, 2004). The expression of P0HA very early in flower development caused the formation of extra anthers and styles, anther fusion and early petal separation (Fig. 9, 11), all of which are the outcome of floral boundary disruption. In *Arabidopsis*, boundaries were found to be regulated by miR164. This miRNA targets the *NAM* transcription factor genes *CUC1* and *CUC2* which play key roles in floral boundaries formation (Aida *et al.*, 1997; Takada *et al.*, 2001). In *Arabidopsis*, the upregulated *CUC1/2* in *eep1* mutants (*miR164c* loss-of-function mutants) caused to formation of extra petals in early flowers. Together these phenotypes demonstrated that expression of P0HA through transactivation could interfere with miRNA activities in tomato and suggest that flower boundary specification and polarity are regulated by miRNAs.

In *Arabidopsis* profiling of miRNA pathway mutants identified the single most upregulated miRNA target transcript as the major contributor to the abnormal phenotype (Nodine and Bartel, 2010; Jay *et al.*, 2011). Thus, at that stage a genome-wide transcript profiling of wild-type and *AP1/3>>P0HA* floral organs was required to uncover the most upregulated miRNA target mRNAs, which are likely responsible for the observed flower phenotypes. However, since radially and extra organ

phenotypes were already characterized in *Arabidopsis* and associated with the upregulation of *HD-ZIP III* and *CUC* miRNA-target genes, respectively, the upregulation of their tomato homologues genes was first tested. Expression analysis of the *HD-ZIP III* homologues genes revealed that their transcript levels were not upregulated, suggesting that the radial phenotype was caused by other genes (data not shown). Lately, Yifhar et al. (2012) demonstrated in tomato *ago7* mutants that the elevated levels of *ARF3* and *ARF4*, tasi-ARF target genes, caused to the formation of narrow floral-organs. Since *ARF3* and *ARF4* transcript levels were not tested, I cannot rule out that they contributed to the radial phenotypes of *AP1/3>>P0HA* petals. In tomato I have found that a single miR164 species guide the cleavage of four mRNAs (Fig. 13) one of which was *GOB* (Berger *et al.*, 2009). Expression analysis of these transcripts found that *SlNAM2* was significantly upregulated (Fig. 7, 11) which hinted on its contribution to the phenotype.

D.3. SlNAM2, a boundary gene?

Hence, my next objective was to analyze the function of *SlNAM2* in flower development. I*n-situ* hybridization of *SlNAM2* in buds revealed that early in flower development, the *SlNAM2* is expressed as bands that mark the boundaries between sepals and between different floral whorls (Fig. 17) suggesting that it might be involved in their separation.

Cell proliferation is greatly reduced in the boundaries which separate two areas of high growth rates (Breuil-Broyer *et al.*, 2004); this process is controlled by regulatory boundary genes which caused to growth repression (Aida and Tasaka, 2006*b*). Therefore, gain-of-function mutants of those genes will usually cause growth suppression and extra organ phenotypes (Hiratsu *et al.*, 2002; Brewer *et al.*, 2004; Laufs *et al.*, 2004; Baker *et al.*, 2005; Berger *et al.*, 2009; Busch *et al.*, 2011). To test whether *SlNAM2* has similar boundary gene activity when accumulated, two responder lines were generated that are able to express wild-type (*SlNAM2*) and sly-miR164-resistant (*mSlNAM2*) versions of the gene upon transactivation. Transcript accumulation of *SlNAM2* in *35S>>mSlNAM2*and *AP1>>mSlNAM2* flowers, resulted in various growth-repression-associated phenotypes typically observed in plants overexpressing boundary genes such as, reduction in organ size, abnormal lobed margins and extra floral organ formation suggesting similar activity for *SlNAM2* (Fig.

19, 20). In addition, molecular analysis showed a positive correlation between the accumulation levels of SlNAM2-encoding transcript and the severity of the phenotype. Taken together, these results further support the assumption that *SlNAM2* function as a boundary gene.

In *Arabidopsis* leaves, complementation of the *cuc2* mutant by a NAC-domain gene did not occur unless they had redundant functions. Attempting to complement *cuc2* mutants with *NAC1*, *ANAC019* and to some extent *CUC3*, which have different functionalities than that of *CUC2*, failed to restore leaf morphogenesis, whereas the redundant gene *CUC1*, could (Hasson *et al.*, 2011). Therefore, my next experiment was to test whether *SlNAM2* can complement the floral-boundary fusion phenotypes of *AP1>>MIR164* mutant. To my surprise, the flowers of *AP1>>MIR164>>mSlNAM2* plants which accumulated m*SlNAM2* transcript had a wild-type-like phenotype (Fig. 21). These results demonstrated that when precociously expressed, SlNAM2 is able to restore the formation of floral boundaries suggesting that it is involved in their establishment. Still, the relatively over-accumulation of SlNAM2-encoding transcripts needed for boundary restoration and the milder phenotypes of *35S>>mSlNAM2* compared to ectopic expression of the GOB^{4d} gain-of-function version (*35S>>Gob-4d*) plants (Berger *et al.*, 2009), suggest that *SlNAM2* activities are less suitable for boundary formation than *GOB*.

D.4. The role of SlNAM2 in floral boundary morphogenesis

Arabidopsis leaf serration occurs in two different phases: an early phase, requiring *CUC2*, during which the boundaries which surround the emerging tooth are initiated, and a later phase, requiring both *CUC2* and *CUC3*, which maintains the boundaries to sustain teeth formation (Hasson *et al.*, 2011). In accordance with that,*CUC2* is expressed in the leaf primordium margins already before teeth outgrowth whereas *CUC3* can hardly be detected at that stage, and afterwards both are detected in the sinuses of the developing serrations (Nikovics *et al.*, 2006; Hasson *et al.*, 2011). In a reminiscent way, since the non-overlapping expression patterns of *GOB* (Blein *et al.*, 2008) and *SlNAM2* in floral boundaries (Fig. 17), where *GOB* precedes *SlNAM2* expression and was found in the boundaries between floral meristem and floral-organ primordia while *SlNAM2* was not detected at that stages but only at later stages in boundaries between whorls and between sepals, may suggest that they function at

different stages of boundary morphogenesis. The occurrence of *SlNAM2* in floral-boundary after they initiated by *GOB* might imply its function in boundary maintenance rather than their formation. However, to support the hypothesis that *SlNAM2* function in floral-boundary maintenance, analysis of *SlNAM2* loss-of-function mutant is required.

In the absence of *SlNAM2* loss-of-function mutant, two approaches based on and artificial miRNA were taken to downregulate *SlNAM2*. The RNAi approach turned out to be a failure as in all *35S>>SlNAM2IR* transgenic lines *SLNAM2* transcript levels were not changed. A possible explanation may be that the silencing of *SlNAM2* occurred by translational inhibition rather than transcript cleavage and generation of specific antibodies against SlNAM2 are required to test that assumption. Another possibility is that a feedback mechanism is presents, which compensate for relatively weak *SlNAM2* downregulation. Thus, a new inverted repeat construct need to be constructed against other regions of *SlNAM2* which may yield better silencing than the chosen 3' UTR. The attempt to downregulate the related *SlNAM2* and *SlNAM3* by specific amiRNA is still ongoing and further analysis of *35S>>aMIRSlNAM* plants need to be performed.

D.5. The biological significance of SlNAM2 regulation by sly-miR164 in the flower

The final objective of my work was to determine the biological role of *SlNAM2* regulation by sly-miR164 in the flower. Several miRNAs modes of regulation are known in plants: spatial restriction, buffering function and temporal regulation (Garcia, 2008). In *Arabidopsis*, miR164 act to restrict the expression of the *CUC1* and *CUC2* transcripts during flower development as well as a buffer (Sieber *et al.*, 2007). Using gain- and loss-of-function mutants of *GOB*, Berger et al. (2009) showed that as in *Arabidopsis*, sly-miR164 act to fine-tune the levels, as well as restrict the expression domains of *GOB* in tomato leaves. In the absence of such *SlNAM2* mutants, an alternative way to investigate this was to express *SlNAM2* in its native version or in a miRNA-resistant version under its endogenous promoter and to analyze the resulted expression pattern and phenotypes (Sieber *et al.*, 2007). To do so, a driver line of the putative *SlNAM2* native promoter was generated and crossed with *OP:SlNAM2* and *OP:mSlNAM2* reporter lines. However, the selected 1.9 kb promoter region turned out to be not informative in planta as its expression domain was not

identical to that of the native *SlNAM2* (Fig. 25). Since the promoter sequence possesses most of the transcriptional regulatory elements, a possible explanation to this result is that the selected region lacks some of the important elements which are essential for genuine transcription. Generation of new driver lines with modified promoter will help to determine the importance of *SlNAM2* regulation by sly-miR164 in the flowers.

In summary, in this work I have generated a unique system to suppress SlAGO1 silencing pathways in tomato and in turn reveal processes regulated by miRNAs and other types of SlAGO1-dependent siRNAs. My results demonstrate the strength of the P0HA in combination with the transactivation system, that enable to investigate the involvement of the miRNA pathway in a desired organ or developmental stage without the influence of preceded abnormal development. Using this system, I showed that SlAGO1s is required for normal flower development, boundary specification and polarity and identified *SlNAM2*, a new tomato sly-miR164 regulated NAM gene member that functions in the maintenance of tomato flower whorl and sepal boundaries. In a parallel work, which I was a major contributor, *SlARF10*, a miR160 target gene that was found to be upregulated due to expression of P0HA in leaves, was implicated in compound leaf blade outgrowth.

D.6. Future studies

An important aspect of *SlNAM2* functionality is the mechanism by which SlNAM2 maintain the flower boundaries. This can be done by analyzing the morphological characteristics of *SlNAM2* expressing cells. Recently, Pei et al. (2013) showed that in Rose the *RhNAC100* gene, a homolog of *Arabidopsis ANAC100*, functions to negatively regulate petals cell expansion and slow the rate of petal growth. Overexpression of *RhNAC100* in *Arabidopsis* reduced petal size, while silencing of *RhNAC100* by VIGS increased petal size by promoting cell expansion. Moreover, they were able to identify several downstream genes that are regulated by *RhNAC100* and may participate in cell expansion (Pei *et al.*, 2013). Further characterization of the *35S>>mSLNAM2* smaller organs will reveal if the suppression activity of *SlNAM2* is made by negative regulation of cell expansion or proliferation. In addition transgenic expression of SlNAM2-GFP under its native promoter will label the SlNAM2

expressing cells and enable to characterize their morphology. In addition Chip-Seq (chromatin-immunoprecipitation followed by massively-parallel sequencing) assay using anti-GFP antibody will assist in establishing the *SlNAM2*-dependent regulatory network involved in boundary establishment. Finally, profiling of *AP1>>mSlNAM2* and *AP1>>SlNAM2* will assist in identifying the downstream genes that are affected by SlNAM2.

E. References

Achard P, Herr A, Baulcombe DC, Harberd NP. 2004. Modulation of floral development by a gibberellin-regulated microRNA. Development (Cambridge, England) **131**, 3357–3365.

Aida M, Ishida T, Fukaki H, Fujisawa H, Tasaka M. 1997. Genes involved in organ separation in Arabidopsis: an analysis of the cup-shaped cotyledon mutant. The Plant Cell Online **9**, 841–857.

Aida M, Tasaka M. 2006*a*. Genetic control of shoot organ boundaries. Current Opinion in Plant Biology **9**, 72–77.

Aida M, Tasaka M. 2006*b*. Morphogenesis and patterning at the organ boundaries in the higher plant shoot apex. Plant molecular biology **60**, 915–928.

Allen RS, Li J, Stahle MI, Dubroué A, Gubler F, Millar AA. 2007. Genetic analysis reveals functional redundancy and the major target genes of the Arabidopsis miR159 family. Proceedings of the National Academy of Sciences of the United States of America **104**, 16371–16376.

Allen E, Xie Z, Gustafson AM, Carrington JC. 2005. microRNA-directed phasing during trans-acting siRNA biogenesis in plants. Cell **121**, 207–221.

Alonso-Peral MM, Li J, Li Y, Allen RS, Schnippenkoetter W, Ohms S, White RG, Millar AA. 2010. The microRNA159-regulated GAMYB-like genes inhibit growth and promote programmed cell death in Arabidopsis. Plant physiology **154**, 757–771.

Alvarez JP, Pekker I, Goldshmidt A, Blum E, Amsellem Z, Eshed Y. 2006. Endogenous and Synthetic MicroRNAs Stimulate Simultaneous, Efficient, and Localized Regulation of Multiple Targets in Diverse Species. The Plant Cell Online **18**, 1134–1151.

Arazi T, Talmor-Neiman M, Stav R, Riese M, Huijser P, Baulcombe DC. 2005. Cloning and characterization of micro-RNAs from moss: miRNAs in moss. The Plant Journal **43**, 837–848.

Aukerman MJ, Sakai H. 2003. Regulation of flowering time and floral organ identity by a MicroRNA and its APETALA2-like target genes. The Plant cell **15**, 2730–2741.

Axtell MJ. 2013. Classification and comparison of small RNAs from plants. Annual review of plant biology **64**, 137–159.

Axtell MJ, Bowman JL. 2008. Evolution of plant microRNAs and their targets. Trends in plant science **13**, 343–349.

Baker CC, Sieber P, Wellmer F, Meyerowitz EM. 2005. The early extra petals1 Mutant Uncovers a Role for MicroRNA miR164c in Regulating Petal Number in Arabidopsis. Current Biology **15**, 303–315.

Baulcombe D. 2004. RNA silencing in plants. Nature **431**, 356–363.

Baumberger N, Baulcombe DC. 2005. Arabidopsis ARGONAUTE1 is an RNA Slicer that selectively recruits microRNAs and short interfering RNAs. Proceedings of the National Academy of Sciences of the United States of America **102**, 11928–11933.

Baumberger N, Tsai C-H, Lie M, Havecker E, Baulcombe DC. 2007. The Polerovirus Silencing Suppressor P0 Targets ARGONAUTE Proteins for Degradation. Current Biology **17**, 1609–1614.

Berger Y, Harpaz-Saad S, Brand A, Melnik H, Sirding N, Alvarez JP, Zinder M, Samach A, Eshed Y, Ori N. 2009. The NAC-domain transcription factor GOBLET specifies leaflet boundaries in compound tomato leaves. Development **136**, 823–832.

Blein T, Pulido A, Vialette-Guiraud A, Nikovics K, Morin H, Hay A, Johansen IE, Tsiantis M, Laufs P. 2008. A conserved molecular framework for compound leaf development. Science (New York, N.Y.) **322**, 1835–1839.

Bohmert K, Camus I, Bellini C, Bouchez D, Caboche M, Benning C. 1998. AGO1 defines a novel locus of Arabidopsis controlling leaf development. The EMBO journal **17**, 170–180.

Borsani O, Zhu J, Verslues PE, Sunkar R, Zhu J-K. 2005. Endogenous siRNAs derived from a pair of natural cis-antisense transcripts regulate salt tolerance in Arabidopsis. Cell **123**, 1279–1291.

Bortolamiol D, Pazhouhandeh M, Marrocco K, Genschik P, Ziegler-Graff V. 2007. The Polerovirus F box protein P0 targets ARGONAUTE1 to suppress RNA silencing. Current biology: CB **17**, 1615–1621.

Breuil-Broyer S, Morel P, de Almeida-Engler J, Coustham V, Negrutiu I, Trehin C. 2004. High-resolution boundary analysis during Arabidopsis thaliana flower development. The Plant journal: for cell and molecular biology **38**, 182–192.

Brewer PB, Howles PA, Dorian K, Griffith ME, Ishida T, Kaplan-Levy RN, Kilinc A, Smyth DR. 2004. PETAL LOSS, a trihelix transcription factor gene, regulates perianth architecture in the Arabidopsis flower. Development (Cambridge, England) **131**, 4035–4045.

Brukhin V, Hernould M, Gonzalez N, Chevalier C, Mouras A. 2003. Flower development schedule in tomato Lycopersicon esculentum cv. sweet cherry. Sexual Plant Reproduction **15**, 311–320.

Burgyán J, Havelda Z. 2011. Viral suppressors of RNA silencing. Trends in Plant Science **16**, 265–272.

Busch BL, Schmitz G, Rossmann S, Piron F, Ding J, Bendahmane A, Theres K. 2011. Shoot branching and leaf dissection in tomato are regulated by homologous gene modules. The Plant cell **23**, 3595–3609.

Buxdorf K, Hendelman A, Stav R, Lapidot M, Ori N, Arazi T. 2010. Identification and characterization of a novel miR159 target not related to MYB in tomato. Planta **232**, 1009–1022.

Chen X. 2004. A microRNA as a translational repressor of APETALA2 in Arabidopsis flower development. Science (New York, N.Y.) **303**, 2022–2025.

Chen X. 2009. Small RNAs and Their Roles in Plant Development. Annual Review of Cell and Developmental Biology **25**, 21–44.

Chitwood DH, Guo M, Nogueira FTS, Timmermans MCP. 2007. Establishing leaf polarity: the role of small RNAs and positional signals in the shoot apex. Development (Cambridge, England) **134**, 813–823.

Csorba T, Lózsa R, Hutvágner G, Burgyán J. 2010. Polerovirus protein P0 prevents the assembly of small RNA-containing RISC complexes and leads to degradation of ARGONAUTE1. The Plant Journal **62**, 463–472.

Csorba T, Pantaleo V, Burgyán J. 2009. RNA silencing: an antiviral mechanism. Advances in virus research **75**, 35–71.

Dai X, Zhao PX. 2011. psRNATarget: a plant small RNA target analysis server. Nucleic acids research **39**, W155–159.

Deleris A, Gallego-Bartolome J, Bao J, Kasschau KD, Carrington JC, Voinnet O. 2006. Hierarchical action and inhibition of plant Dicer-like proteins in antiviral defense. Science (New York, N.Y.) **313**, 68–71.

Derrien B, Baumberger N, Schepetilnikov M, Viotti C, De Cillia J, Ziegler-Graff V, Isono E, Schumacher K, Genschik P. 2012. Degradation of the antiviral component ARGONAUTE1 by the autophagy pathway. Proceedings of the National Academy of Sciences of the United States of America **109**, 15942–15946.

Fernandez AI, Viron N, Alhagdow M, *et al.* 2009. Flexible tools for gene expression and silencing in tomato. Plant physiology **151**, 1729–1740.

Garcia D. 2008. A miRacle in plant development: role of microRNAs in cell differentiation and patterning. Seminars in cell & developmental biology **19**, 586–595.

Gasciolli V, Mallory AC, Bartel DP, Vaucheret H. 2005. Partially redundant functions of Arabidopsis DICER-like enzymes and a role for DCL4 in producing trans-acting siRNAs. Current biology: CB **15**, 1494–1500.

Gleave AP. 1992. A versatile binary vector system with a T-DNA organisational structure conducive to efficient integration of cloned DNA into the plant genome. Plant molecular biology **20**, 1203–1207.

Griffith ME, da Silva Conceição A, Smyth DR. 1999. PETAL LOSS gene regulates initiation and orientation of second whorl organs in the Arabidopsis flower. Development (Cambridge, England) **126**, 5635–5644.

Guo H-S, Xie Q, Fei J-F, Chua N-H. 2005. MicroRNA Directs mRNA Cleavage of the Transcription Factor NAC1 to Downregulate Auxin Signals for Arabidopsis Lateral Root Development. The Plant Cell Online **17**, 1376–1386.

Hasson A, Plessis A, Blein T, Adroher B, Grigg S, Tsiantis M, Boudaoud A, Damerval C, Laufs P. 2011. Evolution and diverse roles of the CUP-SHAPED COTYLEDON genes in Arabidopsis leaf development. The Plant cell **23**, 54–68.

Havecker ER, Wallbridge LM, Hardcastle TJ, Bush MS, Kelly KA, Dunn RM, Schwach F, Doonan JH, Baulcombe DC. 2010. The Arabidopsis RNA-directed DNA methylation argonautes functionally diverge based on their expression and interaction with target loci. The Plant cell **22**, 321–334.

Henderson IR, Zhang X, Lu C, Johnson L, Meyers BC, Green PJ, Jacobsen SE. 2006. Dissecting Arabidopsis thaliana DICER function in small RNA processing, gene silencing and DNA methylation patterning. Nature genetics **38**, 721–725.

Hiratsu K, Ohta M, Matsui K, Ohme-Takagi M. 2002. The SUPERMAN protein is an active repressor whose carboxy-terminal repression domain is required for the development of normal flowers. FEBS letters **514**, 351–354.

Huang T, López-Giráldez F, Townsend JP, Irish VF. 2012. RBE controls microRNA164 expression to effect floral organogenesis. Development (Cambridge, England) **139**, 2161–2169.

Hunter C, Sun H, Poethig RS. 2003. The Arabidopsis heterochronic gene ZIPPY is an ARGONAUTE family member. Current biology: CB **13**, 1734–1739.

Irish VF. 2008. The Arabidopsis petal: a model for plant organogenesis. Trends in plant science **13**, 430–436.

Ishida T, Aida M, Takada S, Tasaka M. 2000. Involvement of CUP-SHAPED COTYLEDON genes in gynoecium and ovule development in Arabidopsis thaliana. Plant & cell physiology **41**, 60–67.

Itaya A, Bundschuh R, Archual AJ, Joung J-G, Fei Z, Dai X, Zhao PX, Tang Y, Nelson RS, Ding B. 2008. Small RNAs in tomato fruit and leaf development. Biochimica et biophysica acta **1779**, 99–107.

Jack T, Brockman LL, Meyerowitz EM. 1992. The homeotic gene APETALA3 of Arabidopsis thaliana encodes a MADS box and is expressed in petals and stamens. Cell **68**, 683–697.

Jay F, Wang Y, Yu A, Taconnat L, Pelletier S, Colot V, Renou J-P, Voinnet O. 2011. Misregulation of AUXIN RESPONSE FACTOR 8 underlies the developmental abnormalities caused by three distinct viral silencing suppressors in Arabidopsis. PLoS pathogens **7**, e1002035.

Jefferson RA, Kavanagh TA, Bevan MW. 1987. GUS fusions: beta-glucuronidase as a sensitive and versatile gene fusion marker in higher plants. The EMBO journal **6**, 3901–3907.

Jones L, Keining T, Eamens A, Vaistij FE. 2006. Virus-induced gene silencing of argonaute genes in Nicotiana benthamiana demonstrates that extensive systemic silencing requires Argonaute1-like and Argonaute4-like genes. Plant physiology **141**, 598–606.

Jones-Rhoades MW, Bartel DP. 2004. Computational Identification of Plant MicroRNAs and Their Targets, Including a Stress-Induced miRNA. Molecular Cell **14**, 787–799.

Karlova R, van Haarst JC, Maliepaard C, van de Geest H, Bovy AG, Lammers M, Angenent GC, de Maagd RA. 2013. Identification of microRNA targets in tomato fruit development using high-throughput sequencing and degradome analysis. Journal of experimental botany **64**, 1863–1878.

Kasschau KD, Fahlgren N, Chapman EJ, Sullivan CM, Cumbie JS, Givan SA, Carrington JC. 2007. Genome-wide profiling and analysis of Arabidopsis siRNAs. PLoS biology **5**, e57.

Katiyar-Agarwal S, Gao S, Vivian-Smith A, Jin H. 2007. A novel class of bacteria-induced small RNAs in Arabidopsis. Genes & development **21**, 3123–3134.

Khraiwesh B, Arif MA, Seumel GI, Ossowski S, Weigel D, Reski R, Frank W. 2010. Transcriptional control of gene expression by microRNAs. Cell **140**, 111–122.

Kidner CA, Martienssen RA. 2004. Spatially restricted microRNA directs leaf polarity through ARGONAUTE1. Nature **428**, 81–84.

Kidner CA, Martienssen RA. 2005. The role of ARGONAUTE1 (AGO1) in meristem formation and identity. Developmental biology **280**, 504–517.

Kim J, Jung J-H, Reyes JL, *et al.* 2005. microRNA-directed cleavage of ATHB15 mRNA regulates vascular development in Arabidopsis inflorescence stems. The Plant journal: for cell and molecular biology **42**, 84–94.

Kim JH, Woo HR, Kim J, Lim PO, Lee IC, Choi SH, Hwang D, Nam HG. 2009. Trifurcate feed-forward regulation of age-dependent cell death involving miR164 in Arabidopsis. Science (New York, N.Y.) **323**, 1053–1057.

Kim YJ, Zheng B, Yu Y, Won SY, Mo B, Chen X. 2011. The role of Mediator in small and long noncoding RNA production in Arabidopsis thaliana. The EMBO Journal **30**, 814–822.

Krizek BA, Fletcher JC. 2005. Molecular mechanisms of flower development: an armchair guide. Nature reviews. Genetics **6**, 688–698.

Krizek BA, Lewis MW, Fletcher JC. 2006. RABBIT EARS is a second-whorl repressor of AGAMOUS that maintains spatial boundaries in Arabidopsis flowers. The Plant Journal **45**, 369–383.

Lakatos L, Csorba T, Pantaleo V, Chapman EJ, Carrington JC, Liu Y-P, Dolja VV, Calvino LF, López-Moya JJ, Burgyán J. 2006. Small RNA binding is a

common strategy to suppress RNA silencing by several viral suppressors. The EMBO journal **25**, 2768–2780.

Lampugnani ER, Kilinc A, Smyth DR. 2013. Auxin controls petal initiation in Arabidopsis. Development (Cambridge, England) **140**, 185–194.

Laufs P, Peaucelle A, Morin H, Traas J. 2004. MicroRNA regulation of the CUC genes is required for boundary size control in Arabidopsis meristems. Development **131**, 4311–4322.

Li S, Liu L, Zhuang X, *et al.* 2013. MicroRNAs inhibit the translation of target mRNAs on the endoplasmic reticulum in Arabidopsis. Cell **153**, 562–574.

Li F, Pignatta D, Bendix C, Brunkard JO, Cohn MM, Tung J, Sun H, Kumar P, Baker B. 2012. MicroRNA regulation of plant innate immune receptors. Proceedings of the National Academy of Sciences of the United States of America **109**, 1790–1795.

Li XG, Su YH, Zhao XY, Li W, Gao XQ, Zhang XS. 2010. Cytokinin overproduction-caused alteration of flower development is partially mediated by CUC2 and CUC3 in Arabidopsis. Gene **450**, 109–120.

Lifschitz E, Eviatar T, Rozman A, Shalit A, Goldshmidt A, Amsellem Z, Alvarez JP, Eshed Y. 2006. The tomato FT ortholog triggers systemic signals that regulate growth and flowering and substitute for diverse environmental stimuli. Proceedings of the National Academy of Sciences **103**, 6398–6403.

Liu X, Huang J, Wang Y, Khanna K, Xie Z, Owen HA, Zhao D. 2010. The role of floral organs in carpels, an Arabidopsis loss-of-function mutation in MicroRNA160a, in organogenesis and the mechanism regulating its expression. The Plant Journal **62**, 416–428.

Lu C, Tej SS, Luo S, Haudenschild CD, Meyers BC, Green PJ. 2005. Elucidation of the small RNA component of the transcriptome. Science (New York, N.Y.) **309**, 1567–1569.

Lynn K, Fernandez A, Aida M, Sedbrook J, Tasaka M, Masson P, Barton MK. 1999. The PINHEAD/ZWILLE gene acts pleiotropically in Arabidopsis development and has overlapping functions with the ARGONAUTE1 gene. Development (Cambridge, England) **126**, 469–481.

Mallory AC, Bartel DP, Bartel B. 2005. MicroRNA-Directed Regulation of Arabidopsis AUXIN RESPONSE FACTOR17 Is Essential for Proper Development and Modulates Expression of Early Auxin Response Genes. The Plant Cell Online **17**, 1360–1375.

Mallory AC, Dugas DV, Bartel DP, Bartel B. 2004*a*. MicroRNA Regulation of NAC-Domain Targets Is Required for Proper Formation and Separation of Adjacent Embryonic, Vegetative, and Floral Organs. Current Biology **14**, 1035–1046.

Mallory AC, Reinhart BJ, Jones-Rhoades MW, Tang G, Zamore PD, Barton MK, Bartel DP. 2004*b*. MicroRNA control of PHABULOSA in leaf development: importance of pairing to the microRNA 5' region. The EMBO journal **23**, 3356–3364.

Mallory AC, Vaucheret H. 2009. ARGONAUTE 1 homeostasis invokes the coordinate action of the microRNA and siRNA pathways. EMBO reports **10**, 521–526.

Mallory A, Vaucheret H. 2010. Form, function, and regulation of ARGONAUTE proteins. The Plant cell **22**, 3879–3889.

Mandel MA, Gustafson-Brown C, Savidge B, Yanofsky MF. 1992. Molecular characterization of the Arabidopsis floral homeotic gene APETALA1. Nature **360**, 273–277.

Margis R, Fusaro AF, Smith NA, Curtin SJ, Watson JM, Finnegan EJ, Waterhouse PM. 2006. The evolution and diversification of Dicers in plants. FEBS letters **580**, 2442–2450.

McConnell JR, Emery J, Eshed Y, Bao N, Bowman J, Barton MK. 2001. Role of PHABULOSA and PHAVOLUTA in determining radial patterning in shoots. Nature **411**, 709–713.

Mi S, Cai T, Hu Y, *et al.* 2008. Sorting of small RNAs into Arabidopsis argonaute complexes is directed by the 5' terminal nucleotide. Cell **133**, 116–127.

Mohorianu I, Schwach F, Jing R, Lopez-Gomollon S, Moxon S, Szittya G, Sorefan K, Moulton V, Dalmay T. 2011. Profiling of short RNAs during fleshy fruit development reveals stage-specific sRNAome expression patterns. The Plant Journal **67**, 232–246.

Montgomery TA, Howell MD, Cuperus JT, Li D, Hansen JE, Alexander AL, Chapman EJ, Fahlgren N, Allen E, Carrington JC. 2008. Specificity of ARGONAUTE7-miR390 interaction and dual functionality in TAS3 trans-acting siRNA formation. Cell **133**, 128–141.

Moore I, Gälweiler L, Grosskopf D, Schell J, Palme K. 1998. A transcription activation system for regulated gene expression in transgenic plants. Proceedings of the National Academy of Sciences of the United States of America **95**, 376–381.

Mosher RA, Schwach F, Studholme D, Baulcombe DC. 2008. PolIVb influences RNA-directed DNA methylation independently of its role in siRNA biogenesis. Proceedings of the National Academy of Sciences of the United States of America **105**, 3145–3150.

Moxon S, Jing R, Szittya G, Schwach F, Rusholme Pilcher RL, Moulton V, Dalmay T. 2008. Deep sequencing of tomato short RNAs identifies microRNAs targeting genes involved in fruit ripening. Genome research **18**, 1602–1609.

Nag A, King S, Jack T. 2009. miR319a targeting of TCP4 is critical for petal growth and development in Arabidopsis. Proceedings of the National Academy of Sciences **106**, 22534–22539.

Nikovics K, Blein T, Peaucelle A, Ishida T, Morin H, Aida M, Laufs P. 2006. The Balance between the MIR164A and CUC2 Genes Controls Leaf Margin Serration in Arabidopsis. The Plant Cell Online **18**, 2929–2945.

Niu Q-W, Lin S-S, Reyes JL, Chen K-C, Wu H-W, Yeh S-D, Chua N-H. 2006. Expression of artificial microRNAs in transgenic Arabidopsis thaliana confers virus resistance. Nature biotechnology **24**, 1420–1428.

Nodine MD, Bartel DP. 2010. MicroRNAs prevent precocious gene expression and enable pattern formation during plant embryogenesis. Genes & development **24**, 2678–2692.

Ooka H, Satoh K, Doi K, *et al.* 2003. Comprehensive analysis of NAC family genes in Oryza sativa and Arabidopsis thaliana. DNA research: an international journal for rapid publication of reports on genes and genomes **10**, 239–247.

Ori N, Cohen AR, Etzioni A, *et al.* 2007. Regulation of LANCEOLATE by miR319 is required for compound-leaf development in tomato. Nature Genetics **39**, 787–791.

Palatnik JF, Wollmann H, Schommer C, *et al.* 2007. Sequence and Expression Differences Underlie Functional Specialization of Arabidopsis MicroRNAs miR159 and miR319. Developmental Cell **13**, 115–125.

Park W, Li J, Song R, Messing J, Chen X. 2002. CARPEL FACTORY, a Dicer homolog, and HEN1, a novel protein, act in microRNA metabolism in Arabidopsis thaliana. Current biology: CB **12**, 1484–1495.

Pazhouhandeh M, Dieterle M, Marrocco K, *et al.* 2006. F-box-like domain in the polerovirus protein P0 is required for silencing suppressor function. Proceedings of the National Academy of Sciences of the United States of America **103**, 1994–1999.

Pei H, Ma N, Tian J, Luo J, Chen J, Li J, Zheng Y, Chen X, Fei Z, Gao J. 2013. A NAC Transcription Factor Controls Ethylene-Regulated Cell Expansion in Flower Petals. Plant physiology.

Pilcher RLR, Moxon S, Pakseresht N, Moulton V, Manning K, Seymour G, Dalmay T. 2007. Identification of novel small RNAs in tomato (Solanum lycopersicum). Planta **226**, 709–717.

Qi Y, He X, Wang X-J, Kohany O, Jurka J, Hannon GJ. 2006. Distinct catalytic and non-catalytic roles of ARGONAUTE4 in RNA-directed DNA methylation. Nature **443**, 1008–1012.

Rast MI, Simon R. 2008. The meristem-to-organ boundary: more than an extremity of anything. Current opinion in genetics & development **18**, 287–294.

Rehmsmeier M, Steffen P, Hochsmann M, Giegerich R. 2004. Fast and effective prediction of microRNA/target duplexes. RNA (New York, N.Y.) **10**, 1507–1517.

Rhoades MW, Reinhart BJ, Lim LP, Burge CB, Bartel B, Bartel DP. 2002. Prediction of plant microRNA targets. Cell **110**, 513–520.

Rogers K, Chen X. 2013. Biogenesis, Turnover, and Mode of Action of Plant MicroRNAs. The Plant cell **25**, 2383–2399.

Ron M, Alandete Saez M, Eshed Williams L, Fletcher JC, McCormick S. 2010. Proper regulation of a sperm-specific cis-nat-siRNA is essential for double fertilization in Arabidopsis. Genes & development **24**, 1010–1021.

Schwab R, Palatnik JF, Riester M, Schommer C, Schmid M, Weigel D. 2005. Specific effects of microRNAs on the plant transcriptome. Developmental cell **8**, 517–527.

Shalit A, Rozman A, Goldshmidt A, Alvarez JP, Bowman JL, Eshed Y, Lifschitz E. 2009. The flowering hormone florigen functions as a general systemic regulator of growth and termination. Proceedings of the National Academy of Sciences of the United States of America **106**, 8392–8397.

Shani E, Burko Y, Ben-Yaakov L, Berger Y, Amsellem Z, Goldshmidt A, Sharon E, Ori N. 2009. Stage-specific regulation of Solanum lycopersicum leaf maturation by class 1 KNOTTED1-LIKE HOMEOBOX proteins. The Plant cell **21**, 3078–3092.

Shivaprasad PV, Chen H-M, Patel K, Bond DM, Santos BACM, Baulcombe DC. 2012. A microRNA superfamily regulates nucleotide binding site-leucine-rich repeats and other mRNAs. The Plant cell **24**, 859–874.

Sieber P, Wellmer F, Gheyselinck J, Riechmann JL, Meyerowitz EM. 2007. Redundancy and specialization among plant microRNAs: role of the MIR164 family in developmental robustness. Development **134**, 1051–1060.

Smyth DR. 2005. Morphogenesis of flowers--our evolving view. The Plant cell **17**, 330–341.

Souer E, van Houwelingen A, Kloos D, Mol J, Koes R. 1996. The No Apical Meristem Gene of Petunia Is Required for Pattern Formation in Embryos and Flowers and Is Expressed at Meristem and Primordia Boundaries. Cell **85**, 159–170.

Stav R, Hendelman A, Buxdorf K, Arazi T. 2010. Transgenic expression of tomato bushy stunt virus silencing suppressor P19 via the pOp/LhG4 transactivation system induces viral-like symptoms in tomato. Virus genes **40**, 119–129.

Sun X, Dong B, Yin L, Zhang R, Du W, Liu D, Shi N, Li A, Liang Y, Mao L. 2013. PMTED: a plant microRNA target expression database. BMC bioinformatics **14**, 174.

Takada S, Hibara K, Ishida T, Tasaka M. 2001. The CUP-SHAPED COTYLEDON1 gene of Arabidopsis regulates shoot apical meristem formation. Development **128**, 1127–1135.

Takeda A, Iwasaki S, Watanabe T, Utsumi M, Watanabe Y. 2008. The mechanism selecting the guide strand from small RNA duplexes is different among argonaute proteins. Plant & cell physiology **49**, 493–500.

Takeda S, Matsumoto N, Okada K. 2004. RABBIT EARS, encoding a SUPERMAN-like zinc finger protein, regulates petal development in Arabidopsis thaliana. Development **131**, 425–434.

Talmor-Neiman M, Stav R, Frank W, Voss B, Arazi T. 2006. Novel micro-RNAs and intermediates of micro-RNA biogenesis from moss. The Plant journal: for cell and molecular biology **47**, 25–37.

Tamura K, Dudley J, Nei M, Kumar S. 2007. MEGA4: Molecular Evolutionary Genetics Analysis (MEGA) software version 4.0. Molecular biology and evolution **24**, 1596–1599.

Thompson JD, Higgins DG, Gibson TJ. 1994. CLUSTAL W: improving the sensitivity of progressive multiple sequence alignment through sequence weighting, position-specific gap penalties and weight matrix choice. Nucleic acids research **22**, 4673–4680.

Tolia NH, Joshua-Tor L. 2007. Slicer and the argonautes. Nature chemical biology **3**, 36–43.

Tomato Genome Consortium. 2012. The tomato genome sequence provides insights into fleshy fruit evolution. Nature **485**, 635–641.

Várallyay E, Válóczi A, Agyi A, Burgyán J, Havelda Z. 2010. Plant virus-mediated induction of miR168 is associated with repression of ARGONAUTE1 accumulation. The EMBO journal **29**, 3507–3519.

Vaucheret H. 2008. Plant ARGONAUTES. Trends in plant science **13**, 350–358.

Vaucheret H, Mallory AC, Bartel DP. 2006. AGO1 homeostasis entails coexpression of MIR168 and AGO1 and preferential stabilization of miR168 by AGO1. Molecular cell **22**, 129–136.

Vaucheret H, Vazquez F, Crété P, Bartel DP. 2004. The action of ARGONAUTE1 in the miRNA pathway and its regulation by the miRNA pathway are crucial for plant development. Genes & development **18**, 1187–1197.

Voinnet O. 2005. Induction and suppression of RNA silencing: insights from viral infections. Nature reviews. Genetics **6**, 206–220.

Weir I, Lu J, Cook H, Causier B, Schwarz-Sommer Z, Davies B. 2004. CUPULIFORMIS establishes lateral organ boundaries in Antirrhinum. Development **131**, 915–922.

Williams L, Grigg SP, Xie M, Christensen S, Fletcher JC. 2005. Regulation of Arabidopsis shoot apical meristem and lateral organ formation by microRNA miR166g and its AtHD-ZIP target genes. Development **132**, 3657–3668.

Wollmann H, Weigel D. 2010. Small RNAs in flower development. European journal of cell biology **89**, 250–257.

Wu H-J, Ma Y-K, Chen T, Wang M, Wang X-J. 2012. PsRobot: a web-based plant small RNA meta-analysis toolbox. Nucleic acids research **40**, W22–28.

Wu M-F, Tian Q, Reed JW. 2006. Arabidopsis microRNA167 controls patterns of ARF6 and ARF8 expression, and regulates both female and male reproduction. Development (Cambridge, England) **133**, 4211–4218.

Xie Z, Allen E, Fahlgren N, Calamar A, Givan SA, Carrington JC. 2005. Expression of Arabidopsis MIRNA Genes. Plant Physiology **138**, 2145–2154.

Xie Q, Frugis G, Colgan D, Chua NH. 2000. Arabidopsis NAC1 transduces auxin signal downstream of TIR1 to promote lateral root development. Genes & development **14**, 3024–3036.

Xie Z, Johansen LK, Gustafson AM, Kasschau KD, Lellis AD, Zilberman D, Jacobsen SE, Carrington JC. 2004. Genetic and functional diversification of small RNA pathways in plants. PLoS biology **2**, E104.

Xie Z, Kasschau KD, Carrington JC. 2003. Negative feedback regulation of Dicer-Like1 in Arabidopsis by microRNA-guided mRNA degradation. Current biology: CB **13**, 784–789.

Yang L, Huang W, Wang H, Cai R, Xu Y, Huang H. 2006. Characterizations of a hypomorphic argonaute1 mutant reveal novel AGO1 functions in Arabidopsis lateral organ development. Plant molecular biology **61**, 63–78.

Yifhar T, Pekker I, Peled D, Friedlander G, Pistunov A, Sabban M, Wachsman G, Alvarez JP, Amsellem Z, Eshed Y. 2012. Failure of the tomato trans-acting short interfering RNA program to regulate AUXIN RESPONSE FACTOR3 and ARF4 underlies the wiry leaf syndrome. The Plant cell **24**, 3575–3589.

Zhai J, Jeong D-H, De Paoli E, *et al.* 2011. MicroRNAs as master regulators of the plant NB-LRR defense gene family via the production of phased, trans-acting siRNAs. Genes & development **25**, 2540–2553.

Zhang X, Henderson IR, Lu C, Green PJ, Jacobsen SE. 2007. Role of RNA polymerase IV in plant small RNA metabolism. Proceedings of the National Academy of Sciences of the United States of America **104**, 4536–4541.

Zhang X, Yuan Y-R, Pei Y, Lin S-S, Tuschl T, Patel DJ, Chua N-H. 2006. Cucumber mosaic virus-encoded 2b suppressor inhibits Arabidopsis Argonaute1 cleavage activity to counter plant defense. Genes & development **20**, 3255–3268.

Zhao L, Kim Y, Dinh TT, Chen X. 2007. miR172 regulates stem cell fate and defines the inner boundary of APETALA3 and PISTILLATA expression domain in Arabidopsis floral meristems. The Plant journal: for cell and molecular biology **51**, 840–849.

Zhao Y, Medrano L, Ohashi K, Fletcher JC, Yu H, Sakai H, Meyerowitz EM. 2004. HANABA TARANU is a GATA transcription factor that regulates shoot apical meristem and flower development in Arabidopsis. The Plant cell **16**, 2586–2600.

Zheng X, Zhu J, Kapoor A, Zhu J-K. 2007. Role of Arabidopsis AGO6 in siRNA accumulation, DNA methylation and transcriptional gene silencing. The EMBO journal **26**, 1691–1701.

Zhu Q-H, Helliwell CA. 2011. Regulation of flowering time and floral patterning by miR172. Journal of experimental botany **62**, 487–495.

Zhu H, Hu F, Wang R, Zhou X, Sze S-H, Liou LW, Barefoot A, Dickman M, Zhang X. 2011. Arabidopsis Argonaute10 Specifically Sequesters miR166/165 to Regulate Shoot Apical Meristem Development. Cell **145**, 242–256.

F. Publications arising from this work

Hendelman A, Stav R, Zemach H, Arazi T. The tomato NAC transcription factor SlNAM2 is involved in flower-boundary morphogenesis. J Exp Bot. 2013 Dec;64(18):5497-507.

Hendelman A, Kravchik M, Stav R, Zik M, Lugassi N, Arazi T. The developmental outcomes of P0-mediated ARGONAUTE destabilization in tomato. Planta. 2013 Jan;237(1):363-77.

Hendelman A, Buxdorf K, Stav R, Kravchik M, Arazi T. Inhibition of lamina outgrowth following Solanum lycopersicum AUXIN RESPONSE FACTOR 10 (SlARF10) derepression. Plant Mol Biol. 2012 Apr;78(6):561-76.

Buxdorf K, **Hendelman A**, Stav R, Lapidot M, Ori N, Arazi T. Identification and characterization of a novel miR159 target not related to MYB in tomato. Planta. 2010 Oct;232(5):1009-22.

Stav R, **Hendelman A**, Buxdorf K, Arazi T. Transgenic expression of tomato bushy stunt virus silencing suppressor P19 via the pOp/LhG4 transactivation system induces viral-like symptoms in tomato. Virus Genes. 2010 Feb;40(1):119-29.

צימחוני *35S>>m/SlNAM2* ניתן היה להבחין בעיכוב הגדילה בפסיגים, אשר היו קטנים יותר, מאונים ובחלקם ניתן היה להבחין בריבוי פסיגים. פנוטיפ דומה התקבל בעגבנייה בביטוי ייתר של הגן *GOB* בתצורתו הרגישה והעמידה לבקרה על ידי sly-*miR164*, דבר המחדד עוד יותר את האפשרות שהגן *SlNAM2* מתפקד כגן גבולות. בפרחי *35S>>mSlNAM2* ניתן היה להבחין שהצטברות הגן *mSlNAM2* גרמה לעיכוב גדילה ולעיוות בכל ארבעת הדורים. הפרחים קטנים יותר ביחס לפרחי הבקורת, האבקנים קצרים יותר ומסתלסלים, השחלה גדולה כתוצאה מריבוי לשכות ועמוד העלי קצר ועבה כתוצאה מריבוי עלי השחלה. ביטוי עודף של הגן *SlNAM2* בתצורתו הרגישה, גרם לעיוותים קלים ולא משמעותיים ולכן, ביטוי זה לא פגע בחיוניות הפרח. ביטוי עודף של הגן *mSlNAM2* תחת הפרומוטור הפרחי *AP1* (*AP1>>m/SlNAM2*) גרם למופע ממוקד בפרח, להקטנה משמעותית של עלי הגביע, לאינוי קל של עלי הכותרת ולהקטנת עמוד העלי. יכולת העיכוב של הגן *SlNAM2* כמו גם הדימיון בפנוטיפים המתקבלים כתוצאה מביטוי ייתר של הגן *SlNAM2* לפנוטיפים המתקבלים בצמחים מוטנטים המבטאים גני גבולות בעודף, עוד יותר מחזקת את ההשערה שגן זה הוא גן גבולות.

במטרה לבדוק האם פעילותו של הגן *SlNAM2* יכולה ליצור גבול, הכלאתי את הצמחים המדווחים המבטאים את הגן *SlNAM2* בתצורתו הרגישה והעמידה לצמחים המבטאים בייתר miR164 ולהם פרחים עם מופע מאוחה. אנליזה פנוטיפית ומולקולרית לפרחי *AP1>>MIR164 >>SlNAM2* הראתה שכיוון שהתעתיקים המבוטאים בייתר מבוקעים על ידי miR164 המבוטא גם כן בעודף, רמת הביטוי המתקבלת של הגן *SlNAM2* נמוכה מאוד ולכן לא היתה לתצורה זו כל השפעה על הפנוטיפ המאוחה. מאידך, ביטוי בייתר של הגן *mSlNAM2* בתצורתו העמידה (*AP1>>MIR164 >>mSlNAM2*) הצליחה להציל את הפנוטיפ המאוחה הן בעלי הגביע והן בין הדורים. תוצאות אלו מחזקות את ההשערה שהגן SlNAM2 משתתף בתהליך קביעת הגבולות בפרח.

לסיכום, בעבודה זו יצרתי מערכת להשתקת מסלול ה-miRNA המאפשרת לחשוף גני מטרה ולשייכם לתהליך ההתפתחותי הנלמד. באמצעות מערכת זו, נמצאו שני גנים המבוקרים על ידי miRNA ומשחקים תפקיד חשוב בהתפתחות האיברים הלטארליים בעגבנייה. הגן *SlNAM2*, המבוקר על ידי sly-miR164, וכנראה מעורב בשמירה על הגבולות בפרח. הגן *SlARF10*, המבוקר על ידי sly-miR160 ומשחק תפקיד בהתפתחות הטרף בעלה. פיתוח של צמחים משפעלים נוספים יאפשר בעתיד להשתמש במערכת זו במגוון רקמות ושלבי התפתחות בהתאם לשאלות הנלמדות. אנליזת ריצוף של התעתיקים ב- *AP1>>P0HA* ו- *AP3>>P0HA*, תחשוף גנים נוספים אשר מבוקרים על ידי miRNAs ועולים כתוצאה מביטוי P0HA ותוביל להבנה טובה יותר של התפתחות הפרח בעגבנייה.

פולריות ולמופע של עלעלים חוטיים, מעוגלים ודקים בדומה למוטנט *ago1-3* בארבידופסיס. ביטוי P0HA בשלב התפתחותי מאוחר יותר גרם למופעים קלים יותר. תוצאות אלו איששו את ההנחה שניתן באמצעות ביטוי ספציפי של P0HA במרחב ובזמן לעכב את מסלול ה-miRNAs ולבחון את חשיבותו לאותו שלב התפתחותי.

על מנת ללמוד על מעורבות מסלול ה-miRNAs בהתפתחות הפרח בעגבנייה, באמצעות מערכת הטרנס-אקטיבציה, נבחרו צמחים משפעלים המכילים פרומוטורים הפעילים בשלבי התפתחות שונים של מוטנט נוסף שנמצא לגן זה, הגורם לביטוי ייתר כתוצאה מעמידות לביקוע על ידי miR164, הראתה שמנגד, ביטוי עודף של הגן *GOB* גורם לריבוי איברים בפרח בכל הדורים, מחקר זה הוכיח של-*GOB* תפקיד חשוב בקביעת הגבולות בפרח. בנוסף, בשלב הזה של העבודה, פורסם גנום העגבנייה ואנליזה ביואינפורמטית מחודשת חשפה שבנוסף לשני גנים אלו בפרח, sly-miR164 מנחה לביקוע שני גנים נוספים ממשפחה זו (*SlNAM3* ו-*SlNAC1*).

על מנת ללמוד את מעורבות הגנים המבוקרים על ידי miR164 בפרח, ביטאתי בייתר את miR164 על ידי הפרומוטורAP1 (*AP1>>MIR164*). אנליזה פנוטיפית של הפרחים חשפה שביטוי ייתר של miR164 בשלבים מוקדמים בהתפתחות הפרח, גורם לאיחוי עלי הגביע ובנוסף לאיחוי של הדורים השונים. אנליזה מולקולרית חשפה שרמת הביטוי של כל ארבעת גני המטרה ירדה כתוצאה מביטוי עודף של miR164. כיוון שעד היום נמצא מוטנט רק לגן gob לא ניתן היה להגדיר את התרומה של ייתר הגנים. כיוון שהגן *SlNAM2* מתבטא ברמה הגבוהה ביותר בשלבים שונים בהתפתחות הפרח, ובאברי הפרח המבטאים את P0 בחרנו להמשיך ולאפיין גן זה וללמוד על תפקידו בהתפתחות הפרח. על מנת לבחון את תפקידו של הגן *SlNAM2* בהתפתחות הפרח, תחילה אופיין דגם ביטויו באמצעות אלניזת *in-situ* hybridization בניצנים בגודל 1 מ״מ. אנליזה זו חשפה שהגן *SlNAM2* מתבטא בגבולות הלטראליים של עלי הגביע, בין הדורים השונים ומסביב לזיר המתפתח. תוצאה זו מעלה את האפשרות שלגן *SlNAM2* תפקיד באזור זה. איזורי גבול מאופיינים באזורים בהם החלוקה פוחתת, על מנת לאפשר יצירה של אזור חיץ בין שני איזורים בעלי קצב חלוקה מהיר. מחקרים הראו שתהליך זה מבוקר על ידי גנים המבוטאים באזור הגבול, ולכן קרויים גני גבולות. פגיעה בגנים הללו, בדרך כלל פוגעת ביצירת הגבול, דבר אשר יכול להוביל לאיחוי, קרי לאי יצירת גבול או ליצירת גבול רחב יותר, מה שיכול להוביל לריבוי איברים או לריווחם. ביטוי אקטופי של גנים אלו, בהתאם לתפקידם, יגרום לרוב לעיכוב גדילה שיוביל להקטנת איברים, לריבוי איברים או לאונתיות. בהתאם לכך, בשלב הבא בדקתי האם ביטוי בייתר של הגן *SlNAM2*ייגרום לעיכוב גדילה וריבוי איברים. על מנת לעשות כן, יוצרו שני קווים מדווחים המבטאים את הגן *SlNAM2* בצורתו הטבעית (*OP:SlNAM2*) ובתצורה עמידה בפני ביקוע של sly-miR164 (*OP:mSlNAM2*). צמחים מדווחים אלו הוכלאו עם צמחים משפעלים המבטאים LhG4 באופן רציף או תחת פרומוטורים פרחיים. איפיון פנוטיפי כמו גם מולקולרי חשף שביטוי ייתר של הגן *SlNAM2* בתצורתו העמידה הצטבר וגרם לעיכוב גדילה בכל שלבי התפתחות הצמח ושקיים מתאם בין חומרת הפנוטיפ לרמת התעתיק. עם נביטת

בעבודה זו עוכב מנגנון ההשתקה האנדוגני על ידי שימוש בחלבון הויראלי P0. חלבון זה, המקודד על ידי הוירוס Beet Western Yellows Virus (BWYV), הינו חלבון מעכב השתקה מסוג F-box אשר גורם לפירוק של AGO1, ובכך מעכב את מנגנון ההשתקה האנטי ויראלי והאנדוגני של הצמח. במחקרים קודמים,הראו שביטוי רציף של P0 בארבידופסיס גורם להרג הצמח, בדומה לחלק מהמוטנטים החסרים את הגן *ago1*. ביטוי מושרה של P0 גורם לעלייה ברמת תעתיקי המטרה של מספר miRNAs ולשיבוש בהתפתחות הצמח, בדומה למוטנטים היפומורפים של *ago1*. מצאתי שבעגבנייה, כמו בטבק, AGO1 מקודד על ידי שני גנים (SlAGO1-1/2). ידוע ש-AGO1 מבוקר בתר שעתוק על ידי miR168. כדי לבדוק האם גם בעבגנייה SlAGO1s מבוקרים על ידי sly-miR168, תחילה אפיינתי את אוכלוסיית miR168, ומצאתי שקיים רק מופע יחיד של sly-miR168 המקודד על ידי שני גנים. אנליזה ביואינפורמטית הראתה שייתכן ו-SlAGO1s מבוקרים על ידי sly-miR168, ואנליזת 5' RACE הוכיחה כי שניהם עוברים חיתוך מונחה על ידי sly-miR168. מכאן שהם מייצגים הומולוגים של הגן AGO1. אכן הראיתי באמצעות אנליזה של western-blot עם נוגדן כנגד AGO1 בארבידופסיס, ששניהם דועכים בנוכחות P0. כיוון שביטוי רציף של P0, גרם להרג בארבידופסיס, בעבודה זו נעשה שימוש במערכת הטראנס-אקטיבציה על מנת לבטא את P0. מערכת זו פותחה על מנת לגבור על בעיית ההרג העלולה להתרחש כתוצאה מביטוי טרנסגנים רעילים, עובדה בעייתית במיוחד בצמחים כדוגמת עגבנייה, שתהליך הטרנספורמציה בהם כולל שלב ארוך של רגנרציה בתרבית ריקמה. מערכת זו מבוססת על יצירת צמחים "מדווחים" המכילים את הטרנסגן במצב לא פעיל תחת בקרת הפרומוטור OP וצמחים "משפעלים" המבטאים את LhG4, שהינו אקטיבטור סינטטי של OP, תחת בקרה של פרומוטור צמחי רציף או ספציפי. הכלאה בין צמח "מדווח" לצמח "משפעל" תבטא בצאצאים את הטרנסגן רק ברקמות בהן LhG4 מתבטא. בהתאם, יוצרו צמחים טרנסגניים מדווחים (*OP:P0HA*) אשר משופעלים בנוכחות LhG4 ומבטאים את החלבון הויראלי P0 המחובר ל-HA tag. ביטוי P0HA בעגבנייה גרם לירידה בביטוי של SlAGO1 ולמופעים התפתחותיים שונים אשר בחלקם מזכירים מופעים הקיימים במספר צמחי ארבידופסיס מוטנטים ל- *ago1*. בצמחי *35S>>P0HA* בהם מבוטא P0HA באופן רציף קיימת ירידה ברמה של SlAGO1 ועלייה ברמת תעתיקי מטרה נבחרים. בהתאם, צמחים אלו הראו פגמים מורפולוגיים מרובים וצמיחתם נעצרה לאחר הנביטה כמו בצמחי ארבידופסיס מוטנטים המבטאים P0 באופן רציף. תוצאות אלו מעידות שביטוי P0HA גרם לפגיעה במסלול ה-miRNAs מתווך SlAGO1 בצמחוני *35S>>P0HA*. בהמשך, על מנת לוודא שהשימוש ב-P0HA הינו רגיש מספיק ויכול לעכב את מסלול ה-miRNA בביטוי ספציפי ופחות חזק, צמחי *OP:P0HA* הוכלאו עם צמחים משפעלים המאופיינים היטב בעגבנייה ומבטאים LhG4 באזורים ובשלבים התפתחותיים שונים בעלה (*FIL:LhG4*/*BLS:LhG4* / *650:LhG4*). טראנס-אקטיבציה של P0HA בשלבים פרימורדיאליים בהתפתחות העלה (*FIL>>P0HA*) שינתה באופן דרמטי את מורפולוגיית העלה וגרמה לאיבוד

תקציר

לפני כעשור זוהתה מערכת בקרת גנים חדשה בצמחים המתרחשת בתר שעתוק (post -PTGS transcriptional gene silencing). מערכת זו התגלתה לראשונה כמערכת הגנה של הצמח כנגד וירוסים ובהמשך התגלה שהיא משמשת את הצמח גם לבקרה על ביטוי גנים אנדוגנים. בקרה זו מבוצעת על ידי מגוון מולקולות רנ״א קטנות אשר חוברות לאחד מחלבוני ה-ARGONAUTE (AGOs), שהוא חלק מקומפלקס חלבוני הקרוי RISC (RNA induced silencing complex), ומנחים אותו להשתקה של תעתיק המטרה אשר משלים להם ברצף, באמצעות ביקועו, עיכוב תרגומו או על ידי מודיפיקציה בכרומטין. מיקרו-רנ״א (miRNAs) הינן מולקולות רנ״א קטנות באורך של 21-24 נוקליאוטידים המייצגות את אחת הקבוצות החשובות של רנ״א קטנים ומשמשות כבקרים עיקריים של ביטוי גנים בצמחים ובבעלי חיים. מחקרים בצמחים מוכיחים ש-miRNAs ותעתיקי המטרה המבוקרים על ידם, שחלקם הגדול מקודד לפקטורי שעתוק, ממלאים תפקיד חשוב במטבוליזם, תהליכים פיזיולוגיים ותהליכים התפתחותיים. הפרח, המכיל את אברי הרבייה אשר חשיבותם רבה לדור העתיד, מהווה איבר שפגיעה בהתפתחותו עלולה להשפיע על הדורות הבאים ועל המשכיות בכלל, ולכן, להבנת התפתחותו יש חשיבות רבה. מחקרים מראים ש-miRNAs ממלאים תפקיד חשוב בהתפתחות הפרח בצמחי מודל שונים, אך מעט מאוד ידוע על תפקודם בעגבנייה, אחד מהגידולים החקלאיים החשובים ביותר. מאחר והפירות נוצרים מפרחים מופרים, זיהוי תעתיקי המטרה המבוקרים על ידי miRNAs והתהליכים ההתפתחותיים בהם הם מעורבים, יאפשר בעתיד לנצלם לשיפור ביוטכנולוגי של העגבנייה. מטרת עבודה זו הייתה לזהות ולאפיין תעתיקי מטרה של miRNAs המשתתפים בהתפתחות הפרח בעגבנייה.

מטרות המשנה של המחקר היו:

1. חשיפת תהליכים וגנים המבוקרים על ידי microRNAs החשובים להתפתחות הפרח
2. אפיון הגנים המבוקרים על ידי sly-miR164 וחשיבותם להתפתחות הפרח
3. אפיון הפונקציה של הגן *SlNAM2* בפרח
4. אפיון חשיבות הבקרה של miR164 לפעילותו של הגן *SlNAM2*

קביעה והבנת המעורבות של מנגנון בקרה זה בהתפתחות הפרח בארבידופסיס התאפשרה הודות למוטנטים השונים שנמצאו פגומים במסלול ה-miRNAs. אולם בעגבנייה, בשלב תחילת המחקר לא היה ידוע על מוטנט שכזה, ויצירה של צמחים טרנסגניים המשתיקים גנים במסלול זה לא התאפשרה כיוון שגנום העגבנייה לא היה ידוע וספריות ה-EST לא הכילו רצפים מלאים המקודדים לחלבוני מפתח במסלול זה. בעבר הראו שניתן לחסום את פעילותם של מולקולות ה-miRNAs על ידי ביטוי של חלבונים ויראליים המעכבים את מנגנון ההשתקה האנטי-ויראלי, אשר לו רכיבים משותפים עם מנגנון ההשתקה האנדוגני. ולכן, בהעדר היכולת לחקור את מעורבות ה-miRNAs בשיטות הגנטיות המקובלות,

תוכן העניינים

ברצוני להודות:

לד״ר צחי ארזי, תודה רבה על העזרה, ההנחיה ועל הדיונים במהלך הדרך. על שלימדת אותי לפקפק ולחפש את החסר. על ה״סדנא״ שעברתי במהלך שנות המחקר, שלעיתים לא היתה קלה ומלאה ברגעי משבר, אך בהחלט למדתי ממנה רבות והגעתי לאן שהגעתי בזכותך ועל כך, תודה ענקית.

לפרופ׳ רפי פרל-טרבס, תודה רבה על העזרה, הדלת הפתוחה והאמונה בי.

לרן סתיו, על העזרה היומיומית במעבדה ועל יכולתו המופלאה לייצר עבורי עשרות קווים טרנסגניים.

לד״ר מיכאל קרבצ׳יק, שלעיתים הוציא אותי מדעתי אך תמיד היה לעזר הן ברמה האישית והן ברמה המדעית.

לחני צמח, שלימדה אותי את כל מה שאני יודעת בהיסטולוגיה ועל העזרה והתמיכה האינסופיים.

לד״ר רקפת שוורץ, על הדיונים המדעיים, העזרה עם המאמרים והאמונה בי ובעבודה (גם בימים בהם הכל נראה אבוד).

לפרופ׳ נעמי אורי ולחברי המעבדה על הזרעים, ההקשבה והייעוץ. ובעיקר תודה ענקית להדס בן-גרה שהיתה לי לאוזן קשבת בכל מה שקשור לניסויי ה-in-situ.

לאדי בלאוסוב על הצילומים המרהיבים במיקרוסקופ הקונפוקלי.

למוחמד, אביב, תמר, הדס, קוומי, לין ולכל החבר׳ה בבניין ובמכון בכלל על החברה והתמיכה.

תודה ענקית למשפחתי היקרה והנפלאה שבלעדיהם כל זאת לא היה מתאפשר.

ולבסוף, לחזקי ונועה אהוביי, על האהבה האינסופית והיותם האור של חיי.

עבודה זו נעשתה בהדרכתם של:

ד״ר צחי ארזי מהמכון למדעי הצמח, מינהל המחקר החקלאי, מרכז וולקני.

פרופ׳ רפאל פרל-טרבס מהמחלקה למדעי החיים ע״ש מינה ואבררד גודמן, אוניברסיטת בר אילן.

מעורבות מיקרו-רנ״א 164 והגנים המבוקרים על ידו בהתפתחות פרח העגבנייה

חיבור לשם קבלת התואר ״דוקטור לפילוסופיה״

מאת:

ענת הנדלמן

המחלקה למדעי החיים ע״ש מינה ואבררד גודמן

הוגש לסנט של אוניברסיטת בר-אילן

רמת גן חשון, תשע״ד